SAFETY ANALYSIS REPORT, Y-12 NATIONAL SECURITY COMPLEX, MODEL ES-3100 PACKAGE WITH BULK HEU CONTENTS

Prepared by
Babcock & Wilcox Technical Services Y-12, LLC
Y-12 National Security Complex
P.O. Box 2009
Oak Ridge, Tennessee 37831
Managed by
Babcock & Wilcox Technical Services Y-12, LLC
for the
U. S. Department of Energy
under contract DE-AC05-00OR22800

February 26, 2009

CONTENTS

CONTENTS

Page

CONTENTS

CONTENTS

REVISION LOG

Date	SAR Revision No.	Description	Affected Pages
8/28/08	2, Page Change 2	Revised SAR in response to RAIs dated April 28, 2008, for review of CoC 9315, Revision 8	i, vi, viii, xii, xxiii, xxiv, 1-10, 1-14 through 1-16, 1-22, 2-1, 2-25 through 2-28, 2-894, 3-15, 3-16, 3-165 through 3-290, 4-1, 4-2, 6-1 through 6-3, 6-20 through 6-28, 6-30 6-32 through 6-34, 6-68 through 6-70, 6-70a, 6-70b, 6-75 through 6-77, 6-77a, 6-77b, 6-78, 6-81 through 6-83, 6-85, 6-86, 6-101 through 6-103, 6-103a through 6-103j, 6-104, 6-123 through 6-126, 6-167 through 6-170, 6-177, 6-177a, 6-177b, 6-218a through 6-218f, 6-219 through 6-234, 6-303 through 6-305, 6-331, 6-332, 6-332a, 6-332b, 6-333, 6-394 through 6-398, 6-501, 6-502, 6-502a through 6-502dd

REVISION LOG

Date	SAR Revision No.	Description	Affected Pages
2/26/09	2, Page Change 3	Revised SAR in response to RAIs dated January 12, 2009, for review of CoC 9315, Revision 9	i, viii, ix, xxiv, 1-7, 1-10, 1-12 through 1-16, 1-21 through 1-23, 1-29 1-31, 1-33, 1-35, 1-37, 1-39, 1-41, 1-135, 1-157, 1-177, 2-6, 2-9, 2-18, 2-36 through 2-38, 2-41 through 2-43, 2-53, 2-78, 2-80, 3-15 through 3-17, 3-27, 3-28, 3-30, 3-32, 3-39, 3-41, 3-147, 3-149 through 3-154, 3-154a, 3-154b, 3-155, 3-158 through 3-161, 3-165 through 3-174, 3-289 through 3-344, 4-2, 4-7, 4-9, 4-27 through 4-34, 6-5, 6-29, 6-30, 6-34, 6-73 through 6-86, 6-86a through 6-86d, 6-96, 6-103a through 6-103c, 6-104b, 6-104c, 6-123, 6-124, 6-168, 6-219 through 6-221, 6-221a, 6-221b, 6-222, 7-7, 7-8, 7-10

Table 3.10. Total pressure inside the containment vessel at 87.81°C (190.06°F) [a]

CVA	n_a [b] (lb-mole)	n_v [b] (lb-mole)	n_{po} [b] (lb-mole)	n_{bo} [b] (lb-mole)	n_{tf} [b] (lb-mole)	n_{H2} [b] (lb-mole)	n_{O2} [b] (lb-mole)	n_T [b] (lb-mole)	P_T (psia)
2	5.7148E-04	1.8626E-05	0.0000E+00	0.0000E+00	0.0000E+00	3.1895E-05	1.5948E-05	6.3795E-04	19.238
7	4.5793E-04	1.4926E-05	0.0000E+00	0.0000E+00	2.2296E-05	2.5558E-05	1.2779E-05	5.3349E-04	20.077

[a] This assumes that the internal convenience cans, polyethylene or Teflon FEP bottles, and Cat 277-4 spacer cans are not sealed.
[b] n_a = molar quantity of dry air in the gas mixture;
n_v = molar quantity of water vapor in the gas mixture;
n_{po} = molar quantity of gas due to offgassing of the silicone rubber pads;
n_{bo} = molar quantity of gas due to offgassing of the polyethylene bags, bottles, and lifting sling;
n_{tf} = molar quantity of gas due to offgassing of the Teflon bottles;
n_{H2} = molar quantity of hydrogen gas due to radiolysis of water;
n_{O2} = molar quantity of oxygen gas due to radiolysis of water; and
n_T = total molar quantity in the gas mixture.

order to determine the worst-case shipping configuration, the arrangements that minimize the void volume inside the containment vessel are analyzed as follows:

1. one shipment will contain six cans with external dimensions of 10.8 cm (4.25 in.) diameter by 12.38 cm (4.875 in.) high cans;

2. one shipment will contain five cans with external dimensions of 10.8 cm (4.25 in.) diameter by 12.38 cm (4.875 in.) high cans and three can spacers;

3. one shipment will contain three cans with external dimensions of 10.8 cm (4.25 in.) diameter by 22.23 cm (8.75 in.) high and two can spacers;

4. one shipment will contain three cans with external dimensions of 10.8 cm (4.25 in.) diameter by 25.4 cm (10 in.) high;

5. one shipment will contain six nickel cans with external dimensions of 7.62 cm (3.00 in.) diameter by 12.07 cm (4.75 in.) high;

6. one shipment will contain three polyethylene bottles with external dimensions of 12.54 cm (4.94 in.) diameter by 22.1 cm (8.7 in.) high;

7. one shipment will contain three teflon bottles with external dimensions of 11.91 cm (4.69 in.) diameter by 23.88 cm (9.4 in.) high;

8. one shipment will contain a brazed assembly of two cans with final external dimensions of 10.8 cm (4.25 in.) diameter by 44.46 cm (17.50 in.) high. An empty can with external dimensions of 10.8 cm (4.25 in.) diameter by 22.23 cm (8.75 in.) high will be placed on top of the 44.46 cm (17.50 in.) high can;

9. one shipment will contain fuel rods, or tubes, or plates greater than 43.18 cm (17.00 in.) in length. These items are bundled together and protected on both ends with an open-ended can with external dimensions of ≤12.7 cm (5.0 in.) diameter by ≤ 22.23 cm (8.75 in.) high. Total assembly height will be ≤ 77.47 cm (30.5 in.). If space is available inside the containment vessel, stainless-steel metal scrubbers will be added on the bottom and top of this assembly or an empty can will be placed on top of this partially canned assembly; and

10. one shipment will contain three cans brazed together with external dimensions of 4.25-in. diameter by ~30 in. high.

These arrangements are shown in Fig. 1.4. To determine the ES-3100's maximum normal operating pressure, the following assumptions have been used in the calculations:

1. The HEU contents are loaded into convenience cans, and convenience cans are placed inside the containment vessel at standard temperature (T_{amb}) and pressure (P_t) [25°C (77°F) and 101.35 kPa (14.7 psia)] with air at a maximum relative humidity of 100%;

2. The convenience cans and bottles are assumed to not be sealed to maximize the void volume inside the containment vessel;

3. Convenience can and bottle geometry does not change during pressure increase inside containment vessel;

4. If metal convenience cans are used, the total amount of polyethylene bagging and lifting slings is limited to 500 g per containment vessel shipping arrangement;

5. The mass of offgassing material (polyethylene bagging or bottles, Teflon bottles, silicone pads, lifting slings) is assumed to be 1490 g for the offgassing evaluation of containment vessel arrangement #7 and 500 g for containment vessel arrangement #6; and

6. Containment vessel arrangements that utilize closed convenience cans with a diameter greater than 10.8 cm (4.25 in.) will not contain any materials that off gas at the temperatures associated with Normal Conditions of Transport (NCT).

The offgassing material limits identified in assumptions 4 and 5 have been established based on the needs of shippers. All configurations are limited to 500 g of polyethylene in the form of bags, slings, and/or bottles. When the requirement to ship material in Teflon bottles arose, the upper limit of 1490 g of offgassing material was established. This limit is a combination of three Teflon bottles (330 g per bottle) and the original 500 g allowance for polyethylene material. These offgassing material limits have been used in calculations pertaining to containment vessel pressure, radioactive material leakage criteria, and criticality control. Therefore, portion of the safety basis of this shipping package has been based on these material limits.

NUREG-1609, Sect. 4.5.2.3, requires the applicant to demonstrate that any combustible gases generated in the package during a period of one year do not exceed 5% (by volume) of the free gas volume in any confined region of the package. No credit should be taken for getters, catalysts, or other recombination devices. The analysis conducted in Appendix 3.6.7 ~~further~~ evaluates the different packaging arrangements for the generation of hydrogen gas due to the radiolysis of water vapor, free water, interstitial water, polyurethane bags, and polyurethane or Teflon bottles. By limiting the mass and the material composition as shown in Appendix 3.6.7, the combustible gas concentration limit stated in NUREG-1609 is not exceeded. These limits are further discussed and shown in Tables 1.3 and 1.3a. Getters, catalysts, or other recombination devices are not employed in any of the containment vessel packaging arrangements. The analysis conducted in Appendix 3.6.4 predicts the maximum normal operating pressure inside the containment vessel for the various packaging arrangements and masses discussed previously. This appendix also includes the hydrogen gs generation predicted by Appendix 3.6.7.

3.1.4.2 Maximum HAC Pressures

Table 3.11 summarizes the results from Appendix 3.6.5 in which the pressure of the containment vessel when subjected to the tests and conditions of HAC per 10 CFR 71.73 has been determined for the most restrictive CVAs shipped in the ES-3100. The shipping configurations discussed in Sect. 3.1.4.1 are evaluated for HAC. To determine the maximum pressure generated inside the

ES-3100's containment vessel due to HAC conditions, the following assumptions have been used in the calculations:

1. The initial pressure inside the containment vessel is the maximum normal operating pressure shown in Table 3.10 for each CVA at standard temperature [25°C (77°F)];

2. The convenience cans and bottles are assumed to not be sealed in order to maximize the void volume inside the containment vessel;

3. Convenience can and bottle geometry does not change during pressure increase inside containment vessel or because of damage from compliance testing;

4. If metal convenience cans are used, the total amount of polyethylene bagging and lifting slings is limited to 500 g per containment vessel shipping arrangement;

5. The mass of offgassing material (polyethylene bagging or bottles, Teflon bottles, silicone pads, lifting slings) is assumed to be 1490 g for the offgassing evaluation of containment vessel arrangement #7 and 500 g for containment vessel arrangement #6; and

6. Containment vessel arrangements that utilize closed convenience cans with a diameter greater than 10.8 cm (4.25 in.) will not contain any materials that off gas at the temperatures associated with Hypothetical Accident Conditions (HAC).

The offgassing material limits identified in assumptions 4 and 5 have been established based on the needs of shippers. All configurations are limited to 500 g of polyethylene in the form of bags, slings, and/or bottles. When the requirement to ship material in Teflon bottles arose, the upper limit of 1490 g of offgassing material was established. This limit is a combination of three Teflon bottles (330 g per bottle) and the original 500 g allowance for polyethylene material. These offgassing material limits have been used in calculations pertaining to containment vessel pressure, radioactive material leakage criteria, and criticality control. Therefore, portion of the safety basis of this shipping package has been based on these material limits.

Table 3.11. Total pressure inside the containment vessel at 123.85°C (254.93°F) [a]

CVA	n_{MNOP} [b] (lb-mole)	n_{po} [b] (lb-mole)	n_{bo} [b] (lb-mole)	n_{tf} [b] (lb-mole)	n_{H2} [b] (lb-mole)	n_{O2} [b] (lb-mole)	n_T [b] (lb-mole)	P_T (psia)
2	7.7226E-04	1.7303E-05	3.1529E-04	0.0000E+00	3.1895E-05	1.5948E-05	1.1527E-03	38.229
7	6.4581E-04	0.0000E+00	3.1529E-04	2.2296E-05	2.5558E-05	1.2779E-05	1.0217E-03	42.288

[a] This assumes that the internal convenience cans, polyethylene or Teflon FEP bottles, and Cat 277-4 spacer cans are not sealed.
[b] n_{MNOP} molar quantity of the gas mixture at maximum normal operating pressure at standard temperature [25°C (77°F)];
n_{po} molar quantity of gas due to offgassing of the silicone rubber pads;
n_{bo} molar quantity of gas due to offgassing of the polyethylene bags, bottles, and lifting sling;
n_{tf} molar quantity of gas due to offgassing of the Teflon bottles;
n_{H2} molar quantity of hydrogen gas due to radiolysis of water;
n_{O2} molar quantity of oxygen gas due to radiolysis of water; and
n_T total molar quantity in the gas mixture.

3.2 SUMMARY OF THERMAL PROPERTIES OF MATERIALS

3.2.1 Material properties

Thermal properties at various temperatures for the stainless steel used in the fabrication of the drum, noncombustible cast refractory (Kaolite 1600), noncombustible neutron poison (BoroBond 4 or Cat 277-4), silicone rubber pads, and air are listed in Table 3.12. Properties used to evaluate thermal stresses due to differences in coefficient of thermal expansion are listed in Table 3.13.

3.2.2 Component Specifications

Component specifications are listed in Tables 3.14 and 3.15.

3.3 GENERAL CONSIDERATIONS

Thermal evaluation of the package design for NCT was performed by analysis. Evaluation of the package design for HAC was performed by a combination of testing and analysis.

3.3.1 Evaluation by Analysis

A description of the method and calculations used to perform the thermal and thermal stress analyses of the package for NCT and HAC is presented in detail in Appendices 3.6.1, 3.6.2 and 3.6.3.

3.3.2 Evaluation by Test

Full-scale testing of five ES-3100 test units was conducted in accordance with 10 CFR 71.73 for HAC. A single full-scale ES-3100 (TU-4) was assembled and subjected to both NCT testing and the sequential tests specified in 10 CFR 71.73(c). The furnace used for thermal testing was the No. 3 furnace at Timken Steel Company in Latrobe, Penn., which is a gas-fired furnace. This furnace employs "pulsed" fire burners, in which the natural gas flow rate is varied based on furnace controller demands, but the flow of air through the burners is constant, even when no gas is flowing. This ensures a very rich furnace atmosphere capable of supporting any combustion of package materials of construction.

Oxygen content was not monitored in stack gases of the furnace because it was not anticipated that any of the package's materials of construction were combustible. There was some burning of the silicone pads which are placed between the inner liner and the top plug of the package.

The most significant change to the definition of the HAC thermal test in the current 10 CFR 71 is the requirement for calculation purposes to base convective heat input on "that value which may be demonstrated to exist if the package was exposed to the fire specified." This is not especially significant for this package because it was tested in the gas-fired furnace with burners placed in an attitude which produced a strong convective swirl. Careful examination of the thermal test data indicates that the total heat imparted to the packages was significantly greater than the required total heat specified in 10 CFR 71.73(c)(4).

Table 3.16. Summary of results of evaluation for the ES-3100 under NCT

Conditions	Calculated results	Allowable limit	SARP reference
Minimum package temperature, °C (°F)	-40 (-40)	-40 (-40)	Sect. 3.4.1
Maximum drum assembly stress due to cold conditions per 10 CFR 71.71(c)(2), kPa (psia)	61,150 (8,869)	132,379 (19,200)	Appendix 3.6.3
Minimum containment vessel pressure, kPa (psia)	76.74 (11.13)	0.0 (0.0)	Sect. 3.4.1
Maximum drum temperature with insolation, °C (°F)	117.72 (243.89) [a]	N/A	Appendix 3.6.2 Sect. 3.4.1
Maximum drum assembly stress due to hot conditions per 10 CFR 71.71(c)(1), kPa (psia)	66,934 (9,708)	132,379 (19,200)	Appendix 3.6.3
Containment vessel temperature with insolation, °C (°F)	87.81 (190.06) [a]	427 (800) [b]	Appendix 3.6.2 Sect. 3.4.1
Maximum O-ring temperature, °C (°F)	87.81 (190.06)	150 (302) [c]	Appendix 3.6.2 Sect. 3.4.1
Maximum containment vessel pressure, kPa (psia)	138.43 (20.077) [d]	801.2 (116.2) [e]	Appendix 3.6.4 Sect. 3.4.2

[a] Appendix 3.6.2.
[b] *ASME Boiler and Pressure Code*, Sect. II, Part D, maximum allowable temperature for Sect. III, Div. 1, Subsection NB vessel.
[c] Maximum O-ring seal life up to 150°C (302°F) for continuous service (*Parker O-ring Handbook,* Fig. 2-24).
[d] Appendix 3.6.4.
[e] Appendix 2.10.1 allowable limit.

Table 3.17. Summary of results of evaluation under HAC for the ES-3100 shipping arrangement using bounding case parameters

Condition	Results	Design limits	SARP references
Maximum adjusted containment vessel temperature during testing, °C (°F)	152.22 (306.00)	426.67 (800) [a]	Sect. 3.5.3
Maximum containment vessel pressure during testing, kPa (psia)	280.63 (40.701) [b]	801.2 (116.2) [c]	Appendix 3.6.5 Sect. 3.5.3
Maximum adjusted O-ring temperature, °C (°F)	141.22 (286.20)	150 (302) [d]	Sect. 3.5.3

[a] *ASME Boiler and Pressure Code*, Sect. II, Part D, maximum allowable temperature for Sect. III, Div. 1, Subsection NB vessel.
[b] Appendix 3.6.5.
[c] Appendix 2.10.1 at 148.89°C (300°F).
[d] Maximum O-ring seal life up to 150°C (302°F) for continuous service (*Parker O-ring Handbook,* Fig. 2-24).

3.4 THERMAL EVALUATION UNDER NORMAL CONDITIONS OF TRANSPORT

3.4.1 Heat and Cold

The ambient temperature requirement for NCT is 38°C (100°F). The 35.2 kg of HEU shipped in the ES-3100 package generates a maximum bounding heat load of 0.4 W. The insolation heat flux stipulated in 10 CFR 71.71(c)(1) was used in the calculations. If the package is exposed to solar radiation at 38°C (100°F) in still air, the conservatively calculated temperatures at the top of the drum, on the top surface of the containment vessel, and on the containment vessel near the O-ring sealing surfaces, are 117.72, 87.81, and 87.72°C (243.89, 190.06, 189.90°F), respectively, for the ES-3100. Nevertheless, these temperatures are within the service limits of all packaging components, including the O-rings. The normal service temperature range of the O-rings used in the containment boundary is -40 to 150°C (-40 to 302°F), in accordance with B&PVC, Sect. III; thus, the seal will not be affected by this maximum normal operating temperature.

Using the temperatures calculated for the conditions of 10 CFR71.71(c)(1), Appendix 3.6.4 predicts that the maximum normal operating pressure inside the containment vessel will be 138.43 kPa (20.077 psia). The design absolute pressure of the containment vessel is 801.17 kPa (116.2 psia), and the hydrostatic test pressure is 1135.57 kPa (164.7 psia). Thus, increasing the internal pressure of the containment vessel to a maximum of 138.43 kPa (20.077 psia) during NCT would have no detrimental effect. Stresses generated in the containment vessel at this pressure are insignificant compared to the materials of construction allowable stress. Table 2.20 provides a summary of the pressure and temperature for the various shipping configurations. As discussed in Sect. 2.6.1.4, the containment vessel and vessel closure nut stresses for these pressure conditions are below the allowable stress values.

Summarizing 10 CFR 71.43(f), the tests and conditions of NCT shall not substantially reduce the effectiveness of the packaging to withstand HAC sequential testing. The effectiveness of the ES-3100 to withstand HAC sequential testing is not diminished through application of the tests and conditions stipulated in 10 CFR 71.71. The justification for this statement is provided by physical testing of both the ES-2M and ES-3100 test packages. Due to the similarities in design, fabrication, and material used in construction of both the ES-2M and the ES-3100 package, the Kaolite 1600 physical characteristics will hold true for both designs. The integrity of the Kaolite 1600 is not significantly affected by the NCT vibration and 1.2-m (4-ft) drop tests.

Prior to testing the ES-2M design (a similarly constructed shipping package), each test unit was radiographed to determine the integrity of the Kaolite 1600 impact and insulation material. Following casting of the material inside the drum, some three-dimensional curving cracks were seen in some packages near the top thinner sections from the bottom of the liner to the bottom drum edge. After vibration testing, radiography of the ES-2M Test Unit-4 showed that the lower half of the impact limiter was broken into small pieces (Byington 1997). To evaluate these findings, Test Unit-4 was reassembled and subjected to HAC sequential testing (Byington 1997). After vibration and impact testing, many three-dimensional curving cracks were seen around the impact areas, and the inner liner was also visibly deformed. Nevertheless, temperatures at the containment boundary were also similar to other packages not subjected to vibration testing prior to HAC testing. No inleakage of water was recorded following immersion. Also, Test Unit-4 of the ES-3100 shipping package was subjected to the full NCT test battery including vibration.

Following these tests, the containment vessel of the ES-2M Test Unit-4 was removed, and a full body helium leak check was performed. The test unit passed the leak-tight criteria in accordance with ANSI N14.5-1997. The containment vessel was then reassembled into the previously tested drum

assembly and subjected to the complete HAC testing. Based on the success of this unit and the similar design of the ES-2M, it can be concluded that vibration normally incident to transport does not reduce the effectiveness of the ES-3100 packaging during HAC testing. The ES-3100 has been tested to determine the effectiveness of the package following a sequential NCT 1.2-m (4-ft) drop test and HAC test battery. Throughout all of the vibration and structural testing, the effectiveness of the Kaolite 1600 material as an impact limiter and thermal insulation was not substantially reduced.

Since the components to be shipped have an assumed decay heat load of 0.4 W, a thermal analysis was conducted for the ES-3100 package with and without full solar insolation. The package was analyzed using the ABAQUS/Standard computer code, and the finite element geometry was constructed for each model using MSC.Patran 2004. The predicted temperature, while stored at 38°C (100°F) in the shade, for the drum lid center and the containment vessel flange near the inner O-ring, is 37.89°C (100.20°F) and 38.22°C (100.80°F), respectively. The analysis shows that no accessible surface of the package would have a temperature exceeding 50°C (122°F). Therefore, the requirement of 10 CFR 71.43(g) would be satisfied for either transportation mode (exclusive use or nonexclusive use).

Also, in accordance with 10 CFR 71.71(c)(2), the containment vessel pressure must be calculated at -40°C (-40°F). Given the initial conditions of temperature, relative humidity, no silicone rubber or polyethylene bag offgassing, the pressure is calculated as follows:

$$P_1 @ 25°C = P_a + P_v + P_{fo},$$

where,

P_a	=	98.15 kPa (14.236 psia)	(Appendix 3.6.4)
P_v	=	3.20 kPa (0.464 psia)	(Appendix 3.6.4)
P_{fo}	=	0	(no offgassing, Appendix 3.6.4)

At -40°C (-40°F), the partial pressure of the water vapor is conservatively assumed to be zero. Therefore, the final pressure of the mixture at -40°C (-40°F) is calculated according to the ideal gas law based solely on the partial pressure of the air.

$$\frac{P_1 V_1}{T_1} = \frac{P_2 V_2}{T_2}$$

where,

P_1	=	98.15 kPa (14.236 psia)
T_1	=	25°C (298.15 K)
T_2	=	-40°C (233.15 K)
V_1	=	V_2

rearranging and solving for P_2,

$$P_2 = P_1 (T_2/T_1)$$
$$= (98.15)(233.15/298.15)$$
$$P_2 = 76.76 \text{ kPa } (11.13 \text{ psia}).$$

The cold condition for NCT specified in 10 CFR 71.71 is an ambient temperature in still air and shade of -40°C (-40°F). The 35.2 kg (77.60 lb) of HEU contents in the ES-3100 package generates a maximum bounding decay heat load of 0.4 W. However, in accordance with Regulatory Guide 7.8, the thermal effects of this internal heat source are neglected during evaluation of the package performance at

-40°C (-40°F). When exposed to this condition, the package component temperatures will stabilize over time at a temperature approaching -40°C (-40°F). The package has been examined for use at -40°C (-40°F) (Sect. 2.6.2). No detrimental effects on the package structure or sealing capability result from this minimum temperature requirement. The normal service temperature range of the O-rings used in the containment boundary is -40 to 150°C (-40 to 302°F), in accordance with the *Parker O-ring Handbook*; thus, the seal will not be affected by this minimum package temperature in accordance with 10 CFR 71.71(c)(2). Leak testing conducted on Test Unit-2 to the leak tight criteria stipulated by ANSI N14.5-1997 following compliance testing provides justification of the above statements.

3.4.2 Maximum Normal Operating Pressure

The stainless-steel drum and cast refractory system will not pressurize as a result of temperature increases because of four ventilation holes (0.795 cm [0.313 in.] in diameter) drilled in the drum side wall 3.81 cm (1.5 in.) from the flanged top and equally spaced around the drum. The holes are filled with nylon plugs, but they are not hermetically sealed. The inner liner encapsulating the noncombustible neutron poison (Cat 277-4) will not pressurize as a result of temperature increases because of three ventilation holes (0.635 cm [0.25 in.] in diameter) and a slot (1.63 cm [0.64 in.] in width and 4.17 cm [1.64 in.] in length) drilled into this inner liner. These features are covered during transport with aluminum tape to prevent contamination of the neutron poison. This tape does not represent a hermetic seal.

The maximum normal operating pressure is defined in 10 CFR 71.4 as the maximum gauge pressure that would develop in the containment system in a period of one year under the heat conditions specified in 10 CFR 71.71(c)(1). The internal pressure developed under these conditions in the ES-3100 containment vessel is calculated in Appendix 3.6.4 for the most restrictive containment vessel configurations. For conservatism, the decay heat of 0.4 W was used for the maximum internal heat load in evaluating the package for NCT. The maximum calculated internal absolute pressure in the containment vessel with solar insolation and the bounding case parameters is 138.43 kPa (20.077 psia). This pressure incorporates offgassing of the silicone rubber pads, polyethylene bottles, Teflon bottles, and polyethylene bagging and hydrogen gas generation from the radiolysis of water and/or other packing materials. The initial environment inside the containment vessel when assembled is at ambient temperature and pressure with 100% relative humidity. The heat-transfer capability of the packaging is not degraded due to gap creation caused by differences in the fabrication material's coefficient of thermal expansion. Modeling assumed nominal gaps and position based on the engineering drawings of Appendix 1.4.8.

3.4.3 Maximum Thermal Stresses

The temperature of the package under NCT will vary from a low of -40°C (-40°F) throughout the package to a maximum of 117.72 and 87.81°C (243.89 and 190.06°F) (Appendix 3.6.2) on the surface of the drum and the containment vessel, respectively (Sect. 3.4.1). The slow temperature increase or decrease experienced in normal conditions between these limits will result in an essentially uniform temperature change throughout the package. All materials of construction are within this operating temperature range (Table 3.15). Thermal stresses due to differences in thermal expansion are insignificant, as discussed in Sects. 2.6.1.2 and 2.6.2.

Most of the components of the packaging are completely unrestrained. Therefore, any thermal stresses in the packaging components as the temperature varies between the extremes listed above will

have no effect on the ability of the packaging to maintain containment, shielding integrity, and nuclear subcriticality. The maximum stresses due to pressure under NCT for the containment vessel are given in Tables 2.21 and 2.22. These values are significantly below the allowable stresses for the packaging components. The Kaolite 1600 insulation and Cat 277-4 materials are poured and cast in place during the fabrication of the drum weldment (Drawing M2E801508A002, Appendix 1.4.8). This situation produces a zero gap between the these materials and the bounding drum and inner liners. Due to differences in coefficients of thermal expansion, some radial and axial interference is expected due to thermal growth or contraction of the inner liners. These radial and axial interferences and induced stresses are calculated in Appendix 3.6.3. The results show that the stresses induced are minimal and do not reduce the effectiveness of the drum assembly.

The containment vessel, which is Type 304L austenitic (iron-nickel-chromium) stainless steel, is designed and fabricated in accordance with Sects. III SubSect. NB and IX of the *ASME Boiler and Pressure Vessel Code* (B&PVC Sect. III and B&PVC Sect. IX). The two sealing surfaces of each containment boundary are joined together by torquing the closure nut inside the containment vessel body to 162.7 ±6.8 N·m (120 ±5 lbf-ft). The O-ring material is ethylene-propylene elastomer.

The design temperature range of the containment vessel is -29 to 148.89°C (-20 to 300°F) (Appendix 2.10.1). However, the package has been evaluated to -40°C (-40°F) (Sect. 2.6.2). The thermal properties of the stainless-steel container body, lid, and closure nut are not critical at these temperatures. The O-ring seal is important for the containment properties of the containment vessel. The normal service temperature range for the elastomer O-ring is -40 to 150°C (-40 to 302°F) for continuous service and up to 165°C (329°F) for 72 h (*Parker O-ring Handbook*). The maximum adjusted HAC temperature of the ES-3100 containment vessel was based upon the thermal testing results in the vicinity of the O-rings. The maximum temperature recorded in the vicinity of the ES-3100 O-rings (241°F) is shown in Table 3.9. As shown in Sect. 3.5.3, the maximum temperature for the containment vessel at the O-ring location was adjusted for the ES-3100 package to 141.22°C (286.20°F). Hence, no damage would be expected to the O-rings during HAC.

The test packages were all preheated to above 38°C (100°F) prior to being placed in the furnace, which was heated to over 800°C (1475°F). As noted in the test report (Appendix 2.10.7), the temperatures recorded on the containment vessels of all the test units were fairly uniform, both vertically and circumferentially. The maximum temperature variation on the containment vessels was ~50°F (from the test temperatures reported in Table 3.9). No damage would be expected on the containment vessel from thermal stresses resulting from a temperature differential of this magnitude. This conclusion is based on the guidelines given in B&PVC, Sect. III. Thermal stress is defined as a self-balancing stress produced by a nonuniform distribution of temperature (Paragraph NB-3213.13 of B&PVC, Sect. III). This paragraph further states that there are two types of thermal stresses: general thermal stress and local thermal stress. An example of a general stress is that produced by an axial temperature distribution in a cylindrical shell (Paragraph NB-3213.9). This general stress is further classified (Paragraph NB-3213.9) as a secondary stress (that is, a normal stress or a shear stress developed by the constraint of adjacent materials or by self-constraint of the structure). Paragraph NB-3213.9 further states that the basic characteristic of a secondary stress is that it is self-limiting. Local yielding and minor distortions can satisfy the conditions that cause the stress to occur, and failure from a single application would not be expected. An example of a local thermal stress is a small hot spot in the wall of a pressure vessel (Paragraph NB-3213.13). Local thermal stress is associated with almost complete suppression of the differential expansion and thus produces no significant distortion. Such stresses are considered only from a fatigue standpoint. Fatigue will not result from a one-time cyclic event such as an accidental fire.

Following the thermal test, the volume between the O-rings on the five containment vessels (Sect. 2.7.4) was then leak tested and met the air leak-rate criterion of 10^{-4} ref-cm^3/s. Following the O-ring leak check, the five containment vessels were drilled and tapped for full body helium leak testing. All five containment vessels passed the leak rate criteria for leaktightness per ANSI N14.5-1997. The containment vessels were then submerged under a pressure equivalent to 0.9 m (3 ft) of water for 8 h, with no leakage noted. (Sect. 2.7.5). Visual inspection following testing and disassembly also indicated that no distortion or damage occurred in the containment vessel wall, sealing lid, closure nut, O-rings, or sealing surfaces. These tests and observations demonstrate that thermal stresses produced during testing did not affect the containment capability of the containment vessel.

3.5 HYPOTHETICAL ACCIDENT THERMAL EVALUATION

3.5.1 Initial Conditions

Five full-scale packages were tested in the sequence shown in Table 2.19. Each ES-3100 test package was subjected to the 1.2-m (4-ft) drop test in accordance with 10 CFR 71.71(c)(5) prior to the sequential HAC tests in accordance with 10 CFR 71.73 (free drop, crush, puncture, thermal, and immersion tests). One of these units (Test Unit-4) had previously completed the tests and conditions stipulated in 10 CFR 71.71(c)(5) through (c)(10), excluding (c)(8). Two different mock-up configurations were used to represent the minimum and maximum proposed shipping weight and to simulate various center of gravity locations. The structural and thermal interface between the mock-up component and the containment vessel was designed to match that of the actual hardware proposed for transport. Based on LS-DYNA-3D drop simulations (Appendix 2.10.2) the five test units with their associated test weights represent the worst drop orientations for the ES-3100 package. Test Unit-5 used a near replicate of the lightest weight contents for its mock-up component. NCT free-drop, 9 m (30 ft) free drop, 9 m (30 ft) crush and puncture tests were made as specified in 10 CFR 71.71(c)(1), and 73(c)(1) through (c)(3) on all five full-scale test packages prior to thermal testing. The results of this testing are discussed in Sects. 2.7.1, 2.7.2, and 2.7.3. The 1.2-m (4-ft), 9-m (30-ft) drop and crush test orientations were as follows: two tests with the long axis of drum at an oblique angle of 12° to impact surface; a center of gravity over the corner of the drum lid; a drop with the long axis of drum parallel with the impact surface; and a vertical drop on to the drum's lid. The subsequent 40-in. puncture drops were made at various orientations as shown in Table 2.19.

Prior to the thermal test, each test unit was preheated to the maximum temperature extreme in accordance with 10 CFR 71.73(b)(1). Since the containment vessels were initially assembled at ~101.35 kPa (14.7 psia) at 25°C (77°F), the initial internal containment vessel pressure was ~105.70 kPa (15.33 psia) at 38°C (100°F) using the ideal gas law. In accordance with 10 CFR 71.73(b)(1), the internal pressure should be that calculated for the maximum normal operating pressure or 138.43 kPa (20.077 psia). This slight pressure differential has little or no effect on the thermal test results. The maximum decay heat load of the contents is calculated to be 0.4 W based on 35.2 kg of HEU. Analysis of the ES-3100 package after thermal HAC tests both with and without the decay heat load has been performed. The maximum projected temperature differential between the two packages following furnace exposure, as calculated in Appendix 3.6.2, would be 0.4°C (0.7°F) at the top center of the containment vessel lid , 0.4°C (0.7°F) at the containment vessel flange near the O-rings, 0.45°C (0.8°F) at the containment vessel bottom center, and 0.6°C (1.1°F) at the containment vessel mid body. These temperature differentials are representative for both the Kaolite 1600 densities evaluated.

convenience can from the top. Based on the temperature recorded on the containment vessel wall and convenience can [92.78°C (199°F)], the average temperature of gas in this region is 92.78°C (199°F). Using the temperature adjustment of 27.89°C (50.20°F) for this region, the adjusted average temperature in the second region is 120.67°C (249.20°F). The third and final volume is represented by the gas adjacent to the bottom convenience can. Again based on the convenience can temperature [87.78°C (190°F)] and the containment vessel end cap temperature [98.89°C (210°F)], the average temperature of gas in this region is 93.33°C (200°F). Using the temperature adjustment of 24.94°C (44.90°F) for this region, the adjusted average temperature in the third region is 118.28°C (244.90°F). Averaging these three temperatures, an average adjusted gas temperature of 123.85°C (254.93°F) is determined for the containment vessel.

As shown in Appendix 3.6.5, the maximum adjusted average gas temperature and pressure in the containment vessel during accident conditions was calculated to be 123.85°C (254.93°F), and 280.63 kPa (40.701 psia), respectively.

The maximum adjusted temperature on the surface of the containment vessel, adjacent to the O-rings, was 141.22°C (286.20°F). This is well within the design range for the packaging. The full body helium leak test on all test units following thermal testing meets the "leaktight" criteria in accordance with ANSI N14.5-1997. Visual inspection following testing and unloading indicated that no distortion or damage occurred in the containment vessel wall, sealing lid, closure nut, O-rings, or sealing surfaces. No water was visible inside the containment vessel following the 0.9-m (3-ft) water immersion test or the 15-m (50-ft) water immersion test on Test Unit-6.

The ES-3100 package satisfies the requirements of 10 CFR 71.73 for transport of the 35.2-kg (77.60-lb) arrangements shown in Table 2.8. Section 2.7 has additional details to support this conclusion.

3.5.4 Accident Conditions for Fissile Material Packages for Air Transport

The expanded fire test conditions specified in 10 CFR 71.55(f)(1)(iv) for fissile material package designs for air transportation was not conducted. The issue of subcriticality is addressed in Section 6 with content mass limits as addressed in Section 1 for air transport.

3.6 APPENDICES

Appendix	Description
3.6.1	THERMAL EVALUATION OF THE ES-3100 SHIPPING CONTAINER FOR NCT AND HAC (CONCEPTUAL DESIGN WITH BOROBOND4 NEUTRON ABSORBER)
3.6.2	THERMAL EVALUATION OF THE ES-3100 SHIPPING CONTAINER FOR NCT AND HAC (FINAL DESIGN WITH CATALOG 277-4 NEUTRON ABSORBER)
3.6.3	THERMAL STRESS EVALUATION OF THE ES-3100 SHIPPING CONTAINER DRUM BODY ASSEMBLY FOR NCT (FINAL DESIGN WITH CATALOG 277-4 NEUTRON ABSORBER)
3.6.4	CONTAINMENT VESSEL PRESSURE DUE TO NORMAL CONDITIONS OF TRANSPORT FOR THE PROPOSED CONTENTS
3.6.5	CONTAINMENT VESSEL PRESSURE DUE TO HYPOTHETICAL ACCIDENT CONDITIONS FOR THE PROPOSED CONTENTS
3.6.6	SILICONE RUBBER THERMAL PROPERTIES FROM THERM 1.2 DATABASE
3.6.7	ESTIMATES OF HYDROGEN BUILDUP IN THE ES-3100 PACKAGE CONTAINING HIGHLY ENRICHED URANIUM

Appendix 3.6.4

CONTAINMENT VESSEL PRESSURE DUE TO NORMAL CONDITIONS OF TRANSPORT FOR THE PROPOSED CONTENTS

Prepared by: M. L. Goins
B&W Y-12
December 2007

Reviewed by: Paul Bales
B&W Y-12
January 2008

Revised by: Mark Stansberry
B&W Y-12
February 2009

Reviewed by: Drew Winder
B&W Y-12
February 2009

Appendix 3.6.4

CONTAINMENT VESSEL PRESSURE DUE TO NORMAL CONDITIONS OF TRANSPORT FOR THE PROPOSED CONTENTS

The following calculations determine the pressure of the containment vessel when subjected to the tests and conditions of Normal Condition of Transport per 10 CFR 71.71 for the most restrictive convenience can arrangements shipped in the ES-3100. The following packaging arrangements are evaluated for shipment:

1. one shipment will contain six cans with external dimensions of 4.25-in. diameter by 4.875-in. high;
2. one shipment will contain five cans with external dimensions of 4.25-in. diameter by 4.875-in. high and three can spacers, top can will be empty;
3. one shipment will contain three cans with external dimension of 4.25-in. diameter by 8.75-in. high and two can spacers;
4. one shipment will contain three cans with external dimension of 4.25-in. diameter by 10-in. high; and
5. one shipment will contain six cans with external dimension of 3.00-in. diameter by 4.75-in. high;
6. one shipment will contain three polyethylene bottles with external dimensions of 4.94-in. diameter by 8.7-in. high;
7. one shipment will contain three Teflon FEP bottles with external dimensions of 4.69-in. diameter by 9.4-in. high;
8. one shipment will contain a brazed assembly of two cans with final external dimensions of 4.25 in. diameter by 17.50 in. high. An empty can with external dimensions of 4.25 in. diameter by 8.75 in. high will be placed on top of the 17.50 in. high can;
9. one shipment will contain fuel rods, or tubes, or plates greater than 17.00 in. in length. These items are bundled together and protected on both ends with an open-ended can with external dimensions of ≤5.0 in. diameter by ≤ 8.75 in. high. Total assembly height will be ≤30.5 in. If space is available inside the containment vessel, stainless-steel metal scrubbers will be added on the bottom and top of this assembly or an empty convenience can will be placed on top of the assembly; and
10. one shipment will contain three cans brazed together with external dimensions of 4.25-in. diameter by ~30 in. high.

To determine this pressure, the following assumptions have been made:

1. The HEU contents are loaded into convenience cans which are placed inside the ES-3100 containment vessel at standard temperature (T_{amb}) and pressure (P_t) [25°C (77°F) and 101.35 kPa (14.7 psia)] with air at a maximum relative humidity of 100%.
2. The convenience cans are assumed to not be sealed~~, which minimizes the void volume inside the containment vessel~~.
3. Polyethylene bagging of contents and/or convenience cans is limited to 500 g per containment vessel shipping arrangement.
4. If metal convenience cans are used, the total amount of polyethylene bagging and lifting slings is limited to 500 g per containment vessel shipping arrangement.

5. The mass of offgassing material (polyethylene bagging or bottles, Teflon bottles, silicone pads, lifting slings) is assumed to be 1490 g for the offgassing evaluation of containment vessel arrangement #7 and 500 g for containment vessel arrangement #6.

The offgassing material limits identified in assumptions 4 and 5 have been established based on the needs of shippers. All configurations are limited to 500 g of polyethylene in the form of bags, slings, and/or bottles. When the requirement to ship material in Teflon bottles arose, the upper limit of 1490 g of offgassing material was established. This limit is a combination of three Teflon bottles (330 g per bottle) and the original 500 g allowance for polyethylene material. These offgassing material limits have been used in calculations pertaining to containment vessel pressure, radioactive material leakage criteria, and criticality control. Therefore, portion of the safety basis of this shipping package has been based on these material limits.

Applying Dalton's law concerning a mixture of gases, the properties of each component are considered as though each component exists separately at the volume and temperature of the mixture. Therefore, the molar quantities of each constituent inside the containment vessel (i.e., dry air, water vapor, polyethylene bagging, and silicone rubber) must be calculated individually.

To calculate these molar properties, the void volume of the containment vessel must be determined. The volume inside an empty ES-3100 containment vessel was determined from Algor finite element software to be 637.18 in.^{3} (10,441.51 cm^3).

I. Molar quantity determination for dry air and water vapor

According to *Fundamentals of Classical Thermodynamics*,

"Relative humidity (Φ) is defined as the ratio of the mole fraction in the mixture to the mole fraction of vapor in a saturated mixture at the same temperature and total pressure."

Since the vapor is considered an ideal gas, the definition reduces to the ratio of the partial pressure of the vapor (P_v) as it exists in the mixture to the saturation pressure of the vapor (P_g) at the same temperature.

Therefore,

$$\Phi = P_v / P_g .$$

From the above equation and interpolating the values given in Table A.1.1 of *Fundamentals of Classical Thermodynamics*, the partial pressure of the water vapor at saturation is:

$$P_v = 1.0\ (0.464)\ \text{psia},$$
$$P_v = 0.464\ \text{psia}.$$

The partial pressure of the dry air (P_a) in the volume:

$$P_a = P_t - P_v$$
$$= 14.7 - 0.464$$
$$= 14.236\ \text{psia}.$$

From the ideal gas law, the number of water vapor moles and dry air moles in the void volume (V_V) for each containment vessel arrangement (CVA) is calculated as follows:

$$n_v = \frac{P_v \cdot V_v}{R_u \cdot T_{amb} \cdot 12}, \quad n_a = \frac{P_a \cdot V_v}{R_u \cdot T_{amb} \cdot 12}$$

To determine the number of moles, the void volume of the air mixture must be determined. The void volume (V_V) in the containment vessel for each CVA is calculated as follows:

$$V_V = V_{ECV} - V_{SP} - V_{PB} - V_{SCC} - V_{CS} - V_{CH},$$

where

V_{ECV} = volume inside an empty containment vessel,
V_{SP} = silicone pad volume,
V_{PB} = polyethylene bagging or lifting sling volume,
V_{SCC} = structural volume of the convenience cans or bottles,
V_{CS} = external volume of the can spacers,
V_{CH} = external volume of the convenience can handles.

A summary for each CVA is shown in Table 1.

Table 1. Containment vessel void volume for each CVA

CVA		V_{ECV} (in.^{3})	V_{SP} [a] (in.^{3})	V_{PB} (in.^{3})	V_{SCC} (in.^{3})	V_{CS} (in.^{3})	V_{CH} (in.^{3})	V_V (in.^{3})
1	Six 4.875-in.-high cans Seven silicone pads Six can handles	637.18	9.35	30.51	7.84	0.00	1.02	588.46
2	Five 4.875-high cans Nine silicone pads Three Cat 277-4 spacers Eight can handles	637.18	12.03	30.51	6.47	60.60	1.36	526.21
3	Three 8.75-in.- high cans Two Cat 277-4 spacers Six silicone pads Five can handles	637.18	8.02	30.51	5.14	40.40	0.85	552.26
4	Three 10-in.-high cans Four silicone pads Three can handles	637.18	5.35	30.51	5.56	0.00	0.51	595.26
5	Six 4.75 in.-high nickel cans	637.18	0.00	30.51	12.64	0.00	1.02	593.01
6	Three 4.94 in. OD polyethylene bottles	637.18	0.00	9.46	21.05	0.00	0.00	606.67
7	Three 4.69 in. OD Teflon FEP bottles	637.18	0.00	30.51	27.95	0.00	0.00	578.72
8	One 17.5-in.-high can loaded One 8.75-in.-high can empty Three silicone pads Two can handles	This configuration is bounded by CVA #3						
9	Two open-ended cans One empty convenience can with height ≤ 8.75-in. Three silicone pads Two can handles	This configuration is bounded by CVA #4 [b]						
10	Three 10 in. cans brazed together Two silicone pads One can handle	This configuration is bounded by CVA #4						

[a] This assumes that the internal convenience cans, polyethylene or Teflon FEP bottles, and Cat 277-4 spacer cans are not sealed.

[b] Although CVA #9 may slightly exceed the height of the combined three 25.4 cm (10 in.) can height (CVA #4), the open-ended cans and contents produce a larger void volume and thereby lower overall pressure inside the containment vessel.

The bounding case based on the volumes listed in Table 1 is CVA 2 at 526.21 in.^{3}. To determine the minimum volume for this configuration, the mass limit of 15.13 kg of oxides is used in conjunction with the lowest density oxide of 7.3 kg/L (UO_3). The resulting volume is 15.13 kg / 7.3 kg/L × 1 ft^3 / 28.32 L × 1728 in.^{3} / ft^3 = 126.464 in.^{3}. Therefore, the bounding volume for CVA 2 is 526.21 in.^{3} - 126.464 in.^{3} = 399.746 in.^{3}.

Only CVA 7 can accommodate the uranyl nitrate crystals held in the Teflon bottles. CVA 7 is limited to 9.12 kg of the uranyl nitrate hexahydrate crystals and 11.9 kg of uranyl nitrate trihydrate crystals (see Appendix 3.6.7). For the bounding pressure calculation, the smallest resulting free volume in CVA 7 is then 578.72 - 11.9 kg / 2.81 kg/L × 1 ft^3 / 28.32 L × 1728 in.^{3} / ft^3 = 578.72 in.^{3} - 258.4 in.^{3} = 320.32 in.^{3}.

Using the above molar equations and bounding volumes, the number of moles for water vapor and dry air in the vessel for CVAs 2 and 7 are summarized in Table 2.

Table 2. Water vapor and dry air molar summary for each CVA

CVA	P_a (psia)	P_v (psia)	V_V (in.^{3})	R_u (ft-lb/lb-mole·R)	T_{amb} (R)	n_v (lb-mole)	n_a (lb-mole)
~~1~~	~~14.236~~	~~0.464~~	~~215.83~~	~~1545.32~~	~~537~~	~~1.0057E-05~~	~~3.0855E-04~~
2	14.236	0.464	399.75	1545.32	537	1.0868E-05	5.7148E-04
~~3 or 8~~	~~14.236~~	~~0.464~~	~~211.44~~	~~1545.32~~	~~537~~	~~9.8522E-06~~	~~3.0227E-04~~
~~4, 9, or 10~~	~~14.236~~	~~0.464~~	~~204.62~~	~~1545.32~~	~~537~~	~~9.5344E-06~~	~~2.9252E-04~~
~~5~~	~~14.236~~	~~0.464~~	~~411.27~~	~~1545.32~~	~~537~~	~~1.9163E-05~~	~~5.8795E-04~~
~~6~~	~~14.236~~	~~0.464~~	~~141.34~~	~~1545.32~~	~~537~~	~~6.5858E-06~~	~~2.0206E-04~~
7	14.236	0.464	320.32	1545.32	537	1.4926E-05	4.5793E-04

II. Molar quantity determination due to offgassing for each containment vessel arrangement

The maximum temperature calculated for the containment vessel is 87.81°C (190.06°F). This temperature is assumed to be constant throughout the containment vessel and contents. Therefore, the polyethylene bags, polyethylene bottles, Teflon FEP bottles, and silicone rubber can pads are assumed to be at this temperature.

Using the above calculated results and the specific gas generation of polyethylene bags and silicone rubber pad measurements at temperatures up to 170°C (338°F) conducted by the Y-12 Development Division, the amount of gas (V_{bo} and V_{po}) generated due to offgassing of the polyethylene bags and bottles, and silicone rubber can pads at any temperature is estimated by first determining the offgassing volume per unit mass at temperature and multiplying that by the total mass of the bags and can supports inside the containment vessel. Based on testing at a temperature of 93.33°C (200°F), no recordable offgassing occurred in the polyethylene bags and bottles, or silicone rubber pad material as documented in Y/DZ-2585, Rev. 2 (Appendix 2.10.4). The data showed that the Teflon FEP material offgassing volume per unit mass (V_{tf}) was conservatively assumed to be 0.25 cm^3/g@STP (Appendix 2.10.9). These values are used to determine the offgassing volumes as shown below:

V_{po} = $W_p \times 0.0 / 16.387$ (in.^{3}) (offgassing volume of silicone rubber pads)

V_{bo} = $W_b \times 0.0 / 16.387$ (in.^{3}) (offgassing volume of polyethylene bags and bottles or lifting sling)

V_{tf} = $W_{tf} \times 0.25 / 16.387$ (in.^{3}) (offgassing volume of Teflon bottles)

From the ideal gas law, the number of gas moles in the volume at standard temperature and pressure is as follows:

$$n_{io} = \frac{P_v \cdot V_i}{R_u \cdot T_{amb} \cdot 12}$$

A summary of the results obtained using the above equations for the bounding containment vessel arrangement is presented in Tables 3, 4, and 5.

Table 3. Molar quantity of gas generated due to the silicone rubber pad offgassing

CVA	W_p (g)	V_{po} ($in.^3$)	P_V (psia)	R_u (ft-lb/lb-mole·R)	T_{amb} (R)	n_{po} (lb-mole)
~~1~~	~~186.74~~	~~0.00~~	~~14.7~~	~~1545.32~~	~~537~~	~~0.0000E+00~~
2	240.09	0.00	14.7	1545.32	537	0.0000E+00
~~3 or 8~~	~~160.06~~	~~0.00~~	~~14.7~~	~~1545.32~~	~~537~~	~~0.0000E+00~~
~~4, 9, or 10~~	~~106.71~~	~~0.00~~	~~14.7~~	~~1545.32~~	~~537~~	~~0.0000E+00~~
~~5~~	~~0.00~~	~~0.00~~	~~14.7~~	~~1545.32~~	~~537~~	~~0.0000E+00~~
~~6~~	~~0.00~~	~~0.00~~	~~14.7~~	~~1545.32~~	~~537~~	~~0.0000E+00~~
7	0.00	0.00	14.7	1545.32	537	0.0000E+00

Table 4. Molar quantity of gas generated due to the polyethylene bag, sling and bottle offgassing

CVA	W_b (g)	V_{bo} ($in.^3$)	P_V (psia)	R_u (ft-lb/lb-mole·R)	T_{amb} (R)	n_{bo} (lb-mole)
~~1~~	~~500.00~~	~~0.00~~	~~14.7~~	~~1545.32~~	~~537~~	~~0.0000E+00~~
2	500.00	0.00	14.7	1545.32	537	0.0000E+00
~~3 or 8~~	~~500.00~~	~~0.00~~	~~14.7~~	~~1545.32~~	~~537~~	~~0.0000E+00~~
~~4, 9, or 10~~	~~500.00~~	~~0.00~~	~~14.7~~	~~1545.32~~	~~537~~	~~0.0000E+00~~
~~5~~	~~500.00~~	~~0.00~~	~~14.7~~	~~1545.32~~	~~537~~	~~0.0000E+00~~
~~6~~	~~845.00~~	~~0.00~~	~~14.7~~	~~1545.32~~	~~537~~	~~0.0000E+00~~
7	500.00	0.00	14.7	1545.32	537	0.0000E+00

Table 5. Molar quantity of gas generated due to the Teflon bottle offgassing

CVA	W_{tf} (g)	V_{tf} ($in.^3$)	P_V (psia)	R_u (ft-lb/lb-mole·R)	T_{amb} (R)	n_{tf} (lb-mole)
7	990.00	15.10	14.7	1545.32	537	2.2296E-05

III. Gas generation due to radiolysis of water

Buildup of hydrogen gas (H_2) and Oxygen Gas (O_2) in the ES-3100 containment vessel due to radiolysis is incorporated into the pressure calculation by assuming that 5 mol % of the free volume is hydrogen gas. Since each mole of H_2 generated is accompanied by 0.5 mole of O_2, the concentration of H_2 will reach 5 mol % when volume of H_2 is 0.05405 times the initial void volume (see Sect. 3.6.7.8 of Appendix 3.6.7). Using the ideal gas law, the number of gas moles of hydrogen in the volume at standard temperature and pressure is:

$$n_r = \frac{P_v \cdot V_r}{R_u \cdot T_{amb}\, 12}$$

where

n_r = individual molar quantity for hydrogen and oxygen gas;
V_r = volume of gas assumed generated by radiolysis.

A summary of the results for hydrogen and oxygen generation due to radiolysis using the above equation is presented in Table 6.

Table 6. Molar quantity of oxygen and hydrogen gqas generation due to radiolysis

CVA	V_v (in.^{3})	V_h (in.^{3})	P_v (psia)	R_u (ft-lb/lb-mole · R)	T_{amb} (R)	n_{r-H2} (lb-mole)	n_{r-O2} (lb-mole)
2	399.75	21.61	14.7	1545.32	537.0	3.1895E-5	1.5948E-5
7	320.32	17.31	14.7	1545.32	537.0	2.5558E-5	1.2779E-5

IV. Total pressure due to offgassing and NCT temperatures inside the containment vessel

The total pressure of the mixture at 87.81 °C (190.06 °F), P_T, for the bounding containment vessel arrangement is the sum of each of the previously calculated molar quantities. Table 7 summarizes the molar constituents and total pressure of each bounding containment vessel arrangement. The following equation is used to calculated the final containment vessel pressure:

$$P_{87.81°C} = (\sum n_i \cdot R \cdot T \cdot 12) / V_{GMV},$$

where

n_i = individual molar quantity for each gas,
T = average gas temperature = 87.81 °C (190.06 °F),
V_{GMV} = V_v = gas mixture volume.

Table 7. Total pressure inside the containment vessel at 87.81°C (190.06°F) [a]

CVA	n_a [b] (lb-mole)	n_v [b] (lb-mole)	n_{po} [b] (lb-mole)	n_{bo} [b] (lb-mole)	n_{tf} [b] (lb-mole)	n_{H2} [b] (lb-mole)	n_{O2} [b] (lb-mole)	n_T [b] (lb-mole)	P_T (psia)
~~1~~	~~3.0855E-04~~	~~1.0057E-05~~	~~0.0000E+00~~	~~0.0000E+00~~	~~0.0000E+00~~			~~3.1861E-04~~	~~17.786~~
2	5.7148E-04	1.8626E-05	0.0000E+00	0.0000E+00	0.0000E+00	3.1895E-05	1.5948E-05	6.3795E-04	19.238
~~3 or 8~~	~~3.0227E-04~~	~~9.8522E-06~~	~~0.0000E+00~~	~~0.0000E+00~~	~~0.0000E+00~~			~~3.1212E-04~~	~~17.786~~
~~4, 9, or 10~~ [b]	~~2.9252E-04~~	~~9.5344E-06~~	~~0.0000E+00~~	~~0.0000E+00~~	~~0.0000E+00~~			~~3.0205E-04~~	~~17.786~~
~~5~~	~~1.9163E-05~~	~~5.8795E-04~~	~~0.0000E+00~~	~~0.0000E+00~~	~~0.0000E+00~~			~~6.0711E-04~~	~~17.786~~
~~6~~	~~2.0206E-04~~	~~6.5858E-06~~	~~0.0000E+00~~	~~0.0000E+00~~	~~0.0000E+00~~			~~2.0865E-04~~	~~17.786~~
7	4.5793E-04	1.4926E-05	0.0000E+00	0.0000E+00	2.2296E-05	2.5558E-05	1.2779E-05	5.3349E-04	20.077

[a] This assumes that the internal convenience cans, polyethylene or Teflon FEP bottles, and Cat 277-4 spacer cans are not sealed.

[b] ~~Although CVA #9 may slightly exceed the height of the combined three 25.4 cm (10 in.) can height (CVA #4), the open-ended cans and contents produce a larger void volume and thereby lower overall pressure inside the containment vessel.~~

[b] n_a molar quantity of dry air in the gas mixture;
n_v molar quantity of water vapor in the gas mixture;
n_{po} molar quantity of gas due to offgassing of the silicone rubber pads;
n_{bo} molar quantity of gas due to offgassing of the polyethylene bags, bottles, and lifting sling;
n_{tf} molar quantity of gas due to offgassing of the Teflon bottles;
n_{H2} molar quantity of hydrogen gas due to radiolysis of water;
n_{O2} molar quantity of oxygen gas due to radiolysis of water; and
n_T total molar quantity in the gas mixture.

At −40°C (−40°F), the partial pressure of the water vapor is conservatively assumed to be zero. Therefore, the final pressure of the mixture at −40°C (−40°F) is calculated according to the ideal gas law based solely on the partial pressure of the air.

$$\frac{P_1 V_1}{T_1} = \frac{P_2 V_2}{T_2},$$

where

P_1 = 14.236 psi,
T_1 = 77°F = 536.67 R,
T_2 = −40°F = 419.67 R,
V_1 = V_2.

Rearranging and solving for P_2,

P_2 = $P_1 (T_2/T_1)$,
P_2 = (14.236)(419.67/536.67) = 11.13 psia.

Appendix 3.6.5

CONTAINMENT VESSEL PRESSURE DUE TO HYPOTHETICAL ACCIDENT CONDITIONS FOR THE PROPOSED CONTENTS

Prepared by: M. L. Goins
B&W Y-12
December 2007

Reviewed by: Paul Bales
B&W Y-12
January 2008

Revised by: Mark Stansberry
B&W Y-12
February 2009

Reviewed by: Drew Winder
B&W Y-12
February 2009

Appendix 3.6.5

CONTAINMENT VESSEL PRESSURE DUE TO HYPOTHETICAL ACCIDENT CONDITIONS FOR THE PROPOSED CONTENTS

The following calculations determine the pressure of the containment vessel when subjected to the tests and conditions of Hypothetical Accident Conditions per 10 CFR 71.73 for the most restrictive convenience can arrangements shipped in the ES-3100 package. The following packaging arrangements are evaluated for shipment:

1. one shipment will contain six cans with external dimensions of 4.25-in. diam by 4.875-in. high;

2. one shipment will contain five cans with external dimensions of 4.25-in. diam by 4.875-in. high and three can spacers, the top can is empty;

3. one shipment will contain three cans with external dimensions of 4.25-in. diam by 8.75-in. high and 2 can spacers;

4. one shipment will contain three cans with external dimensions of 4.25-in. diam by 10-in. high;

5. one shipment will contain six nickel cans with external dimensions of 3.00-in. diam by 4.75-in. high;

6. one shipment will contain three polyethylene bottles with external dimensions of 4.94-in. diam by 8.7-in. high;

7. one shipment will contain three Teflon FEP bottles with external dimensions of 4.69-in. diam by 9.4-in. high;

8. one shipment will contain a brazed assembly of two cans with final external dimensions of 4.25 in. diameter by 17.50 in. high. An empty can with external dimensions of 4.25 in. diameter by 8.75 in. high will be placed on top of the 17.50 in. high can;

9. one shipment will contain fuel rods, or tubes, or plates greater than 17.00 in. in length. These items are bundled together and protected on both ends with an open-ended can with external dimensions of ≤5.0 in. diameter by ≤8.75 in. high. Total assembly height will be ≤30.5 in. If space is available inside the containment vessel, stainless-steel metal scrubbers will be added on the bottom and top of this assembly or an empty convenience can will be placed on top of this assembly; and

10. one shipment will contain three cans brazed together with external dimensions of 4.25-in. diameter by ~30 in. high.

To determine this pressure, the following assumptions have been made:

1. The highly enriched uranium (HEU) contents are loaded into convenience cans and placed inside the ES-3100 containment vessel at standard temperature [25°C (77°F)] and at the maximum normal operating pressure (see Table 5 of Appendix 3.6.4) with air at a maximum relative humidity of 100%.

2. The convenience cans are assumed to not be sealed ~~to minimize the void volume inside the containment vessel~~.

3. Polyethylene bagging of contents and/or convenience containers is limited to 500 g per containment vessel shipping arrangement.

4. If metal convenience cans are used, the total amount of polyethylene bagging and lifting slings is limited to 500 g per containment vessel shipping arrangement.

5. The mass of offgassing material (polyethylene bagging or bottles, Teflon bottles, silicone pads, lifting slings) is assumed to be 1490 g for the offgassing evaluation of containment vessel arrangement #7 and 500 g for containment vessel arrangement #6.

The offgassing material limits identified in assumptions 4 and 5 have been established based on the needs of shippers. All configurations are limited to 500 g of polyethylene in the form of bags, slings, and/or bottles. When the requirements to ship material in Teflon bottles arose, the upper limit of 1490 g of offgassing material was established. This limit is a combination of three Teflon bottles (990 g) and the original 500 g allowance for polyethylene material. These offgassing material limits have been used in calculations pertaining to containment vessel pressure, radioactive material leakage criteria, and criticality control. Therefore, portion of the safety basis of this shipping package has been based on these material limits.

Applying Dalton's law concerning a mixture of gases, the properties of each component are considered as though each component exists separately at the volume and temperature of the mixture. Therefore, the molar quantities of each constituent inside the containment vessel (i.e., dry air, water vapor, polyethylene bagging and bottles, silicone rubber pads, and teflon bottles) must be calculated individually.

To calculate these molar properties, the void volume of the containment vessel must be determined. The volume inside an empty ES-3100 containment vessel was determined from Algor finite element software to be 637.18 in.^{3} (10,441.51 cm^3).

I. Molar quantity determination based on MNOP

Table 1. Total pressure inside the containment vessel at 87.81°C (190.06°F) [a]

CVA	n_a [b] (lb-mole)	n_v [b] (lb-mole)	n_{po} [b] (lb-mole)	n_{bo} [b] (lb-mole)	n_{tf} [b] (lb-mole)	n_{H2} [b] (lb-mole)	n_{O2} [b] (lb-mole)	n_T [b] (lb-mole)	P_T (psia)
2	5.7148E-04	1.8626E-05	0.0000E+00	0.0000E+00	0.0000E+00	3.1895E-05	1.5948E-05	6.3795E-04	19.238
7	4.5793E-04	1.4926E-05	0.0000E+00	0.0000E+00	2.2296E-05	2.5558E-05	1.2779E-05	5.3349E-04	20.077

[a] This assumes that the internal convenience cans, polyethylene or Teflon FEP bottles, and Cat 277-4 spacer cans are not sealed.

[b] n_a – molar quantity of dry air in the gas mixture;
n_v – molar quantity of water vapor in the gas mixture;
n_{po} – molar quantity of gas due to offgassing of the silicone rubber pads;
n_{bo} – molar quantity of gas due to offgassing of the polyethylene bags, bottles, and lifting sling;
n_{tf} – molar quantity of gas due to offgassing of the Teflon bottles;
n_{H2} – molar quantity of hydrogen gas due to radiolysis of water;
n_{O2} – molar quantity of oxygen gas due to radiolysis of water; and
n_T – total molar quantity in the gas mixture.

To use the maximum normal operating pressure at standard temperature, the number of lb-mole of gas needs to be increased using the following equation:

$$n_{MNOP} = \frac{P_T \cdot V_v}{R_u \cdot T_{amb} \cdot 12}$$

Using the above molar equations, the total number of moles is summarized in Table 2.

Table 2. Molar summary at MNOP and 25°C (77°F)

CVA	P_T (psia)	V_V (in.^{3})	R_u (ft-lb/lb-mole·R)	T_{amb} (R)	n_{MNOP} (lb-mole)
~~1~~	~~17.786~~	~~215.83~~	~~1545.32~~	~~537~~	~~3.8549E-04~~
2	19.238	399.75	1545.32	537	7.7226E-04
~~3 or 8~~	~~17.786~~	~~211.44~~	~~1545.32~~	~~537~~	~~3.7765E-04~~
~~4, 9, or 10~~	~~17.786~~	~~204.62~~	~~1545.32~~	~~537~~	~~3.6547E-04~~
~~5~~	~~17.786~~	~~411.27~~	~~1545.32~~	~~537~~	~~7.3457E-04~~
~~6~~	~~17.786~~	~~141.34~~	~~1545.32~~	~~537~~	~~2.5245E-04~~
7	20.077	320.32	1545.32	537	6.4581E-04

II. Molar quantity determination due to offgassing for each containment vessel arrangement

To determine the maximum pressure inside the containment vessel as a result of thermal testing, the average adjusted gas temperature must be calculated based on the results shown in Sect. 3.5.3. The approach used is to divide the containment vessel volume into three distinct equal regions and then average the three together. The first volume is represented by the gas adjacent to the containment vessel lid and flange region and the top most convenience can. Based on the temperature recorded near the O-rings [116.11°C (241°F)] and the temperature recorded on the external surface of the convenience can [98.89°C (210°F)], the average temperature of the gas in this region is 107.50°C (225.50°F). Using the temperature adjustment of 25.11°C (45.20°F) for this region, the adjusted average temperature in the first region is 132.61°C (270.70°F). The second volume is represented by the gas adjacent to the second convenience can from the top. Based on the temperature recorded on the containment vessel wall and convenience can [92.78°C (199°F)], the average temperature of gas in this region is 92.78°C (199°F). Using the temperature adjustment of 27.89°C (50.20°F) for this region, the adjusted average temperature in the second region is 120.67°C (249.20°F). The third and final volume is represented by the gas adjacent to the bottom convenience can. Again, based on the convenience can temperature [87.78°C (190°F)] and the containment vessel end cap temperature [98.89°C (210°F), the average temperature of gas in this region is 93.33°C (200°F). Using the temperature adjustment of 24.94°C (44.90°F) for this region, the adjusted average temperature in the third region is 118.28°C (244.90°F). Averaging these three temperatures, an average adjusted gas temperature of 123.85°C (254.93°F) is determined for the containment vessel.

Using the above calculated results and the specific gas generation of polyethylene bags and silicone rubber pads measurements at temperatures up to 170°C (338°F) conducted by the Y-12 Development Division (Appendix 2.10.4), the amount of gas generated due to offgassing of the silicone rubber can pads, the polyethylene bags and bottles, and the Teflon FEP bottles at 123.85°C (254.93°F), (V_{po}, V_{bo}, and V_{tf}) is estimated by first determining the offgassing volume per unit mass at temperature and multiplying that by the total mass of the bags, bottles, slings, and silicone rubber can supports inside

the containment vessel. Based on testing at an approximate temperature of 141.11°C (286.00°F), values of ~7.0 and ~0.8 cm3/g @STP for the polyethylene bagging and bottles, and silicone rubber pads, respectively, were taken from the curves for the offgassing volume per unit mass as documented in Y/DZ-2585, Rev. 2 (Appendix 2.10.4). The data showed that the Teflon FEP material offgassing volume per unit mass (V_{tf}) was conservatively assumed to be 0.25 cm^3/g@STP (Appendix 2.10.9). These values are used to determine the offgassing volume as shown below:

$V_{po} = W_p \times 0.8 / 16.387\ (in.^3)$ (offgassing volume of silicone rubber pads)

$V_{bo} = W_b \times 7.0 / 16.387\ (in.^3)$ (offgassing volume of polyethylene bags, bottles, and lifting sling)

$V_{tf} = W_{tf} \times 0.25 / 16.387\ (in.^3)$ (offgassing bottles of Teflon FEP bottles)

From the ideal gas law, the number of gas moles in the volume is as follows:

$$n_i = \frac{P_v \cdot V_i}{R_u \cdot T_{amb} \cdot 12}$$

A summary of the results obtained using the above equations for each containment vessel arrangement is presented in Tables 3, 4, and 5.

Table 3. Molar quantity of gas generated due to the silicone rubber pad offgassing

CVA	W_p (g)	V_{po} ($in.^3$)	P_V (psia)	R_u (ft-lb/lb-mole·R)	T_{amb} (R)	n_{po} (lb-mole)
~~1~~	~~186.74~~	~~9.12~~	~~14.7~~	~~1545.32~~	~~537~~	~~1.3458E-05~~
2	240.09	11.72	14.7	1545.32	537	1.7302E-05
~~3 or 8~~	~~160.06~~	~~7.81~~	~~14.7~~	~~1545.32~~	~~537~~	~~1.1535E-05~~
~~4, 9, or 10~~	~~106.71~~	~~5.21~~	~~14.7~~	~~1545.32~~	~~537~~	~~7.6901E-06~~
~~5~~	~~0.00~~	~~0.00~~	~~14.7~~	~~1545.32~~	~~537~~	~~0.0000E+00~~
~~6~~	~~0.00~~	~~0.00~~	~~14.7~~	~~1545.32~~	~~537~~	~~0.0000E+00~~
7	0.00	0.00	14.7	1545.32	537	0.0000E+00

Table 4. Molar quantity of gas generated due to polyethylene bag, sling, and bottle offgassing

CVA	W_b (g)	V_{bo} ($in.^3$)	P_V (psia)	R_u (ft-lb/lb-mole·R)	T_{amb} (R)	n_{bo} (lb-mole)
~~1~~	~~500.00~~	~~213.58~~	~~14.7~~	~~1545.32~~	~~537~~	~~3.1529E-04~~
2	500.00	213.58	14.7	1545.32	537	3.1529E-04
~~3 or 8~~	~~500.00~~	~~213.58~~	~~14.7~~	~~1545.32~~	~~537~~	~~3.1529E-04~~
~~4, 9, or 10~~	~~500.00~~	~~213.58~~	~~14.7~~	~~1545.32~~	~~537~~	~~3.1529E-04~~
~~5~~	~~500.00~~	~~213.58~~	~~14.7~~	~~1545.32~~	~~537~~	~~3.1529E-04~~
~~6~~	~~845.00~~	~~360.96~~	~~14.7~~	~~1545.32~~	~~537~~	~~5.3284E-04~~
7	500.00	213.58	14.7	1545.32	537	3.1529E-04

Table 5. Molar quantity of gas generated due to the Teflon FEP bottle offgassing

CVA	W_{tf} (g)	V_{tf} ($in.^3$)	P_V (psia)	R_u (ft-lb/lb-mole·R)	T_{amb} (R)	n_{tf} (lb-mole)
7	990.00	15.10	14.7	1545.32	537	2.2296E-05

III. Total pressure due to offgassing and HAC temperatures inside the containment vessel

The total pressure of the mixture at 123.85°C (254.93°F), P_T, for each containment vessel arrangement is the sum of each of the previously calculated molar quantities. Table 6 summarizes the molar constituents and total pressure of each containment vessel arrangement. The following equation is used to calculated the final containment vessel pressure:

$$P_{123.85°C} = (\sum n_i \cdot R \cdot T \cdot 12) / V_{GMV} ,$$

where

n_i = individual molar quantity for each gas,
T = average gas temperature = 123.85°C (254.93°F),
V_{GMV} = V_v = gas mixture volume.

Table 6. Total pressure inside the containment vessel at 123.85°C (254.93°F) [a]

CVA	n_{MNOP} [b] (lb-mole)	n_{po} [b] (lb-mole)	n_{bo} [b] (lb-mole)	n_{tf} [b] (lb-mole)	n_T [b] (lb-mole)	P_T (psia)
~~1~~	~~3.8549E-04~~	~~1.3458E-05~~	~~3.1529E-04~~	~~0.0000E+00~~	~~7.1424E-04~~	~~43.852~~
2	7.7226E-04	1.7303E-05	3.1529E-04	0.0000E+00	1.1049E-03	36.642
~~3 or 8~~	~~3.7765E-04~~	~~1.1535E-05~~	~~3.1529E-04~~	~~0.0000E+00~~	~~7.0448E-04~~	~~44.151~~
~~4, 9, or 10~~[b]	~~3.6547E-04~~	~~7.6901E-06~~	~~3.1529E-04~~	~~0.0000E+00~~	~~6.8845E-04~~	~~44.585~~
~~5~~	~~7.3457E-04~~	~~0.0000E+00~~	~~3.1529E-04~~	~~0.0000E+00~~	~~1.0499E-03~~	~~33.829~~
~~6~~	~~2.5245E-04~~	~~0.0000E+00~~	~~5.3284E-04~~	~~0.0000E+00~~	~~7.8529E-04~~	~~73.625~~
7	6.4581E-04	0.0000E+00	3.1529E-04	2.2296E-05	9.8340E-04	40.701

[a] This assumes that the internal convenience cans, polyethylene or Teflon FEP bottles, and Cat 277-4 spacer cans are not sealed.

~~[b] Although CVA #9 may slightly exceed the height of the combined three 25.4 cm (10 in.) can height (CVA #4), the open-ended cans and contents produce a larger void volume and thereby lower overall pressure inside the containment vessel.~~

[b] n_{MNOP} molar quantity of the gas mixture at maximum normal operating pressure at standard temperature [25°C (77°F)];
n_{po} molar quantity of gas due to offgassing of the silicone rubber pads;
n_{bo} molar quantity of gas due to offgassing of the polyethylene bags, bottles, and lifting sling;
n_{tf} molar quantity of gas due to offgassing of the Teflon bottles;
n_T total molar quantity in the gas mixture.

Appendix 3.6.7

ESTIMATES OF HYDROGEN BUILDUP IN THE ES-3100 PACKAGE CONTAINING HIGHLY ENRICHED URANIUM

3.6.7.1 Summary

Table 3.6.7.1 below indicates that the ES-3100 package with a containment vessel arrangement (CVA) 2 (see Appendix 3.6.4) can accommodate a 15.13-kg load of uranium oxide with 3 wt % water if the time allowed to generate 5 mol % of hydrogen is assumed to be 1.20 years (14.4 months). For the same time period, with CVA 7, the ES-3100 can accommodate 4.75 kg of uranyl nitrate hexahydrate crystals (X=6, 21.6 wt % water) or 6.70 kg of uranyl nitrate trihydrate crystals (X=3, 12.1 wt % water). If the time allowed is assumed to be 0.5015 years (6.02 months), the ES-3100 can accommodate 9.12 kg of UN6 and 11.90 kg of UN3 crystals. For additional margin of safety (20%), the ES-3100 loading conditions will specify a hydrogen build-up time limit of 5 months and 12 months for these two UNX cases, instead of 6.02 and 14.4 months as analyzed, respectively.

Calculations of permeation and diffusion from closed convenience containers (bottles and cans) indicate that the steady-state concentration of hydrogen can be as high as 0.2 mol % when all conservative assumptions are used. These results do not take into account the leakage of hydrogen that will be experienced through the closed lid of these containers, which would result in a steady-state concentration lower than 0.2 mol %.

The calculated 0.2 mol % hydrogen initial steady-state concentration is accounted for in the mass loading allowables given in Table 3.6.7.1. As indicated, the time to reach 5 mol % hydrogen in the ES-3100 containment vessel (including the initial condition of 0.2 mol %) is 20% greater than the time allowed for shipping these materials (Sect. 1.2.3.8, condition 9). With this safety factor in place, and with other conservative assumptions, it will not be necessary to vent containers before loading into the ES-3100. The time limit for the shipment (5 or 12 months, as appropriate) begins when the containment vessel is sealed.

Table 3.6.7.1. Summary of allowable weights

Weight (kg)	Water		Time to reach 5 mol % hydrogen	
	X	wt %	Years	Months
Oxides (U_3O_8, UO_2, UO_3) [CVA 2][a]				
15.13		3.0	1.20	14.4
$UO_2(NO_3)_2 \times XH_2O$ [CVA 7][b]				
4.75	6	21.6	1.20	14.4
6.70	3	12.1	1.20	14.4
9.12	6	21.6	0.5015	6.02
11.90	3	12.1	0.5015	6.02

[a] CVA 2 consists of five cans of which one is empty (see Sect. 3.1.4.1).
[b] CVA 7 consists of three Teflon bottles (see Sect. 3.1.4.1).

3.6.7.2 Introduction

There is a concern about the possible buildup of hydrogen gas (H_2) in the ES-3100 package, and it is necessary to show that the H_2 concentration in the package will not exceed 5 mol % in one year (established as a limit for the purposes of this analysis). The allowable materials include uranium oxide (UO_3, U_3O_8, and UO_2) and uranyl nitrate crystals [UNX or $UO_2(NO_3)_2 \cdot XH_2O$]. The water in UNX

ranges from X=0 to X=6 (0 to 21.6 wt %) {molecular weights of uranyl nitrate [$UO_2(NO_3)_2$] and H_2O are 391 and 18, respectively, and $6 \times 18 / [391 + 6 \times 18] = 0.216$}. The water associated with oxides ranges from 0 to 3 wt % (Sect. 1.2.3). There is no liquid water (sorbed or interstitial) associated with other authorized contents. The air in the void spaces of the package contains water vapor (humidity). H_2 can be generated from water by radiolysis and/or chemical reaction. Radiolysis applies to any chemical form of HEU, but only the metal can have a chemical reaction with water. Radiolysis can also generate H_2 from other materials containing hydrogen (e.g., polyethylene bags). However, radiolysis of water is the major source of H_2 for uranium oxides and uranyl nitrate crystals.

3.6.7.3 Hydrogen Generation by Chemical Reaction with Water

HEU metal can combine with the oxygen in water to release H_2. The only source of water for HEU metal is the humidity of the air initially in the void spaces of the package. The air is assumed to be at 25°C, 1 atm (101.3 kPa) and 100% relative humidity. The vapor pressure of water at 25°C is 3.1690 kPa (CRC Handbook, p. 6-8), so the initial concentration of water vapor is $3.1690 / 101.3 = 0.031$ mole fraction. Since 1 mole of water vapor produces 1 mole of H_2 and the oxygen is bound up as solid uranium oxide, this reaction does not change the total gas pressure. Therefore, if all the water vapor reacts with the metal, the maximum concentration of H_2 is also 0.031 mole fraction, which is below the 5 mol % limit.

3.6.7.4 Radiation Energy Calculations

The radiation energy that drives radiolysis can be estimated from the decay rate and maximum decay energy of each radionuclide that makes up the HEU. The bounding information to calculate these terms and the results are given in Table 3.6.7.2.

The decay rate per gram of the n^{th} radionuclide is

$D_{Rn} = [\ln(2) / T_{Hn}] \times A_N / MW_n$;
D_{Rn} = the decay rate of the n^{th} radionuclide, atoms/y;
T_{Hn} = half life of the n^{th} radionuclide, y;
A_N = Avogadro's number, 6.022×10^{23} molecules/mol; and
MW_n = the molecular (atomic) weight of the n^{th} radionuclide, g/mol.

Table 3.6.7.2. Radiation energy calculations

Nuclide	wt % [a]	MW [b] (g/mol)	T_H [b] (y)	α [b] (MeV)	D_R [c] [atms/(g y)]	Nuclide contr [c] [MeV/(g y)]
^{232}U	4.00E-06	232.0371	6.89E+01	5.414	2.61E+19	5.65E+12
^{233}U	6.00E-01	233.0396	1.59E+05	4.909	1.13E+16	3.32E+14
^{234}U	2.00E+00	234.0409	2.45E+05	4.856	7.28E+15	7.07E+14
^{235}U	5.49E+01	235.0439	7.04E+08	4.679	2.52E+12	6.48E+12
^{236}U	4.00E+01	236.0456	2.34E+07	4.569	7.56E+13	1.38E+14
^{238}U	0.00E+00	238.0508	4.46E+09	4.185	3.93E+11	0.00E+00
Transuranic	4.00E-03			5.476 [d]	4.73E+17	1.04E+14
^{237}Np	2.50E+00	237.0482	2.14E+06	4.957	8.23E+14	1.02E+14
Total	1.00E+02					1.39E+15

[a] wt % from Appendix 4.6.1 (Table 1). Maximum transuranic is 40 μg/gU and 0.60 MBq/gU activity.
[b] MW is molecular weight; T_H is half life; and α is the maximum energy emitted. (*CRC Handbook of Chemistry and Physics*, D. R. Lide, ed., 79th ed., CRC Press, Boca Raton, Fla., 1998, pp. 11-140 and 11-141)
[c] D_R is decay rate, and Nuclide contr is the contribution of each nuclide to the total rate of decay energy.
[d] Transuranic α assumed to be equal to ^{246}Cm.

All the radionuclides in Table 3.6.7.2 are primarily α emitters, and the total rate of radiation dose is given as

$$D_E = \sum_{n=1}^{N} [wt\%_n \times D_{Rn} \times \alpha_{Mn}] / 100$$

where

D_E = the total rate of decay energy, Mev/(g y);
$wt\%_n$ = the weight percent of the n^{th} radionuclide;
α_{Mn} = the α energy emitted in the decay of the n^{th} radionuclide, MeV; and
N = the total number of radionuclides.

The above calculation of D_E for HEU is 1.39×10^{15} MeV/(g y).

3.6.7.5 Hydrogen Generation by Radiolysis from Polyethylene

Almost all the radiation energy from HEU is due to alpha particles with energies of 4–5 MeV (Table 3.6.7.2). These particles are not very penetrating and will only deposit their energy into materials that are in intimate contact with the uranium atoms (i.e., the water of hydration in uranyl nitrate crystals and the water associated with the oxides). The polyethylene is in the form of bottles and bags that surround the uranium and the only alpha particles that reach the polyethylene come from the outer range of alpha particle penetration within the HEU.

Equation 2 on page 6 in *Evaluation of Radiolysis-Induced Hydrogen Generation in DOT 6M Drums from INTEC* (WSRC-TR-2007-00200) gives the following expression for calculating the range of alpha particle penetration in the HEU (metal, oxide, or crystals).

$$R = 2.3 \times 10^{-6} \times (1.24 \times \alpha_{MA} - 2.62) \times (MW_A)^{1/3} / \rho$$

where

R = the range of alpha particle penetration in the HEU, m;
α_{MA} = the average α energy emitted by the HEU, ~4.9 MeV (Table 3.6.7.2);
MW_A = the average molecular weight of the HEU, ~235.5 g/mol (Table 3.6.7.2); and
ρ = the density of the HEU, g/cm^3.

The range increases with decreasing ρ, and the smallest value for ρ is about 1.5 g/cm^3 {the smallest approximate bulk density of HEU oxide from *Cost-Effectiveness of Utilizing Surplus Depleted Uranium (DU)*, [WM-4009]}. The resulting range is 8.1×10^{-5} m.

The radius of a polyethylene bottle is 0.0627 m [4.94-in. diam (Fig. 1.4), configuration designated as CVA 6]. If the HEU oxide fills the bottle, the alpha particles generated in the outer range come from the HEU between 0.0627 and $(0.0627 - 8.1 \times 10^{-5})$ m. For an infinite cylinder, the fraction of the total radiation within this range is $[(0.0627)^2 - (0.0627 - 8.1 \times 10^{-5})^2] / (0.0627)^2 = 0.00259$. Half of this radiation would be directed toward the center of the cylinder, and much of the outward-directed portion would be absorbed passing through the HEU. Consequently, the radiation absorbed by the polyethylene would be much less than 1% of that absorbed by the water, and the H_2 generated in the polyethylene would be correspondingly less than that generated in the water.

3.6.7.6 Hydrogen Generation by Radiolysis from Water

Assuming an infinite amount of water is available, the radiolytic hydrogen generation rate is given by the following expression (based on NUREG/CR-6673, p. 31, Eq. 4.7):

$$d(n_{H2}) / dt = (D_H / 100) \times [G(H_2) / A_N]$$

where

n_{H2} = the amount of hydrogen generated, mol;
t = time, y;
D_H = the decay energy absorbed by the water, eV/y; and
$G(H_2)$ = a radiolytic hydrogen generation factor for alpha radiation in water, molecules H_2/100 eV absorbed by water.

3.6.7.7 Radiolytic Hydrogen Generation Factors for Alpha Radiation in Water

A bounding value for $G(H_2)$ with alpha radiation is 1.6 molecules H_2/100 eV absorbed by water. (NUREG/CR-6673, p. 12, Table 3.1) However, recent (2003) experimental data from Oak Ridge National Laboratory suggest lower $G(H_2)$ values [*Alpha Radiolysis of Sorbed Water on Uranium Oxides and Uranium Oxyfluorides* (ORNL/TM-2003/172) and *Water Sorption and Radiolysis Studies for Neptunium Oxides* (ORNL/TM-2003/194), included in this appendix]. Table 3.6.7.3 lists the $G(H_2)$ values derived from these experiments. The largest of the ORNL values (1.02) is used for the hydrogen generation calculations.

Table 3.6.7.3. $G(H_2)$ values derived from alpha radiolysis experiments

Sample description					Molecules/100 eV		
	$e^-(H_2O)$	e^-(rem)	f_{H2O}	Gf	G'(gas)[a]	G'(H_2)	G(H_2)
Icenhour and Toth, ORNL/TM-2003/172, 2003							
Fig. 3.3. Samp A-2-2, UO_3, 10% H_2O, 350°C	0.0556	0.3689	0.1000	0.1309	0.1507	0.1005	0.77
Fig. 3.5. Samp A-4-1 U_3O_8, 2% H_2O, 650°C	0.0111	0.4000	0.0200	0.0270	0.0113	0.0075	0.28
Icenhour et. al., ORNL/TM-2003/194, 2004							
Fig. 4.12. Samp Al 3, NpO_2, 8% H_2O, 650°C	0.0444	0.3728	0.0800	0.1065	0.1100	0.0733	0.69
Fig. 4.11. Samp Al 2, NpO_2, 1% H_2O, 650°C	0.0056	0.4012	0.0100	0.0137	0.0210	0.0140	1.02
Fig. 4.13. Samp Al 4, NpO_2, 1% H_2O, 800°C	0.0056	0.4012	0.0100	0.0137	0.0060	0.0040	0.29
Fig. 4.14. Samp Al 5, NpO_2, 0.5% H_2O, 650°C	0.0028	0.4032	0.0050	0.0068	0.0043	0.0029	0.42

[a] G'(gas) for ORNL/TM-2003/172 is based on a measured slope in Fig. 3.3 or 3.5. For ORNL/TM-2003/194, the values are listed on Figs. 4.11–4.14.

The G'(gas) value is the initial slope of the gas yield (mmol/g material) versus the decay energy (MGy) converted to units of molecules of gas per 100 eV. G'(gas) for ORNL/TM-2003/172 is based on a measured slope in Fig. 3.3 or 3.5 while the values for ORNL/TM-2003/194 are listed on Figs. 4.11–4.14. Figure 3.6.7.1 is from ORNL/TM-2003/172 (p. 9, Fig. 3.5) with lines added to outline the initial slope and facilitate reading values. From Fig. 3.6.7.1, the gas yield difference along the slope is 0.023 – (–0.0005) = 0.0235 millimol/g or $0.0235 \times A_N / 1000 = 1.42 \times 10^{19}$ molecules/g. The decay energy difference along the slope is 20.0 MGy or $20.0 \times 6.24 \times 10^{21} = 1.25 \times 10^{23}$ eV (6.24×10^{21} eV/g = 1 MGy). Therefore, G'(gas) is $1.42 \times 10^{19} / (1.25 \times 10^{23}) \times 100 = 0.0113$ molecules gas/100 eV. It is assumed the gas is due to the decomposition of H_2O and has a molar composition of 2/3 H_2 and 1/3 O_2. The derived G'(H_2) is 2/3 of the G'(gas) value or 0.00756 molecules H_2/100 eV decay energy.

The radiation calculated in Table 3.6.7.2 is the decay energy rather than the energy absorbed by the water associated with the material. The energy absorbed by the associated water, D_H, is approximately equal to the decay energy, D_E, multiplied by the fraction of electrons associated with the water or

$$Gf = e(H_2O) / e(mat)$$

where

Gf = the fraction of electrons associated with the water;
$e^-(H_2O)$ = the number of electrons associated with the water, electrons/molecule;

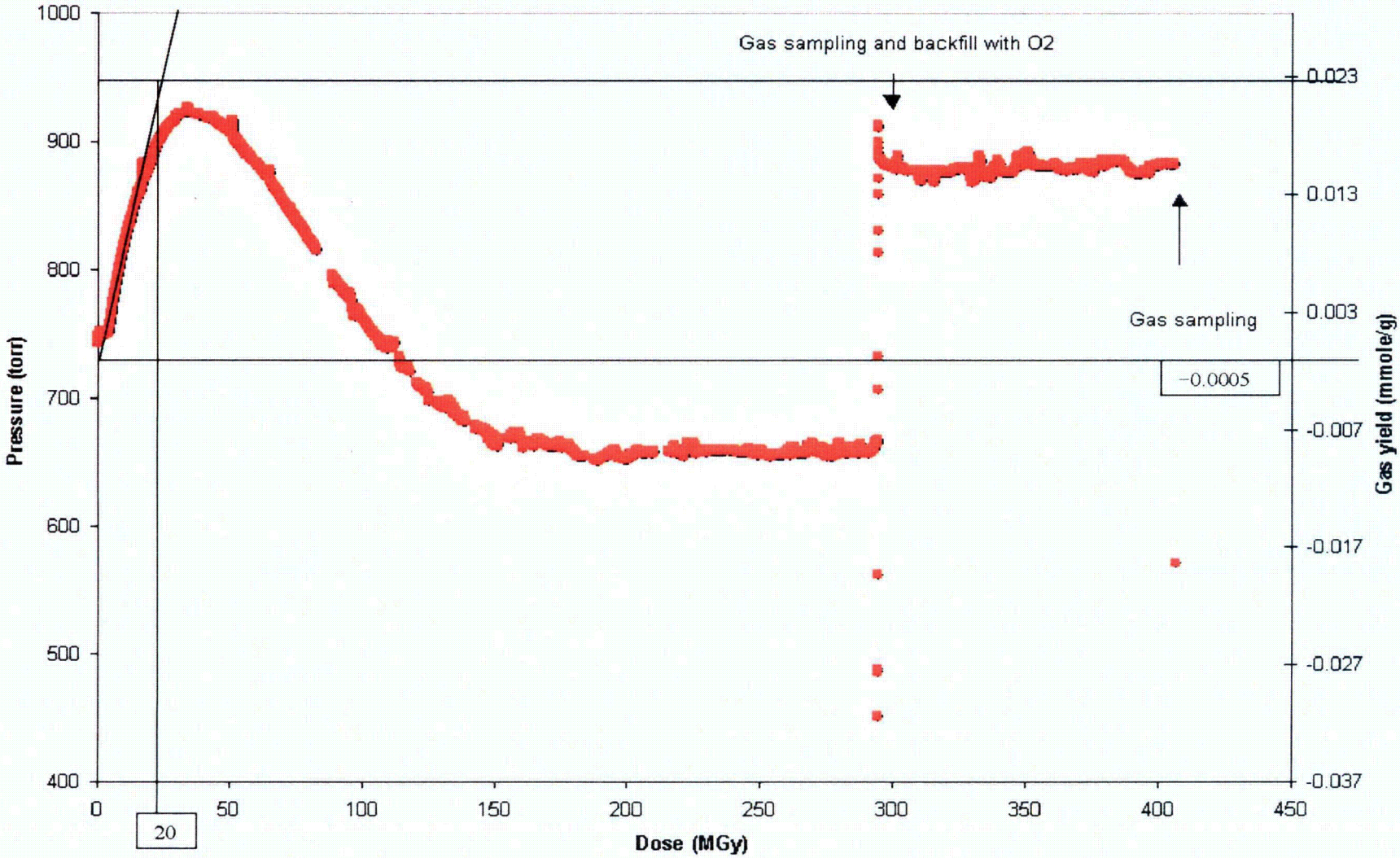

Fig. 3.6.7.1. Pressure and gas yield as a function of dose. Based on Fig. 3.5 in *Alpha Radiolysis of Sorbed Water on Uranium Oxides and Uranium Oxyfluorides* (ORNL/TM-2003/172), Sample A-4-1 (5.64 g U_3O_8 with 2 wt % H_2O, spiked with 0.0249 g ^{244}Cm).

$$e^-(mat) = \sum_{i=1}^{I} e^-(mat_i) =$$ the total number of electrons associated with the molecular species; electrons/molecule ;

$e^-(mat_i)$ = the contribution of the i^{th} molecular species to $e^-(mat)$; and
I = the total number of molecular species. The energy absorbed by the water is
D_H = $Gf \times D_E$ and
$G'(H_2)$ = $Gf \times G(H_2)$ · $G(H_2) = G'(H_2) / Gf$.

Two methods to calculate Gf are reported in *Calculation of Hydrogen Generation Rates for Storage of Post-KIS Oxide in 9975 Shipping Containers* (Calculation No. N-CLC-K-00219, p. 9 and 10). In the more rigorous of the two methods, Gf is estimated from the material stoichiometry and molecular weights. Using this more rigorous method, $e^-(mat_i)$ is calculated as

$$e^-(mat_i) = f_i \times \sum_{j=1}^{J} [n_{i,j} \times Z_{i,j}] / MW_i$$

where

f_i = the weight fraction of the i^{th} molecular species;
MW_i = the molecular weight of the i^{th} species;
$n_{i,j}$ = the number of moles of the j^{th} element in the i^{th} species;
J = the total number of elements in the i^{th} species; and
$Z_{i,j}$ = the atomic number of the j^{th} element in the i^{th} species.

According to the preceding equation, the expression for the number of electrons associated with the water is

$$e^-(H_2O) = f_{H2O} \times 10 / (16 + 2) = f_{H2O} \times 0.5556.$$

A mixture of water and U_3O_8 (assuming all the uranium is ^{235}U) is

$$e^-(mat) = f_{H2O} \times 0.5556 + f_{U3O8} \times (3 \times 92 + 8 \times 8) / (3 \times 235 + 8 \times 16)$$
$$= f_{H2O} \times 0.5556 + f_{U3O8} \times 0.4082$$

where

f_{H2O} = the weight fraction of water and
f_{U3O8} = the weight fraction of $U_3O_8 = 1 - f_{H2O}$ if no other material is present.

A $G'(H_2)$ value of 0.00756 molecules H_2/100 eV decay energy is derived from the experiment by Icenhour and Toth with a U_3O_8 sample (5.64 g) containing 2% water and spiked with 0.0249 g ^{244}Cm (ORNL/TM-2003/172, p. 7, Table 3.1). The mass of ^{244}Cm can be neglected, so the calculation of $G(H_2)$ for this sample is $e^-(H_2O) = 0.02 \times 0.5556 = 0.0111$; $e^-(mat) = 0.0111 + 0.98 \times 0.4082 = 0.4111$; $Gf = 0.0111 / 0.4111 = 0.0270$; and $G(H_2) = 0.00756 / 0.0270 = 0.280$ molecules H_2/100 eV absorbed by the water. Since the largest of the ORNL values (1.02) is used for the hydrogen generation calculations, the $G'(H_2)$ value for any other water content is the corresponding value of $Gf \times 1.02$.

To calculate Gf for $UO_2(NO_3)_2 \cdot XH_2O$, the two components are $UO_2(NO_3)_2$ and H_2O, where f_{H2O} is

$$f_{H2O} = X \times (2 + 16) / [235 + 2 \times 16 + 2 \times (14 + 3 \times 16) + X \times (2 + 16)]$$
$$= 1 / [1 + 391 / (X \times 18)]$$

$$e\ (mat) = f_{H2O} \times 0.5556 + f_{UN2O8} \times (92 + 8 \times 8 + 2 \times 7) / (391)$$
$$= f_{H2O} \times 0.5556 + f_{UN2O8} \times 0.4348$$

f_{UN2O8} = the weight fraction of $UO_2(NO_3)_2 = 1 - f_{H2O}$.

3.6.7.8 Time to Reach 5 mol %

The time at which the H_2 concentration in the void spaces of the package reaches 5 mol % depends on the H_2 generation rate and the volume of the void spaces. The void spaces are assumed to be initially filled with air at 25°C and 1 atm (101.3 kPa). The initial amount of air is given by

$$n_I = 101.3 \times V_{VT} / [8.3145 \times (25 + 273.15)]$$

where

n_I = the initial amount of air, mol;
V_{VT} = the total volume of the void spaces, L; and
8.3145 = the gas constant, J/(mol × K).

Since each mole of H_2 generated is accompanied by 0.5 mole of O_2, the concentration of H_2 will reach 5 mol % when

$$(n_{H2} + y \times n_I) / [1.5 \times (n_{H2} + y \times n_I) + n_I] = 0.05 \text{ or}$$
$$n_{H2} = (0.05405 - y) \times n_I$$

where

y is the initial mole fraction of hydrogen or 0.002.

The value of V_{VT} depends on the configuration and sizes of the convenience containers in the package and the amount of material in the containers. The configuration designated as CVA 7 is used for crystals and oxides may be placed in CVAs 1 through 6. The empty void volume (before the material is placed in the containers) is 9.4835 L (578.72 in.^{3}) for CVA 7 (Appendix 3.6.4, Table 1). The smallest (most conservative) empty void volume of CVAs 1 through 6 is 8.6230 L (526.21 in.^{3}) for CVA 2 (Appendix 3.6.4, Table 1).

If all the interstitial space is included, the total void volume is given by

$$V_{VT} = V_{BT} - Wt / \rho$$

where

V_{BT} = empty void volume, 8.6230 and 9.4835 L for CVA 2 and CVA 7, respectively;
Wt = the total weight of the material in the containers, kg; and
ρ = the theoretical density of the material in the containers, (10.97 kg/L for UO_2, 8.38 kg/L for U_3O_8, 7.3 kg/L for UO_3, and 2.81 kg/L for UNH). (CRC Handbook, p. 4-94)

Since UO_3 has the smallest theoretical density of the oxides, it will produce the smallest (most conservative) total volume of the void spaces.

As shown in Table 3.6.7.2, the bounding value of the decay energy is 1.39×10^{15} MeV/(g y). The fraction of uranium in UO_3 is $(1 - f_{H2O}) \times 235 / (235 + 3 \times 16) = 0.8055$ gU/g material for $f_{H2O} = 0.03$ (3% water). The corresponding fraction for crystals is $235 / [235 + 2 \times 16 + 2 \times (14 + 3 \times 16) + X \times (2 + 16)] = 0.4709$ gU/g material for X = 6 [$UO_2(NO_3)_2 \cdot 6H_2O$]. The decay energies are 1.12×10^{15} MeV/y g material for UO_3 with 3% H_2O and 6.57×10^{14} MeV/y g material for $UO_2(NO_3)_2 \cdot 6H_2O$.

The hydrogen generation rates for oxides (UO_2, U_3O_8, and UO_3) and uranyl nitrate crystals ($UO_2(NO_3)_2 \cdot XH_2O$) are calculated with the expression presented earlier in this appendix. The amounts of hydrogen for 5 mol % are divided by the corresponding generation rate to give the time to reach 5 mol %.

Table 3.6.7.4 gives the total weight of the material in the containers (Wt) that will generate enough hydrogen to reach 5 mol % in 1.20 or 0.5015 years as a function of the water content. The time limits for shipping the material are set at 1 year and 5 months and the additional 0.20 year allows a margin of safety in both cases. The water content considered is 3% for oxides and X values of 6 and 3 (21.64 and 12.13%) for crystals. As indicated in the table, the weight for UO_3 is the smallest for the oxides (15.13 kg).

The above calculations did not include the water from the humidity in the air. As indicated in Sect. 3.6.7.3, the mole fraction of water in the humid air is 0.031. Table 3.6.7.4 indicates the largest initial air in empty void volume is on the order of 0.32 moles so the water from the humidity in the air is on the order of $0.32 \times 0.031 = 0.01$ moles. The water content in the oxides is less than the crystals and is on the order of 3% so this water is on the order of $15{,}130 \times 0.03 / 18 = 25$ moles. Therefore, the radiolytic H_2 due to water from the humidity in the air is negligible.

3.6.7.9 Initial H_2 concentration

The results in Table 3.6.7.4 were calculated with the assumption that the initial H_2 concentrations were zero. It was suggested that a container stored for a long period of time would need to be vented before being placed in the ES-3100 in order to remove any H_2 that accumulated in the container during the storage period. An estimate of the accumulated H_2 is calculated in this section.

The H_2 generated in a container can leak out through tiny spaces in imperfect lids and by permeation or diffusion through the walls of the container. The largest leaks are through the tiny spaces but they are difficult to characterize. Consequently, this calculation conservatively considers only permeation and diffusion. Because permeation is usually a faster mechanism than diffusion and is more likely with plastics, the permeation model was used for the Teflon bottles. Since metals are not very permeable, the diffusion model was used for the cans.

The rate of gas loss through permeation is given by

$$d(n_P) / dt = P_m \times P \times A/\tau \times \rho_G$$

where

n_P is the amount of gas lost through permeation, mol;
P_m is the permeability, $cm^2/(Pa\ y)$;
P is the pressure increase over the initial value, Pa;
A is the cylindrical area of the Teflon bottle (4.69-in. diam × 9.4-in. tall, see Sect. 1), 893.5 cm^2 ;
τ is the thickness of the bottle (0.05-in. nominal thickness), 0.1270 cm; and
ρ_G is the gas density, 4.087×10^{-5} mol/cm^3 for an ideal gas at 25°C and 1 atm.

At steady state, the permeation rate is balanced by the gas generation rate.

$$1.5 \times d(n_{H2}) / dt = P_m \times P \times A/\tau \times \rho \quad \rightarrow \quad P = [1.5 \times d(n_{H2}) / dt] / [P_m \times A/\tau \times \rho_G]$$

where

$d(n_{H2}) / dt$ is the H_2 generation rate in the bottle due to radiolysis, mol/y and
1.5 is a factor to account for the oxygen released with the hydrogen.

Table 3.6.7.4. Combinations of weight and water content that will generate 5 mol % hydrogen in 1.20 or 0.5015 years

Density (kg/L)	Weight (kg)	Total void volume (L)	Gas amounts (mol)		Water		Material uranium content (gU/g mat)	Annual radiation rate [MeV/(g mat y)]	Gf	G'(H_2) (molecules H_2/100 eV)	n_{H2} rate (mol/y)
			Initial air	H_2 for 5 mol %	X	(wt %)					
U Oxides (UO_2) [CVA 2]											
10.97	15.51	7.2095	0.29468	0.01593		3.0	0.8537	1.19E+15	0.0407	0.0416	1.27E-02
U Oxides (U_3O_8) [CVA 2]											
8.38	15.33	6.7939	0.27769	0.01501		3.0	0.8209	1.15E+15	0.0404	0.0412	1.20E-02
U Oxides (UO_3) [CVA 2]											
7.3	15.13	6.5511	0.26777	0.01447		3.0	0.8055	1.12E+15	0.0402	0.0410	1.16E-02
$UO_2(NO_3)_2 \cdot XH_2O$ [CVA 7]											
2.81	4.75	7.7946	0.31852	0.01722	6	21.64	0.4709	6.57E+14	0.2609	0.2661	1.38E-02
2.81	6.70	7.0981	0.29006	0.01568	3	12.13	0.5281	7.37E+14	0.1500	0.1530	1.25E-02
2.81	9.12	6.2389	0.25495	0.01378	6	21.64	0.4709	6.57E+14	0.2609	0.2661	2.65E-02
2.81	11.90	5.2494	0.21451	0.01160	3	12.13	0.5281	7.37E+14	0.1500	0.1530	2.23E-02

The steady-state mole fraction is

$$f_{H2} = (2/3) \times P / P_0$$

where

f_{H2} = is the mole fraction of H_2 ;
2/3 is a factor to account for the fact that 1/3 of the pressure increase is due to oxygen; and
P_0 is the initial pressure in the bottle, 101325 Pa (1 atm).

The largest H_2 generation rate is 0.0265 mol/y (Table 3.6.7.4) for 3 Teflon bottles (see Sect. 3.1.4.1). The value for one bottle is 0.0265 / 3 = 0.00882 mol/y. Permeability values for Teflon bottles can be found at the Nalgene Labware Web site. In units of (cc • mm)/(m^2 • day • Bar), these permeability values are 4960 for N_2, 11,625 for O_2, and 34,100 for CO_2. The value for H_2 would be expected to be larger than these values; however, the smallest value (4960 for N_2) was conservatively assumed for H_2. When converted to consistent units, the permeability used for H_2 is 0.000181 cm^2/(Pa • y). With these values, the steady-state pressure rise is 254.1 Pa, and the H_2 mole fraction is 0.00167 or less than 0.2%.

The rate of H_2 loss through diffusion is given by

$$d(n_D) / dt = D \times C \times A/\tau$$

where

n_D is the amount of H_2 lost through diffusion, mol;
D is the diffusivity, cm^2/y; and
C is the H_2 concentration increase over the initial value, mol/cm^3.

At steady state, the diffusion rate is balanced by the H_2 generation rate.

$$d(n_{H2}) / dt = D \times C \times A/\tau \rightarrow C = [d(n_{H2}) / dt] / [D \times A/\tau]$$

The steady-state mole fraction is

$$f_{H2} = (V_C \times C) / n_I ; \quad n_I = V_C \times \rho_G \rightarrow f_{H2} = C / \rho_G$$

where

V_C is the volume of the can (4.25-in. diam × 4.88-in. tall; see Sect. 1), 1134.5 cm^3.

The largest H_2 generation rate (0.0265 mol/y, Table 3.6.7.4) is also conservatively applied to four cans (see Sect. 3.1.4.1), and the value for one can is 0.0265 / 4 = 0.00662 mol/y. The cylindrical area of the can is 420.4 cm^2, and the thickness is 0.0762 cm (0.03-in. nominal thickness for a nickel can). Presentation view graphs about hydrogen diffusion through metal pipelines indicate a wide range of diffusivity values at room temperatures and suggest that a value of about 5×10^{-7} cm^2/s is probably a low number for plain steel without welds or rough surfaces. (Sudersanam 2005) Using these values, the H_2 mole fraction is 0.00186, also less than 0.2%.

Both permeation and diffusion lead to H_2 concentrations less than 0.2 mole percent, which are negligible compared to the 5% limit. Also, these are conservative calculations in that they do not consider leaks through can and bottle closure lids, which are expected to be much larger. The small concentration (0.2 mol %) was used as an initial condition in the hydrogen generation calculations that gave rise to mass loadings and the time limits to complete shipment of this material. Therefore, it will not be necessary to vent the containers before loading them into an ES-3100 containment vessel.

ORNL/TM-2003/194

Water Sorption and Radiolysis Studies for Neptunium Oxides

January 2004

Prepared by
A. S. Icenhour
R. M. Wham
R. R. Brunson
L. M. Toth

DOCUMENT AVAILABILITY

Reports produced after January 1, 1996, are generally available free via the U.S. Department of Energy (DOE) Information Bridge:

Web site: http://www.osti.gov/bridge

Reports produced before January 1, 1996, may be purchased by members of the public from the following source:

National Technical Information Service
5285 Port Royal Road
Springfield, VA 22161
Telephone: 703-605-6000 (1-800-553-6847)
TDD: 703-487-4639
Fax: 703-605-6900
E-mail: info@ntis.fedworld.gov
Web site: http://www.ntis.gov/support/ordernowabout.htm

Reports are available to DOE employees, DOE contractors, Energy Technology Data Exchange (ETDE) representatives, and International Nuclear Information System (INIS) representatives from the following source:

Office of Scientific and Technical Information
P.O. Box 62
Oak Ridge, TN 37831
Telephone: 865-576-8401
Fax: 865-576-5728
E-mail: reports@adonis.osti.gov
Web site: http://www.osti.gov/contact.html

ORNL/TM-2003/194

WATER SORPTION AND RADIOLYSIS STUDIES FOR NEPTUNIUM OXIDES

A. S. Icenhour
R. M. Wham
R. R. Brunson
L. M. Toth

Date Published: January 2004

Prepared by
OAK RIDGE NATIONAL LABORATORY
P.O. Box 2008
Oak Ridge, Tennessee 37831-6285
managed by
UT-Battelle, LLC
for the
U.S. DEPARTMENT OF ENERGY
under contract DE-AC05-00OR22725

CONTENTS

Page

LIST OF FIGURES

LIST OF FIGURES (continued)

LIST OF TABLES

ACRONYMS, ABBREVIATIONS, AND DEFINITIONS

ATR	Advanced Test Reactor
DOE	U.S. Department of Energy
G-value	the number of molecules of gas either produced or destroyed per 100 eV of energy deposited in the sample
HEPA	high-efficiency particulate air (filter)
HFIR	High Flux Isotope Reactor
INEEL	Idaho National Engineering and Environmental Laboratory
LANL	Los Alamos National Laboratory
MGy	megagray, 1 MGy = 10^6 J/kg (1 Gy = 100 rad)
ORNL	Oak Ridge National Laboratory
PCV	primary containment vessel
REDC	Radiochemical Engineering Development Center
SNF	spent nuclear fuel
SRS	Savannah River Site

ABSTRACT

Plans are to convert the ^{237}Np that is currently stored as a nitrate solution at the Savannah River Site to NpO_2 and then ship it to the Y-12 National Security Complex in Oak Ridge for interim storage. This material will serve as feedstock for the ^{238}Pu production program, and some will be periodically shipped to the Oak Ridge National Laboratory (ORNL) for fabrication into targets. The safe storage of this material requires an understanding of the radiolysis of moisture that is sorbed on the oxides, which, in turn, provides a basis for storage criteria (namely, moisture content). A two-component experimental program has been undertaken at ORNL to evaluate the radiolytic effects on NpO_2: (1) moisture uptake experiments and (2) radiolysis experiments using both gamma and alpha radiation.

These experiments have produced two key results. First, the water uptake experiments demonstrated that the 0.5 wt % moisture limit that has been typically established for similar materials (e.g., uranium and plutonium oxides) cannot be obtained in a practical environment. In fact, the uptake in a typical environment can be expected to be at least an order of magnitude lower than the limit.

The second key result is the establishment of steady-state pressure plateaus as a result of the radiolysis of sorbed moisture. These plateaus are the result of back reactions that limit the overall pressure increase and H_2 production. These results clearly demonstrate that 0.5 wt % H_2O on NpO_2 is safe for long-term storage—if such a moisture content could even be practically reached.

1. INTRODUCTION

The Department of Energy (DOE) Office of Space and Defense Power, NE-50, is reestablishing domestic production of ^{238}Pu using existing DOE facilities. The feed material for the production is ^{237}Np, which is currently stored at the Savannah River Site (SRS). This material will be stabilized as an oxide, packaged, and then transported to the Y-12 National Security Complex for interim storage. Y-12 will then transfer material as needed to Oak Ridge National Laboratory (ORNL). Target fabrication will occur at the Radiochemical Engineering Development Center (REDC) Building 7930. The High Flux Isotope Reactor (HFIR) at ORNL and the Advanced Test Reactor (ATR) at the Idaho National Engineering and Environmental Laboratory (INEEL) will be used to irradiate ^{237}Np-containing targets to produce ^{238}Pu. The irradiated targets will undergo chemical processing at the REDC to (1) recover ^{238}Pu for shipment to Los Alamos National Laboratory (LANL) and (2) recover ^{237}Np for recycle.

Safety issues concerning transportation and long-term storage of neptunium are of a particular concern to the program. The material and its packaging must comply with shipping standards as well as provide for safe storage.

One aspect relative to the safe transport and storage of NpO_2 is radiolysis of sorbed water. Current safety analyses assume that all of the water absorbed on the surface of the NpO_2 can be radiolyzed to gaseous hydrogen and oxygen, thus generating significant gas pressures within the storage containers. Also, the potential for detonation of the hydrogen has been identified as a safety issue for transportation. However, experimental work by Icenhour et al.[1–4] using uranium oxides and uranium oxyfluorides has demonstrated that radiolysis does not convert all of the water to H_2 and O_2 because of competing back reactions that result in a pressure plateau, demonstrating that a steady state has been reached. In some cases, the vessel actually goes to vacuum conditions as a result of the dominance of back reactions.

The use of high-dose-rate gamma and/or alpha irradiation capable of radiolyzing significant quantities of the proposed materials in a short period of time is the only practical way to achieve the necessary doses and thus assess potential long-term storage problems. A set of experiments was performed to irradiate NpO_2 samples that have sorbed moisture. This report provides a description of the experiments and the results.

2. BACKGROUND

The neptunium to be used as feed material currently exists in a nitrate solution in the SRS H-Canyon. The neptunium solution, which contains about 500 ppm ^{238}Pu,[5] will undergo chemical processing in a glove-box line (HB-Line Phase II) to remove impurities and convert it to an oxide as depicted in Fig. 2.1.

The neptunium solution first undergoes a feed adjustment to 6–8 *M* HNO_3. The adjusted solution is then fed into anion-exchange columns, where the neptunium nitrate complex absorbs, allowing most metal impurities to pass through the column. Next, a decontamination wash is performed to remove residual impurities. Finally, a weak nitric acid solution is passed through the column to elute the neptunium.

Once the anion-exchange process has been completed, the resulting neptunium solution is combined with oxalic acid, which forms an insoluble neptunium oxalic precipitant. This product is filtered, and the neptunium oxalate is then calcined at ~600°C to convert the oxalate to oxide.

The oxide will be packaged in a can–bag–can configuration for shipment (Fig. 2.1). The inner can, which contains up to 6 kg neptunium, is a screw-top, food-pack convenience can. Because no gasket or sealing compounds are used on the closure, this inner can will not be gastight. The inner can is contained in a heat-sealed polyethylene bag, which has an installed HEPA (high-efficiency particulate air) filter. The can–bag will then be placed inside an outer can, which has a HEPA filter in its lid.* Finally, the can–bag–can will be placed inside a 9975 primary containment vessel (PCV).[6] SRS currently plans to evacuate the PCV and backfill with argon. Because of the installed HEPA filters and the screw-top lid on the inner can, the entire contents of the PCV will be evacuated and backfilled. This operation is expected to reduce the O_2 concentration inside the PCV to less than 5 vol %.

Concerns related to the long-term storage of the NpO_2 are the potential for container pressurization and/or the formation of H_2 as a result of radiolytic decomposition of moisture that is sorbed on the oxide. To address these concerns, NpO_2 radiolysis experiments have been conducted at ORNL using both gamma and alpha radiation sources. Samples of NpO_2 were prepared by the method expected to be used at SRS (i.e., oxalate precipitation and calcination). Moisture was added to the samples to simulate water uptake.

The equipment and experimental facilities described in this report have been used in similar studies concerning gamma irradiation of uranium oxides and fluoride salts with various amounts of sorbed water.[1–4]

*Because of ergonomic considerations, two bagged inner cans may be used instead of just one.

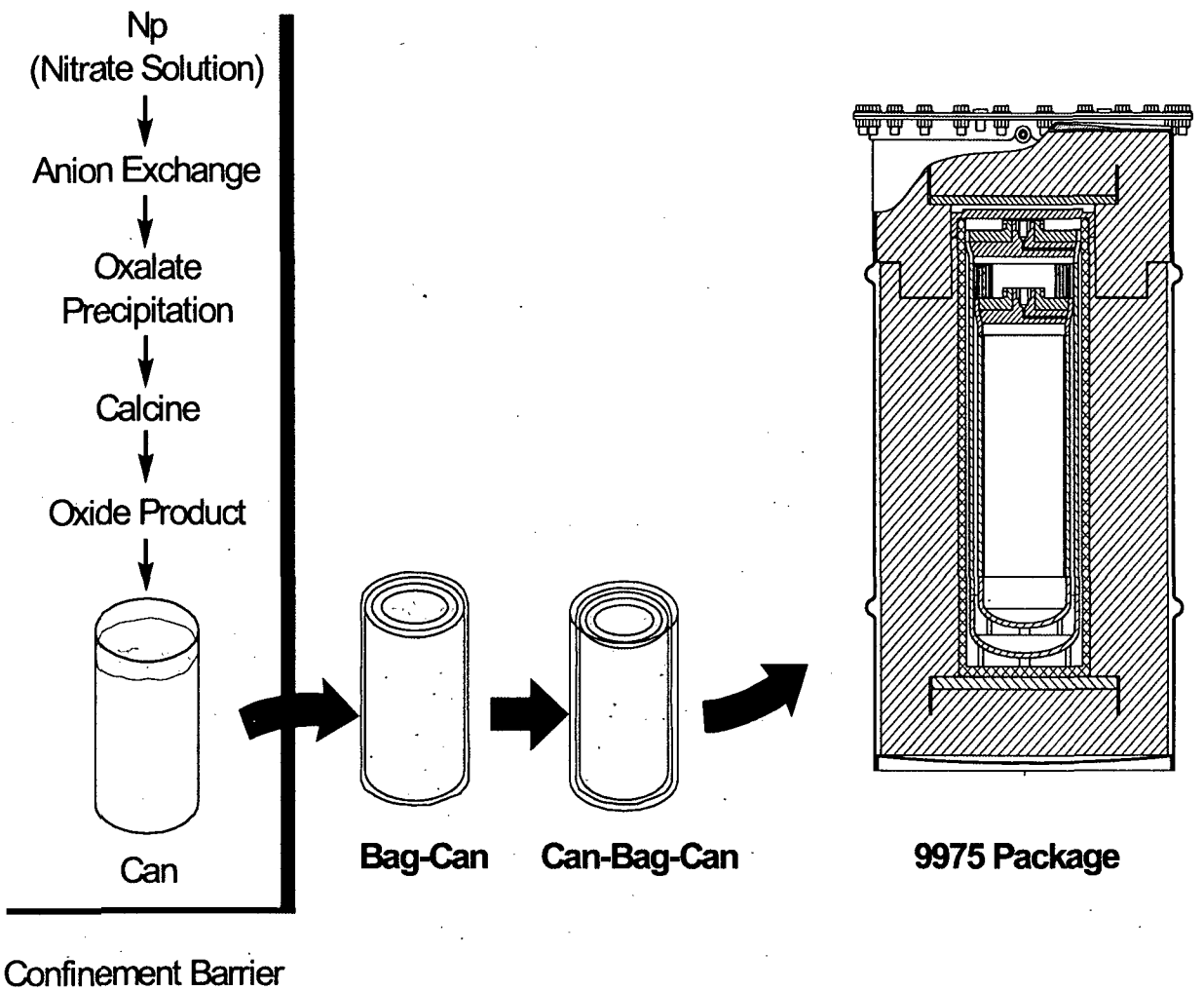

Fig. 2.1. Schematic depiction of neptunium processing and packaging.

3. EXPERIMENTAL

The experimental program was divided into three distinct activities: sample preparation, water sorption studies, and radiolysis experiments.

3.1 SAMPLE PREPARATION

Twelve samples of NpO_2 were prepared and then irradiated to evaluate radiolytic decomposition of water. The samples first underwent chemical processing at REDC Building 7930 to prepare the NpO_2 in a form similar to that expected from SRS.[7] The water content and the surface area of the samples were varied for the experiments.

In order to prepare NpO_2 for these experiments, a batch of 80–100 g of NpO_2 was dissolved in nitric acid. Some of the feed material was neptunium oxide originally obtained from LANL. The majority of the material had been processed using hydroxide precipitation, oxalate precipitation, and ion-exchange processing at the REDC. Because the neptunium product batches from the hydroxide precipitation and oxalate precipitation processes were calcined at 1400°C, they were extremely difficult to dissolve. Therefore, these various sources of neptunium were dissolved in 8 *M* HNO_3 acid with 0.02 *M* NaF added to the solution, followed by heating over a period of about 24 h to promote the dissolution. After dissolution, the neptunium was adjusted to the 4+ valence state by addition of hydrazine followed by ascorbic acid. A slight excess of oxalic acid was then added to precipitate the neptunium as neptunium oxalate. The resulting material was filtered, dried, and fired to 650°C to convert the oxalate to oxide.* Some material was fired at 800°C to change the surface area. Tables 3.1 and 3.2 provide isotopic and chemical impurity results, respectively, from the analysis of NpO_2 prepared by the method described.

3.2 WATER SORPTION STUDIES

Neptunium oxide with varying amounts of sorbed water was needed for these experiments. The amount of water sorbed as a function of time was determined by placing these materials in a controlled-humidity environment. Humidities of 60 and 97.5% were used. The humidity was controlled by

*Note that at the time of this work, the exact calcination temperature had not yet been established. It is now expected that the SRS material will be fired at temperatures between 600 and 650°C, depending on the capability of the furnace used. This temperature range will have no effect on the results or conclusions described in this report.

Table 3.1. Neptunium isotopic data

	Isotopic abundance (wt %)
^{237}Np	99.97361
$^{239/240}Pu$	0.02558
^{238}Pu	0.0008

Table 3.2. Metal ion impurity in NpO_2 samples

Element	Concentration (μg/g)
Al	$1.38 \times 10^4 \pm 1.38 \times 10^3$
B	$9.19 \times 10^3 \pm 9.19 \times 10^2$
Ba	$6.03 \times 10^3 \pm 6.03 \times 10^2$
Be	$4.25 \times 10^1 \pm 4.25$
Ca	$1.94 \times 10^4 \pm 1.91 \times 10^3$
Cu	$6.79 \times 10^2 \pm 8.49 \times 10^1$
Fe	$6.52 \times 10^3 \pm 1.36 \times 10^3$
K	$8.43 \times 10^3 \pm 2.08 \times 10^3$
Mg	$1.41 \times 10^4 \pm 1.31 \times 10^3$
Mn	$2.34 \times 10^2 \pm 4.25 \times 10^1$
Na	$5.44 \times 10^4 \pm 5.44 \times 10^3$
Sb	$3.27 \times 10^3 \pm 7.22 \times 10^2$
Sr	$3.40 \times 10^2 \pm 3.40 \times 10^1$

placing the NpO_2 sample in a small open glass container, which, in turn, was placed in a glass desiccator. The desiccant had been removed and was replaced with a small open container of dilute sulfuric acid to yield the desired humidity. The NpO_2 samples were periodically removed from the chamber and weighed to determine the uptake of water. Table 3.3 provides relative humidity data for a number of sulfuric acid solutions. (The vapor referred to is pure water.)

Table 3.3. Constant humidity control using sulfuric acid solutions[a]

Density of aqueous H_2SO_4 solution	Relative humidity (%)	Water vapor pressure at 20°C (mm Hg)
1.00	100.0	17.4
1.05	97.5	17.0
1.10	93.9	16.3
1.15	88.8	15.4
1.20	80.5	14.0
1.25	70.4	12.2
1.30	58.3	10.1
1.35	47.2	8.3
1.40	37.1	6.5
1.50	18.8	3.3
1.60	8.5	1.5
1.70	3.2	0.6

[a]From *Handbook of Chemistry and Physics*, 41st ed., Chemical Rubber Publishing Co., Cleveland, 1959, p. 2500.

3.3 RADIOLYSIS EXPERIMENTS

Radiolysis experiments were performed using both gamma and alpha radiation. The equipment used for these experiments is described in Sects. 3.3.1 and 3.3.2.

3.3.1 Gamma Irradiation Experiments

Two different sources of gamma radiation were used: (1) the ORNL ^{60}Co irradiator and (2) the HFIR spent nuclear fuel (SNF) elements. In preparation of the samples, a calibrated pipette was used to add the desired amount of water.

3.3.1.1 ^{60}Co irradiation experiments

A J. L. Shepherd model 109-68 (serial no. 654) ^{60}Co gamma irradiator (shown in Fig. 3.1), providing a dose rate of about 10^5 rad/h, was used for the experiments. The sample container itself is shown in Fig. 3.2, while Fig. 3.3 shows the samples installed in the irradiator prior to being lowered into the device. A detailed description of the irradiator and the methods used to calculate the dose to the samples (for both the ^{60}Co source and HFIR SNF elements) is provided in Ref. 8.

The samples to be irradiated were placed in stainless steel containers, each of which had a small-diameter stainless steel tube connected at one end for pressure sensing and a capped opening at the other end for loading samples. The container was connected by small-diameter tubing to a stainless steel Nupro® valve and an MKS Baratron® pressure transducer (Type 127A). The material to be irradiated was loaded through a stainless steel VCR gland on one end of the container.

Preparation of sample containers for their insertion into the ^{60}Co irradiator consisted of leak checks, volume measurements, and loading of the samples into the containers. As part of their fabrication, the containers were leak checked with air to a pressure of about 6.8 atm (100 psia).

Just before their use, the containers were leak checked again, using both pressure (typically ~3 atm) and vacuum. The volume of the irradiation rig (i.e., the sample container, tubing, valve, and pressure transducer) was measured by expanding helium from a known volume into the rig, observing the pressure change, and applying the ideal gas law. The volume of each of the tubes used in the experiments is presented in Table 3.4.

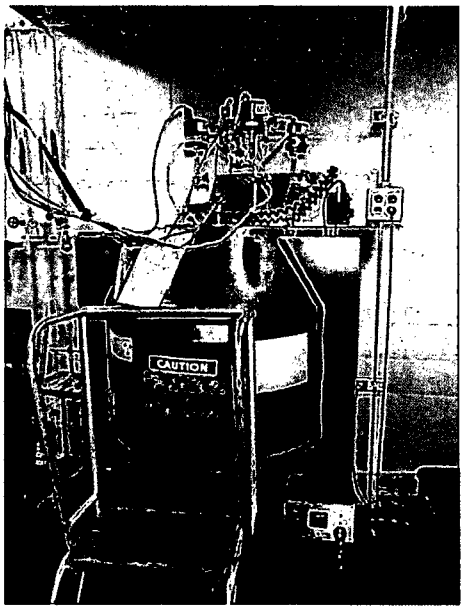

Fig. 3.1. ORNL ^{60}Co irradiator.

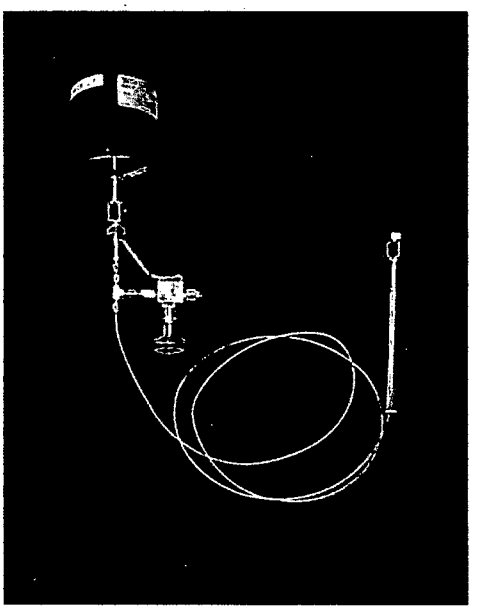

Fig. 3.2. Sample container and pressure transducer used in the ^{60}Co irradiations.

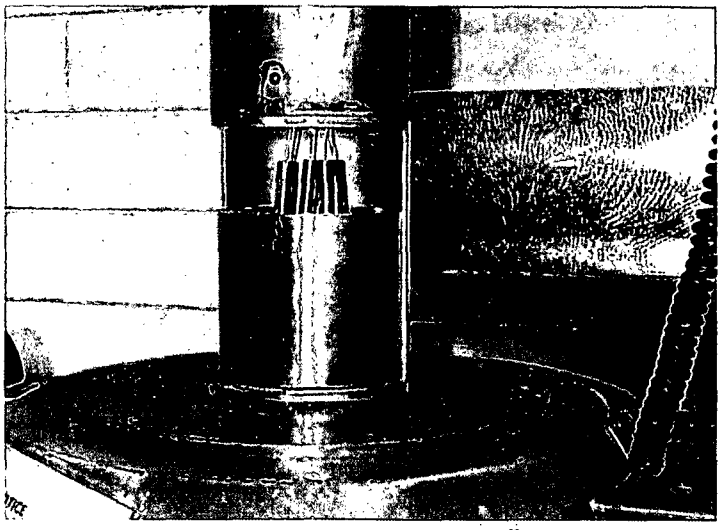

Fig. 3.3. Irradiation chamber of ORNL ^{60}Co irradiator with sample containers installed.

Table 3.4. Volume of sample containers used in irradiation experiments

Container	Volume (cm^3)
^{60}Co Np Tube 1	16.7
^{60}Co Np Tube 2	16.6
^{60}Co Np Tube 3	16.4
^{60}Co Np Tube 4	16.1
HFIR Np Tube 1	34.6
HFIR Np Tube 2	49.7
HFIR Np Tube 3	50.8
HFIR Np Tube 4	35.4
Alpha Np Tube 1	13.1
Alpha Np Tube 2	13.3
Alpha Np Tube 3	13.5
Alpha Np Tube 4	13.7
Alpha Np Tube 5	13.1

A computerized data acquisition system was used to collect data during each irradiation. Validyne® hardware and software were used, providing up to eight data channels per card. The data acquisition system is shown in Fig. 3.4. Typical parameters recorded during an irradiation included container pressure, temperature of selected containers, and ambient pressure and temperature.

3.3.1.2 HFIR SNF irradiation experiments

To obtain higher dose rates, the HFIR SNF gamma irradiation facility (shown in Fig. 3.5) was also used. Figure 3.6 depicts the experimental configuration for these irradiations. Samples can be irradiated in the HFIR SNF pool by inserting them into SNF elements. The SNF elements are cylindrical with a hollow center. In its storage position in the SNF pool, a cadmium sleeve inside the hollow region of the element absorbs neutrons. Hence, the hollow region of the fuel element primarily provides a gamma field for irradiation. The neutron flux in this region is about 100 neutrons • cm^{-2} • s^{-1}. The contribution of neutrons to the radiation damage is negligible when compared with the very large gamma field. Exposure rates vary from about 10^7 to 10^8 R/h, depending on the time since the discharge of the SNF from the reactor.

A multiple-irradiation container was used for the irradiation of four samples at once (Fig. 3.7). Small sample containers consisting of 1.27-cm-diam stainless steel tubing were placed inside an outer container, which was fabricated from 8.9-cm-diam, 44-cm-long stainless steel pipe. The outer container was closed at one end and had a Conflat flange on the other end. The flange contained five penetrations. Four were used to connect the smaller inner containers to 0.318-cm-diam stainless steel tubing, while the fifth connected the void volume of the outer container to 0.318-cm-diam stainless steel tubing. In each case, this tubing was about 6.1 m long and was connected to a pressure transducer and to a valve.

The volume of each of the sample containers, which included sampling lines and pressure transducers, is presented in Table 3.4. Before the experiment was transported to the HFIR for insertion in an SNF element, the samples were loaded in air and the outer container was pressurized to 1.7 atm (10 psig), as required by HFIR operations personnel.

Sensotec® (model FPA, 0–50 psia) pressure transducers were used for the four inner sample containers. A Kobold® (model KPK, 30 in. Hg to 100 psig) compound pressure transducer was used to monitor the pressure in the large outer vessel. A computerized data acquisition system was used to record the pressure throughout the experiments.

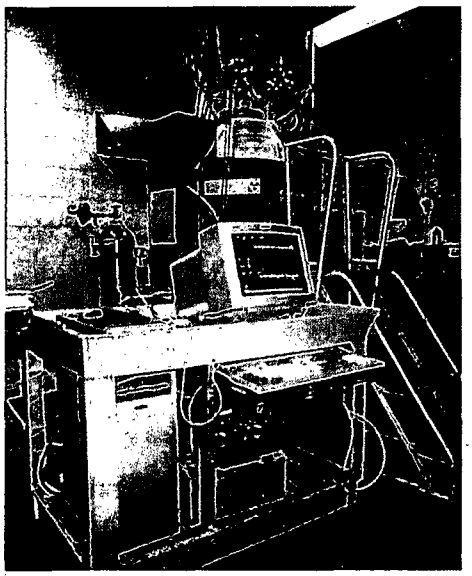

Fig. 3.4. Data acquisition computer in operation at the ORNL ^{60}Co source.

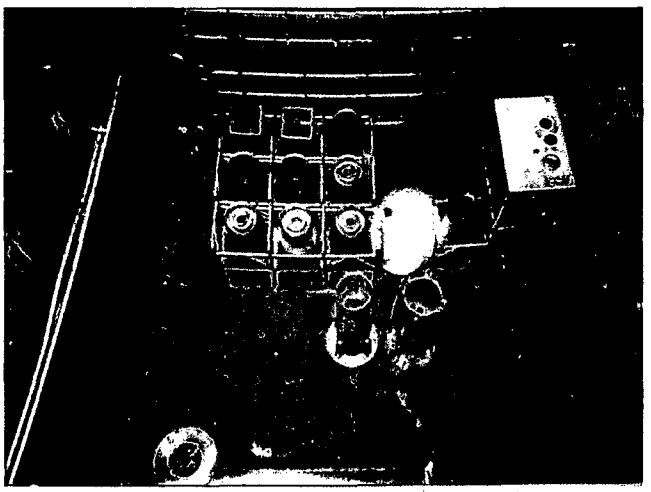

Fig. 3.5. SNF elements in the HFIR SNF pool.

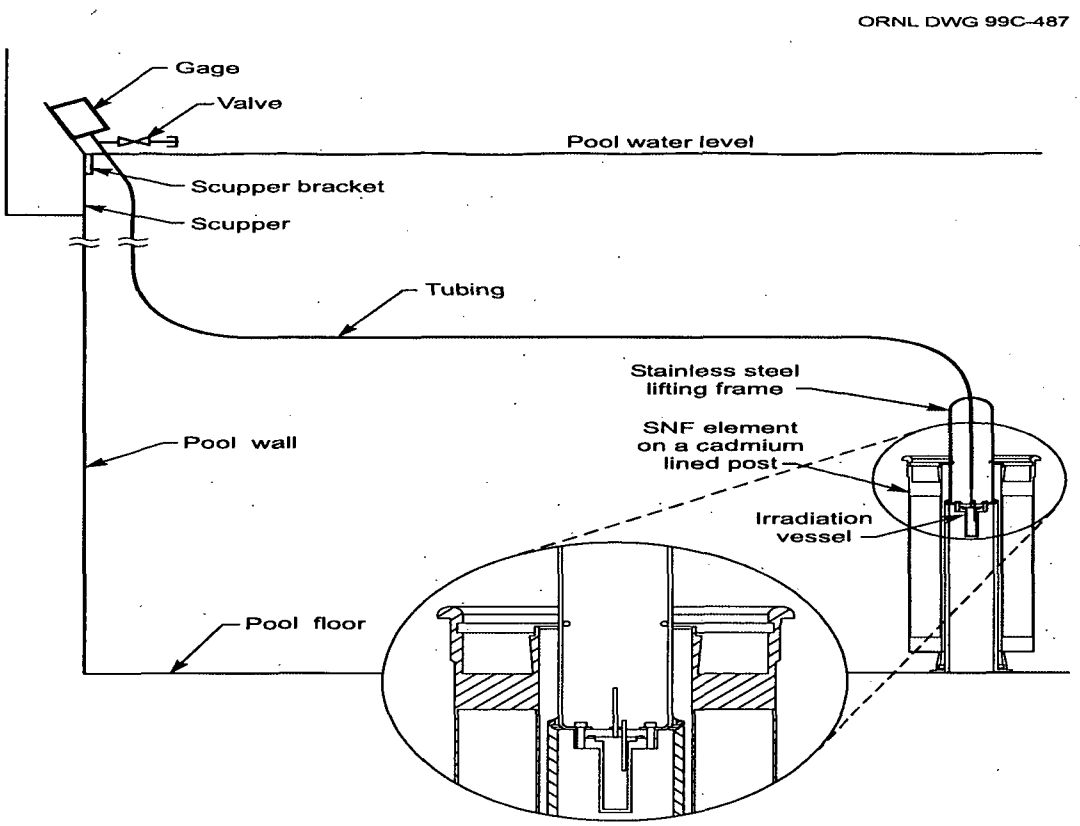

Fig. 3.6. Schematic of the experimental configuration for gamma irradiation experiments with a HFIR SNF element.

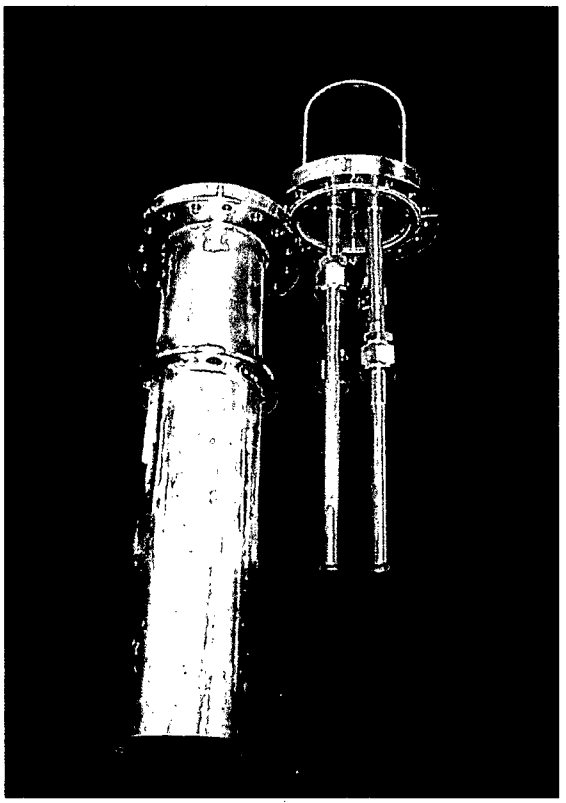

Fig. 3.7. Multiple-irradiation container used in HFIR SNF irradiations.

3.3.2 Alpha Radiolysis Experiments

To perform the alpha radiolysis experiments, neptunium samples were spiked with ^{244}Cm to mimic the dose from ^{238}Pu, but in a shorter time period reasonable for the present experimental study. Note that the neptunium in storage at SRS contains about 500 ppm ^{238}Pu. Samples of NpO_2 containing about 7000 ppm ^{244}Cm realized a dose rate about 70 times that for the SRS material, as illustrated in Figure 3.8. An example of the radionuclide composition and dose contribution data for the curium used is presented in Table 3.5. This table demonstrates that while 40 wt % of the material used to spike the samples was ^{240}Pu, more than 99% of the dose was delivered by the parent isotope, ^{244}Cm.

A portion of the dissolved neptunium was set aside for alpha radiolysis experiments. The neptunium was adjusted to the 4+ valence state and diluted to 1–2 *M* HNO_3. A small aliquot of ^{244}Cm was then mixed with the neptunium solution, and oxalic acid was added to form both neptunium and curium oxalate. The oxalate product was filtered, dried, and calcined at 650°C. The resulting oxide was then divided into four samples, one of which was further heated to 800°C.

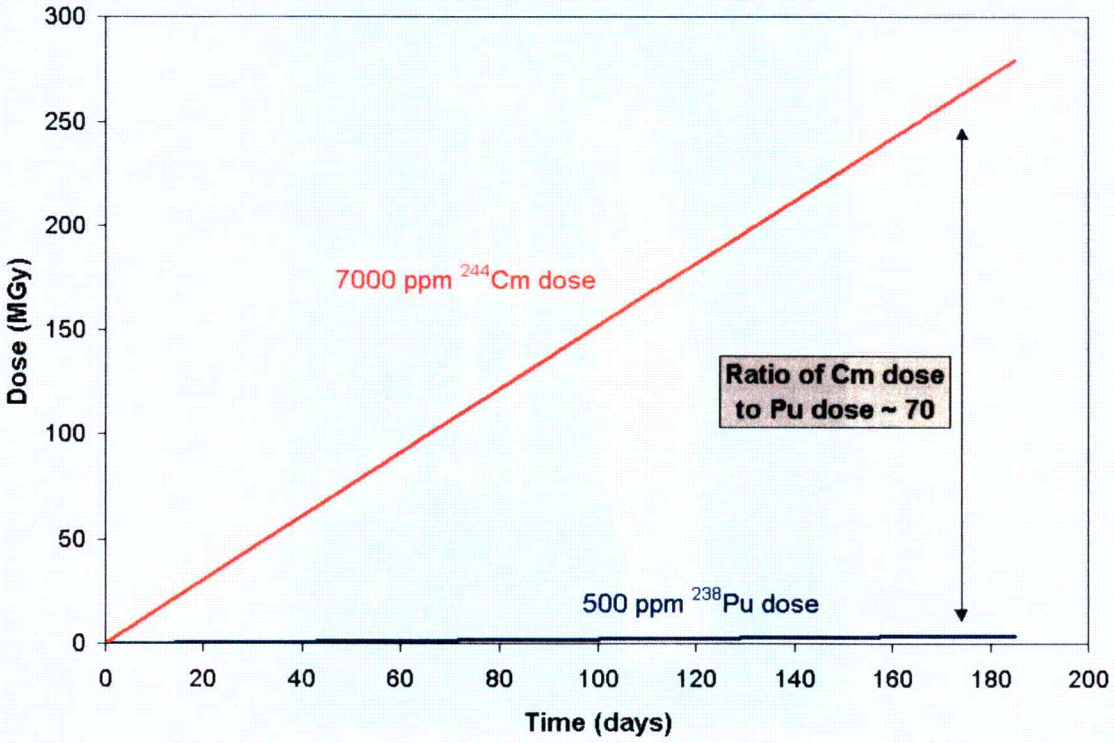

Fig. 3.8. Comparison of doses to NpO_2 samples using 500 ppm ^{238}Pu and 7000 ppm ^{244}Cm.

Table 3.5. Example of radionuclide composition and dose contribution data for a NpO_2 sample spiked with ^{244}Cm

Radionuclide	Half-life (years)	Specific activity (Ci/g)	Average alpha energy (MeV)	Composition (wt %)	Contribution to dose (%)
^{244}Cm	18.11	80.9	5.7965	50.34	99.74
^{245}Cm	8500	0.1717	5.363	1.36	0.01
^{246}Cm	4730	0.3072	5.376	7.31	0.05
^{247}Cm	1.56×10^{7}	9.20×10^{5}	4.9475	0.12	2.34×10^{-7}
^{248}Cm	3.40×10^{5}	0.00424	4.6524	0.07	5.72×10^{-6}
^{240}Pu	6563	0.22696	5.1549	40.04	0.20
^{241}Pu	14.4	103	0.000118	2.01×10^{-6}	1.03×10^{-10}
^{242}Pu	3.76×10^{5}	0.003926	4.89	1.93×10^{-5}	1.57×10^{-9}
^{243}Am	7380	0.1993	5.2656	0.76	3.37×10^{-3}

The samples were placed in stainless steel containers, and the desired amount of water was then added. The containers were connected by a small-diameter stainless steel tube to a Sensotec pressure transducer and to a valve (Fig. 3.9). Filter gaskets (0.5-μm sintered frit) were used in the VCR face-sealed connections to prevent movement of particles and the spread of contamination. An Omega® Type K thermocouple was attached to the outside of each sample container. The void volume of the containers was measured by expanding helium from a known volume. (The measured volumes are shown in Table 3.4.) Samples were prepared and loaded into the containers in a glove box.

3.4 SAMPLING AND ANALYSES

At the completion of the irradiations, gas samples were withdrawn and analyzed by mass spectrometry.

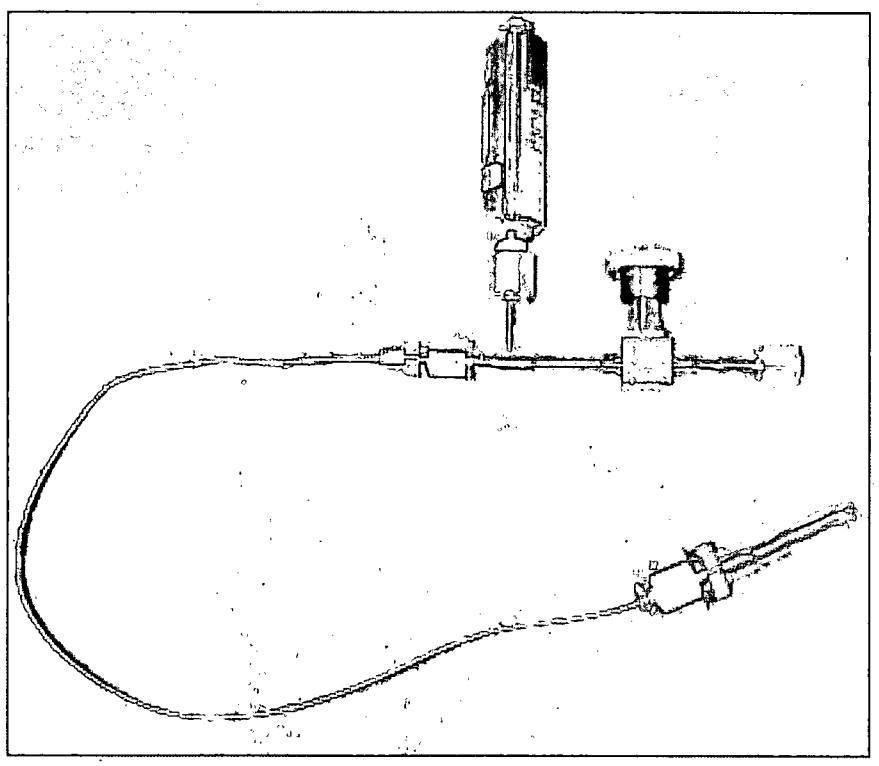

Fig. 3.9. Sample container and pressure transducer used in the alpha radiolysis experiments.

4. RESULTS AND DISCUSSION

4.1 WATER SORPTION EXPERIMENTS

The results for the water sorption on the samples prepared at 650°C are shown in Fig. 4.1, where the weight gain (i.e., amount of water sorption) of the NpO_2 sample is depicted as a function of time for two different relative humidities. The sample exposed to the 97.5% humidity exhibited an increase in moisture uptake to a limiting value of about 1 wt %. Interestingly, at about 30 days, the lid to the chamber containing the sample was left off, thereby lowering the relative humidity over the sample to that of the glove box. The amount of moisture on the sample rapidly decreased, and, when the lid was replaced, the amount of moisture returned to the previous limit. For the sample exposed to the 60% humidity, a much lower moisture uptake limit was reached—about 0.02 wt %. A similar behavior was seen for the samples prepared at 800°C (not shown in this report). For these samples, the maximum moisture uptake was 0.8 wt % in the 97.5% humidity, while the maximum was about 0.02 wt % in the 60% humidity.

The water sorption experiments showed that in practical humidities, NpO_2 sorbs very little water. Even in the case of extreme humidity (i.e., 97.5%), the sample prepared at 650°C sorbed quantities of water only up to ~1 wt % (Fig. 4.1). Furthermore, this water was held very loosely on the surface—as demonstrated by the overnight occurrence described in the paragraph above. However, in the more normal operational case of 60% relative humidity, the maximum water uptake was about 0.02 wt %.

Taking these results in a broader perspective, it is worth noting that the plutonium and ^{233}U storage standards[9,10] have been set with the maximum acceptable moisture content at 0.5 wt %. With such precedents, we expect an identical limit will be established for the NpO_2 that is to be prepared at SRS. In light of the current moisture uptake data for the NpO_2 prepared at 650°C, and based on similar results obtained at 75% relative humidity by the Savannah River Technology Center,[11] the storage standard limit of 0.5 wt % could never be reached in normal operating or storage conditions where humidity levels are controlled at 60–75%.

4.2 GAMMA RADIOLYSIS EXPERIMENTS

Irradiation experiments were conducted for a number of NpO_2 samples using either the ORNL ^{60}Co source or HFIR SNF elements. Table 4.1 provides a summary of the irradiation experiments performed. The results obtained from these radiolysis experiments are presented in Sects. 4.2.1 and 4.2.2.

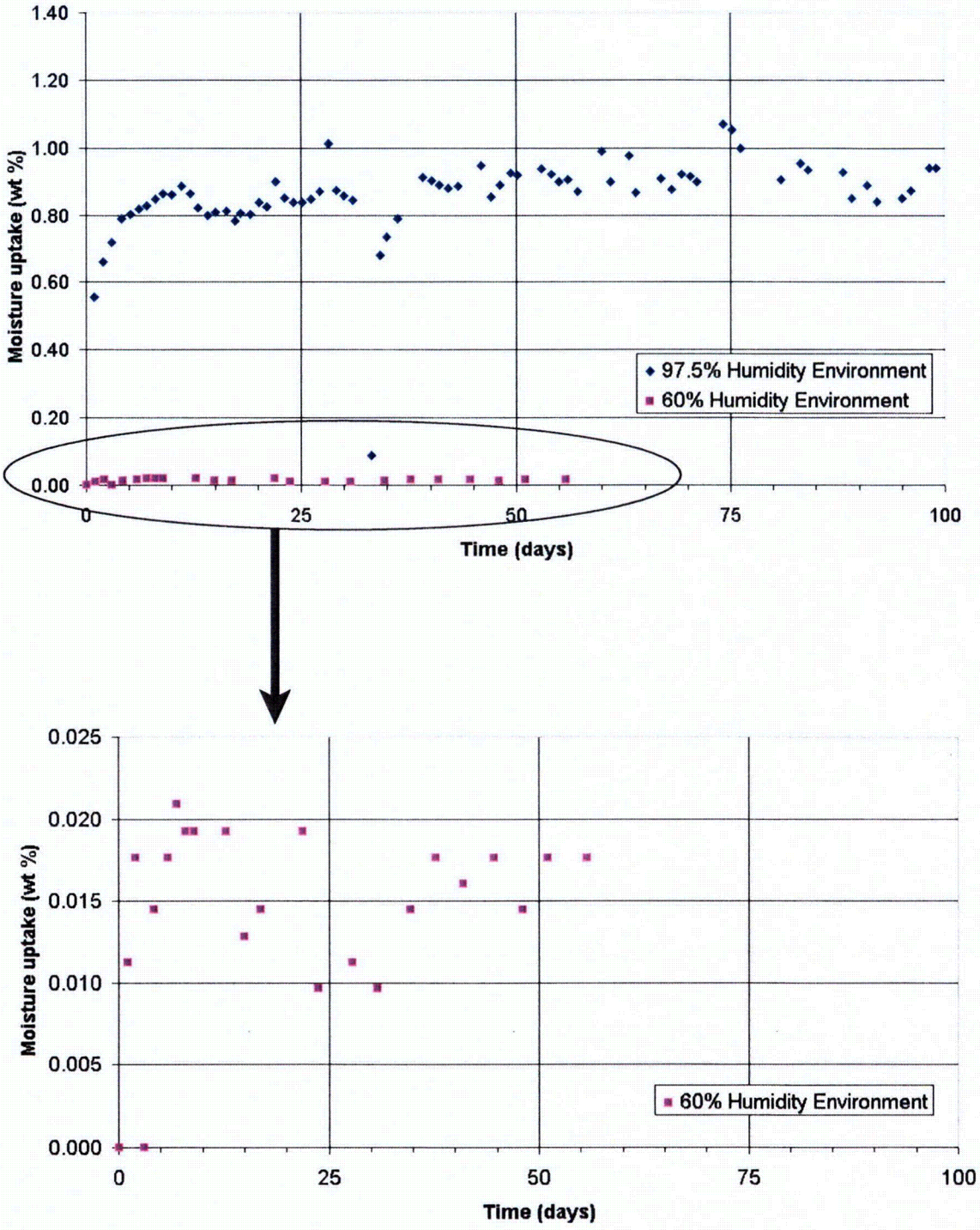

Fig. 4.1. Moisture uptake data for NpO_2 prepared at 650°C.

Table 4.1. Summary of gamma irradiation experiments performed

Experiment	Material[a]	Mass (g)	Total dose (MGy)
^{60}Co Np Tube 1	NpO_2 (650°C)	3.9593	4.2
^{60}Co Np Tube 2	NpO_2 (650°C) + 8 wt % H_2O	4.3152	4.1
^{60}Co Np Tube 3	NpO_2 (650°C) + 1 wt % H_2O	3.9832	4.2
^{60}Co Np Tube 4	NpO_2 (800°C) + 1 wt % H_2O	3.9886	4.2
HFIR Np Tube 1	NpO_2 (650°C)	3.9530	613
HFIR Np Tube 2	NpO_2 (650°C) + 1 wt % H_2O	3.9908	612
HFIR Np Tube 3	NpO_2 (650°C) + 8 wt % H_2O	4.2806	595
HFIR Np Tube 4	NpO_2 (800°C) + 1 wt % H_2O	4.0227	611

[a] Value in parenthesis denotes preparation temperature.

4.2.1 Pressure Measurements

Pressure within the sample containers was monitored throughout the irradiations, and the pressure data from each of the gamma radiolysis experiments are shown in Figs. 4.2–4.9. The pressure and gas yield (millimoles of gas per gram of sample) are plotted as a function of dose in each of the figures. The gas yield was calculated using the ideal gas law.

Container temperatures in the ^{60}Co irradiator were measured to be about 28°C. For the HFIR multiple-vessel irradiations, the temperature was estimated to average about 55°C, based on earlier experiments.[3] For this earlier work, the temperature typically ranged from 50 to 60°C, with several short transients upon insertion of the experiment into a fresh element. The difference in temperature between the ^{60}Co and HFIR irradiations did not appear to have a measurable effect on the irradiation results, other than accounting for the slight pressure differences due to gas expansion.

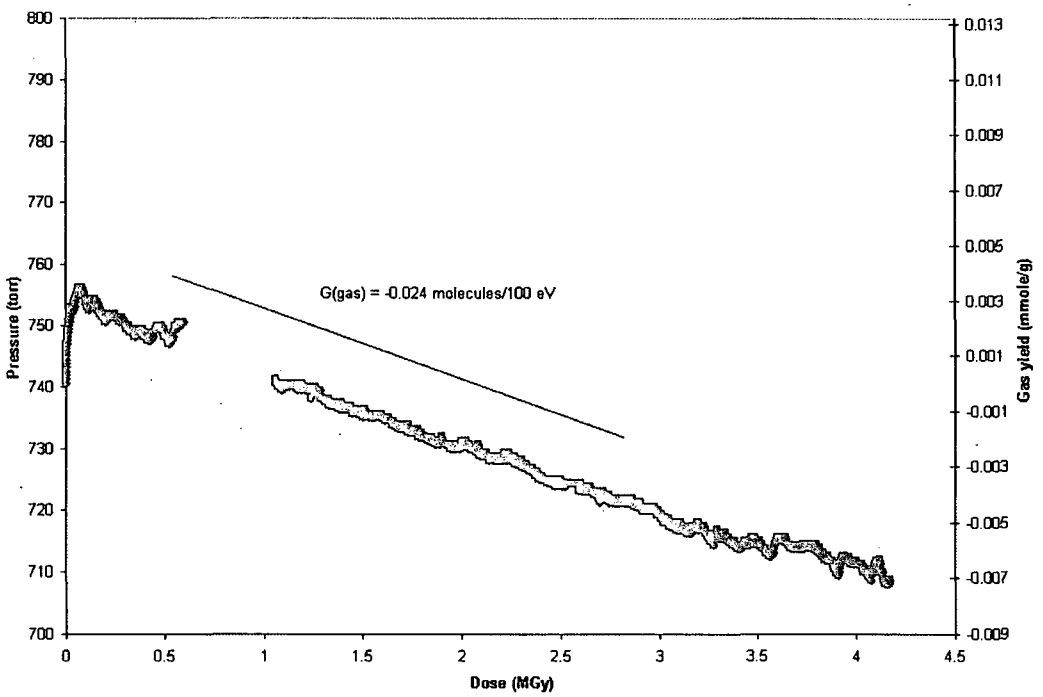

Fig. 4.2. Pressure and gas yield as a function of dose for sample ^{60}Co Np Tube 1 [^{60}Co-irradiated NpO_2 (650°C)].

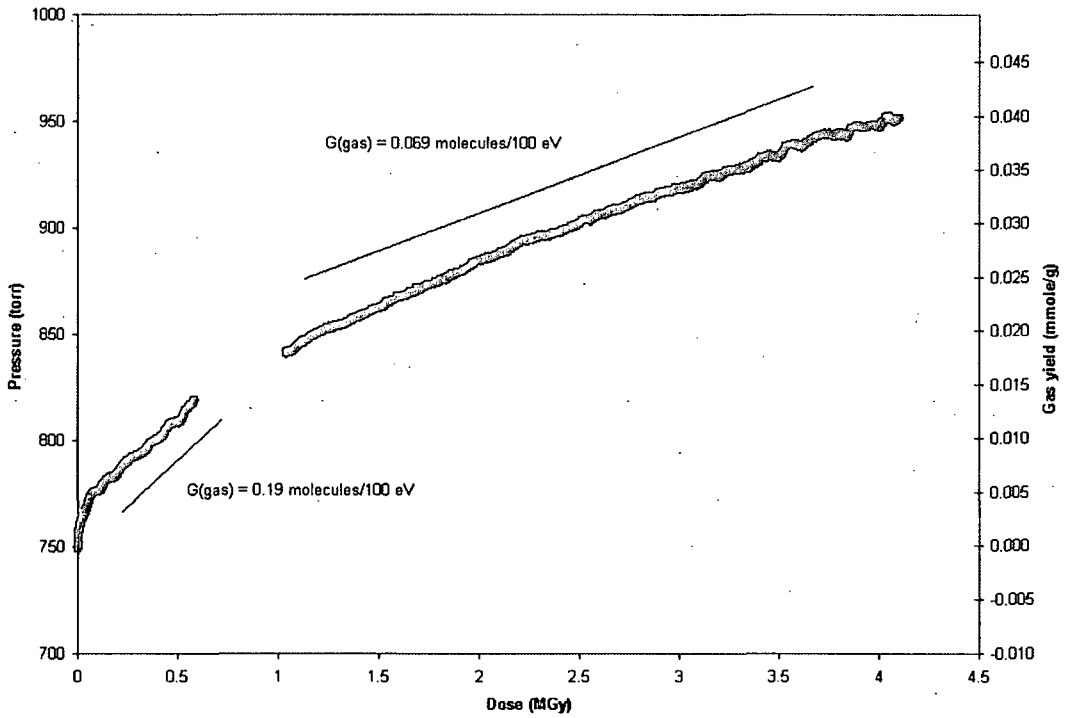

Fig. 4.3. Pressure and gas yield as a function of dose for sample ^{60}Co Np Tube 2 [^{60}Co-irradiated NpO_2 (650°C) + 8 wt % H_2O].

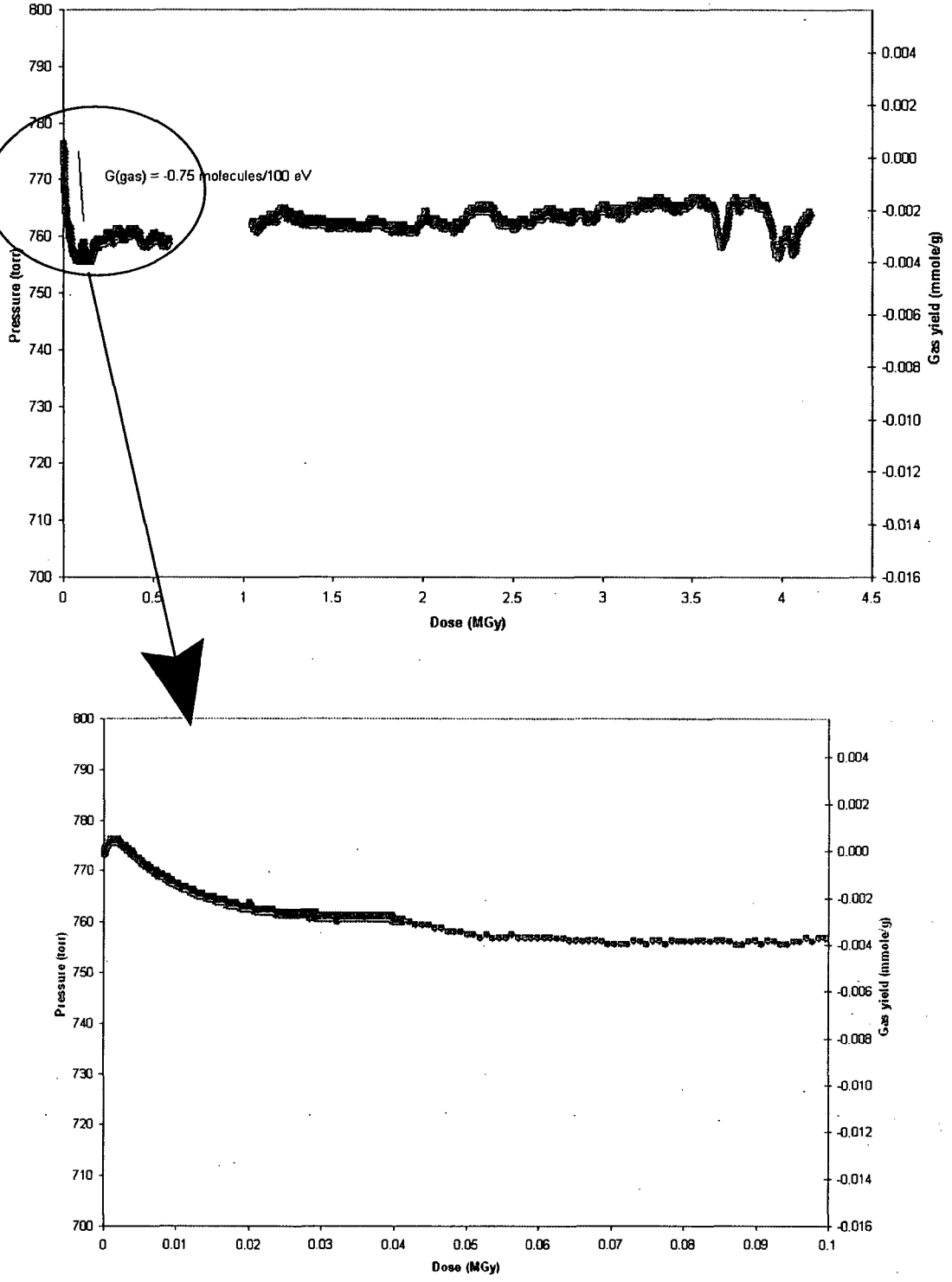

Fig. 4.4. Pressure and gas yield as a function of dose for sample ^{60}Co Np Tube 3 [^{60}Co-irradiated NpO_2 (650°C) + 1 wt % H_2O].

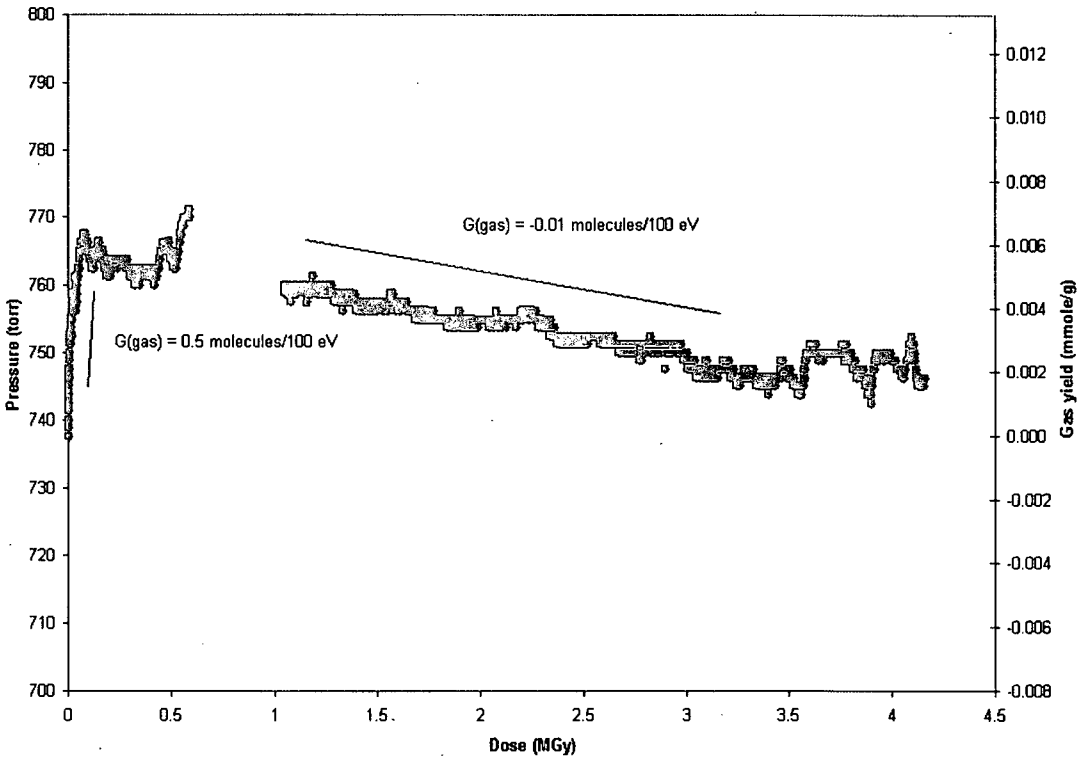

Fig. 4.5. Pressure and gas yield as a function of dose for sample ^{60}Co Np Tube 4 [^{60}Co-irradiated NpO_2 (800°C) + 1 wt % H_2O].

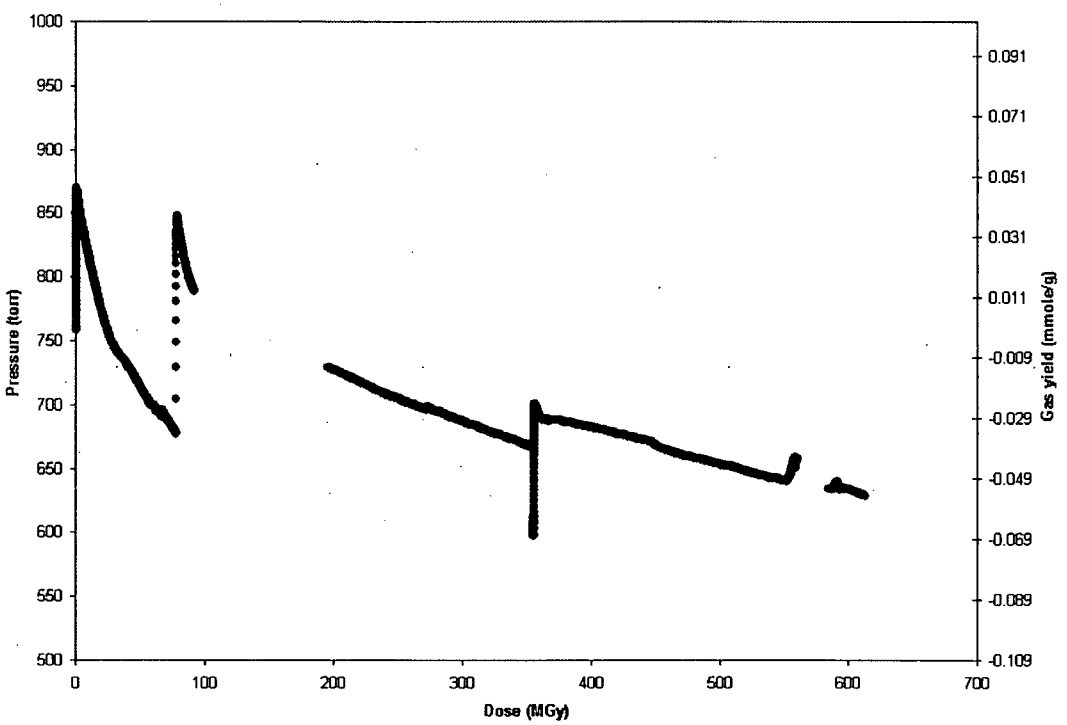

Fig. 4.6. Pressure and gas yield as a function of dose for sample HFIR Np Tube 1 [HFIR SNF-irradiated NpO_2 (650°C)].

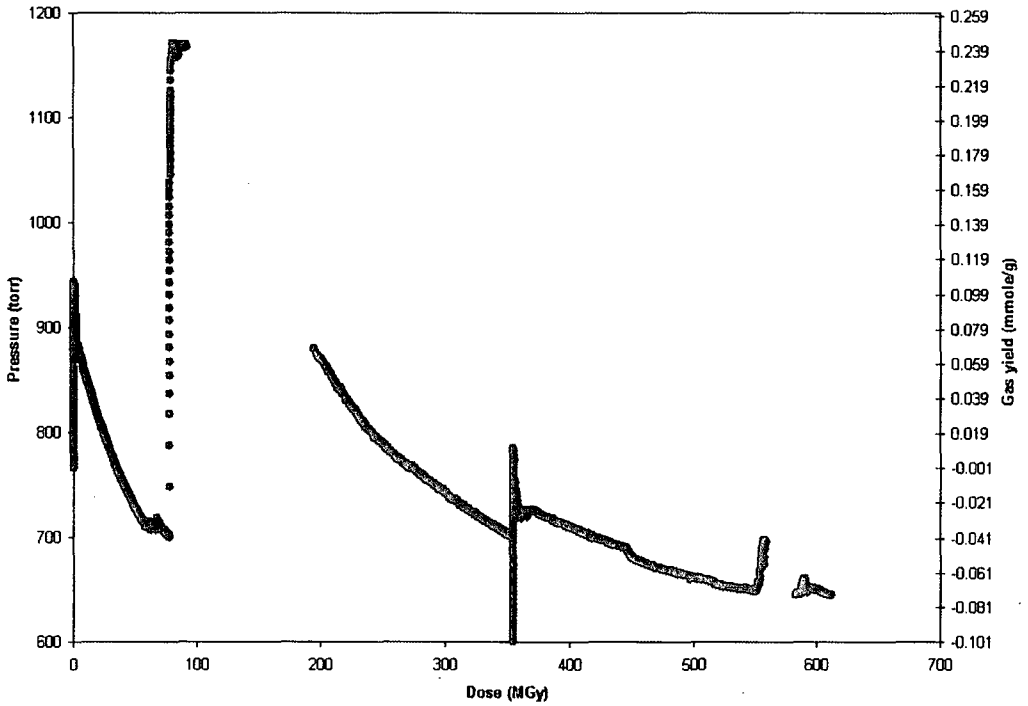

Fig. 4.7. Pressure and gas yield as a function of dose for sample HFIR Np Tube 2 [HFIR SNF-irradiated NpO_2 (650°C) + 1 wt % H_2O].

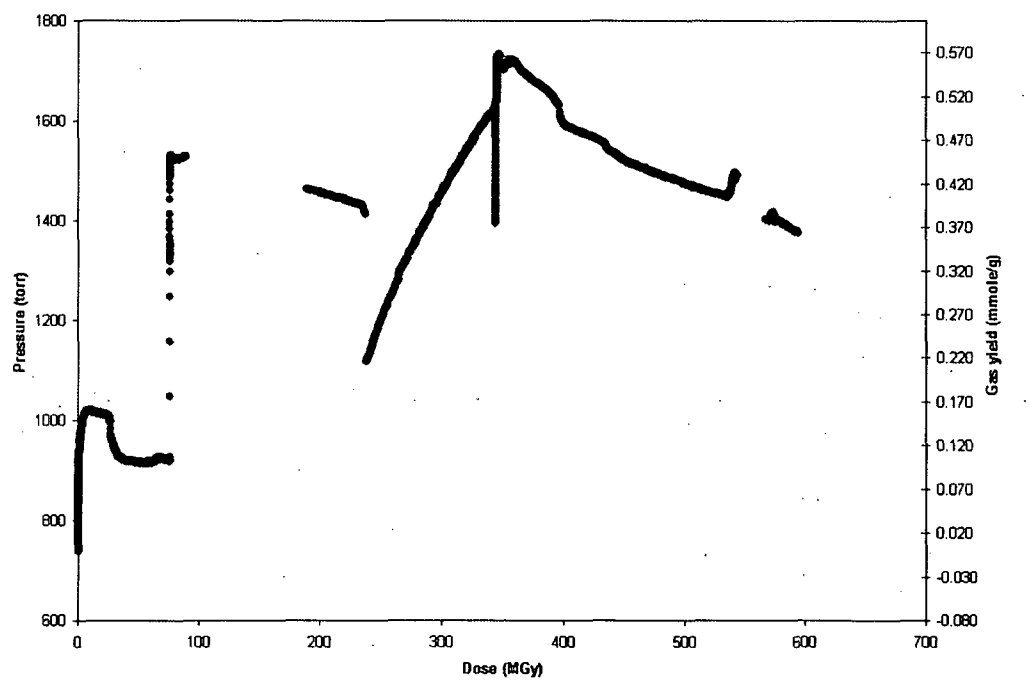

Fig. 4.8. Pressure and gas yield as a function of dose for sample HFIR Np Tube 3 [HFIR SNF-irradiated NpO_2 (650°C) + 8 wt % H_2O].

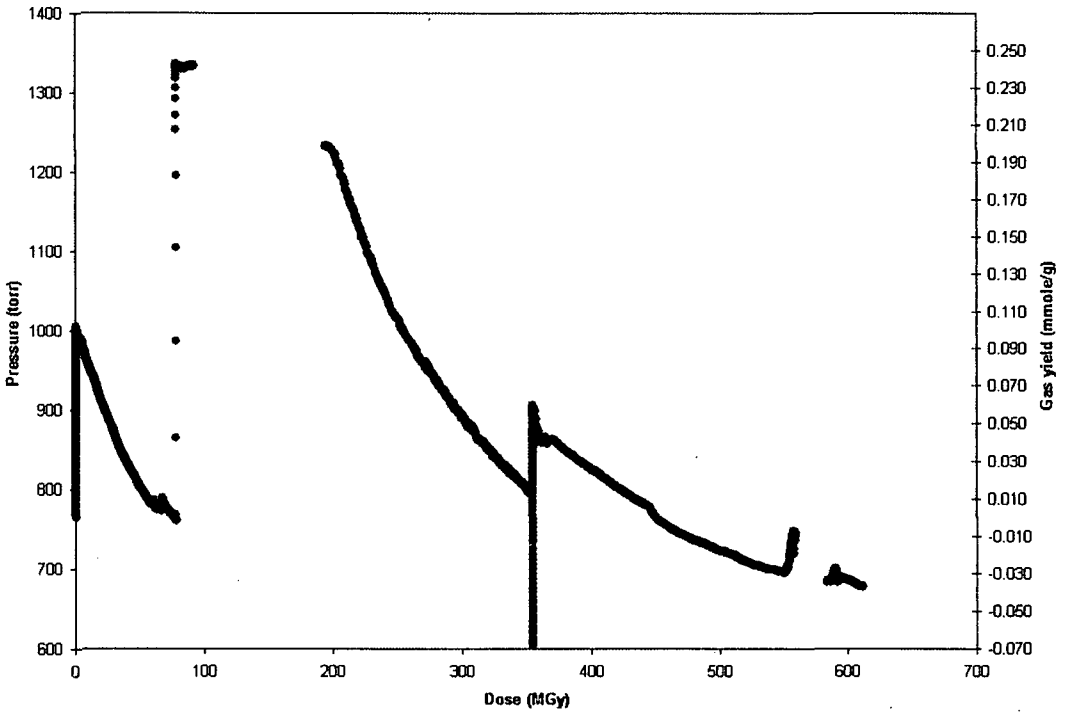

Fig. 4.9. Pressure and gas yield as a function of dose for sample HFIR Np Tube 4 [HFIR SNF-irradiated NpO_2 (800°C) + 1 wt % H_2O].

The gap in the data for the ^{60}Co irradiations between about 0.5 and 1 MGy for Figs. 4.2–4.5 occurs because the data acquisition system was not working properly during that period. The slope of the gas yield vs dose curve gives (with unit conversion) the G-values that are indicated on the figures for the ^{60}Co experiments.

For the ^{60}Co experiments, the sample that was dry (Fig. 4.2) showed a small pressure increase, followed by a steady pressure decrease. Most of the increase can be attributed to the slight heating of the sample upon insertion into the irradiator. For the sample that contained 8 wt % moisture (Fig. 4.3), a steady pressure increase was seen. However, the rate of increase appears to slow with higher doses—as evidenced by the two G-values on the plot. This change in slope (G-value) is typical of an approach to a steady-state kinetic condition. The two ^{60}Co-irradiated samples that contained 1 wt % moisture showed a slightly different behavior. The sample prepared at 650°C (Fig. 4.4) showed a small initial pressure increase (from about 773 to 778 torr, see insert), followed by a rather rapid pressure decrease to essentially a steady-state value of about 760 torr. The sample prepared at 800°C (Fig. 4.5) had an initial pressure increase, which, similar to that presented in Fig. 4.4, could represent the combined effect of heating the sample (with a concomitant increase in vapor pressure of the moisture on the sample) and radiolysis of the moisture on the sample. Afterwards, the pressure was seen to steadily decrease.

For each of the HFIR SNF experiments (Figs. 4.6–4.9), a number of pressure transients are seen (i.e., at about 0, 90, and 350 MGy). These transients correspond to the insertion of the experiment into a fresh SNF element (i.e., one that was more recently discharged from the reactor and therefore of much greater gamma intensity).* The transient seen at about 550 MGy reflects an adjustment in the SNF pool temperature. The gap in the data shown in Figs. 4.6–4.9 between about 100 and 200 MGy occurred because the data acquisition system was not working properly during that period.

Each of the HFIR SNF-irradiated samples generally exhibited a similar behavior. Upon insertion into a fuel element, a pressure increase was observed, followed by a pressure decrease. In fact, if one disregards the transients, the overall trend is a pressure decrease. The increases during the transients are larger for the moisture-loaded samples (Figs. 4.7–4.9) than for the dry sample (Fig. 4.6). Again, the combined effects of heating and radiolysis are occurring during these transients.

In Fig. 4.8, which represents a HFIR sample that is heavily loaded with water, an additional transient is seen between about 220 and 350 MGy. The pressure is observed to quickly drop and then rise steadily. Otherwise, the behavior is very similar to that for the other samples. No explanation has been found for this transient, nor did time permit further exploration of this observation.

4.2.2 Gas Analyses

Results from the gas samples withdrawn from the containers at the completion of the irradiations are presented in Tables 4.2 and 4.3 for the ^{60}Co and the HFIR SNF experiments, respectively. Pressure and temperature data are also included in the tables. The values labeled as "initial" are those at the beginning of the experiment. The "final" values were taken just prior to withdrawal of the gas sample. As indicated in the tables, both the ^{60}Co and HFIR SNF experiments were loaded in air. However, there was a small amount of residual helium in each of the containers after leak testing.

To provide better insight into the change in the gas composition as a result of irradiation, the changes in the number of moles of O_2, CO_2, and H_2 were calculated by assuming that the starting sample atmosphere was the standard air composition (less any residual helium in the sample tubes).[12] The results of these calculations are shown in Table 4.4 . To put the measured H_2 yields in perspective, Table 4.5 provides the H_2 yields as a mole percentage of the initial amount of water available for radiolysis. Additionally, for the samples that had a net oxygen production, the O_2-plus-CO_2 yields as a mole percentage of the initial amount of water available for radiolysis are presented in Table 4.5.

The gas analysis for the ^{60}Co-irradiated samples containing ≤ 1 wt % H_2O showed, in general, O_2 consumption and a small amount of H_2 production (<1 vol %). A small amount of NO_x was also detected

* The insertion into a fresher element increases both the sample temperature and the radiolysis of any moisture that is present.

for each of the samples, which is a typical occurrence in the radiolysis of moist air.[13–15] Because this phenomenon is of no significance in the interpretation of the overall radiolysis experiments, it is not discussed further. The ^{60}Co-irradiated sample containing 8 wt % H_2O—which was clearly much greater than any amount of moisture possible by physi- or chemisorption—exhibited both H_2 and O_2 production. In fact, Table 4.4 shows that this production was nearly stoichiometric. For the 1 wt % moisture-laden samples, the O_2 consumption is nearly balanced by CO_2 production. For the dry NpO_2, the CO_2 production is about one-tenth the O_2 consumption. For each of the ^{60}Co-irradiated samples that contained water, a very small percentage of the available water was found as H_2 gas after irradiation (Table 4.5).

Table 4.2. Results of mass spectrometric analysis of gas composition from ^{60}Co-irradiated NpO_2 samples

	^{60}Co Np Tube 1 [NpO_2 (650°C)]	^{60}Co Np Tube 2 [NpO_2 (650°C) + 8 wt % H_2O]	^{60}Co Np Tube 3 [NpO_2 (650°C) + 1 wt % H_2O]	^{60}Co Np Tube 4 [NpO_2 (800°C) + 1 wt % H_2O]
Initial atmosphere	Air	Air	Air	Air
Initial pressure[a] (torr)	741	749	773	738
Initial temperature[a] (°C)	22	22	22	22
Final pressure[b] (torr)	709	952	764	746
Final temperature[b] (°C)	25	25	25	25
	Gas composition (vol %)			
CO_2	0.89	1.1	2.05	4.9
Ar	1.04	0.8	0.98	1.01
O_2	15.07	21.08	18.22	13.38
N_2	80.13	62.4	74.52	77.32
H_2	0.01	12.01	0.94	0.24
He	2.25	2.07	2.9	1.7
H_2O	0.48	0.35	0.1	0.09
NO_x	0.1	0.03	0.13	1.22

[a] Value at beginning of the experiment.
[b] Value just prior to withdrawal of gas sample.

Table 4.3. Results of mass spectrometric analysis of gas composition from HFIR SNF-irradiated NpO_2 samples

	HFIR Np Tube 1 [NpO_2 (650°C)]	HFIR Np Tube 2 [NpO_2 (650°C) + 1 wt % H_2O]	HFIR Np Tube 3 [NpO_2 (650°C) + 8 wt % H_2O]	HFIR Np Tube 4 [NpO_2 (800°C) + 1 wt % H_2O]
Initial atmosphere	Air	Air	Air	Air
Initial pressure[a] (torr)	759	766	739	766
Initial temperature[a,b] (°C)	40	40	40	40
Final pressure[c] (torr)	629	645	1376	678
Final temperature[c,d] (°C)	55	55	55	55
	Gas composition (vol %)			
CO_2	2.32	0.04	0.005	1.68
Ar	1.23	1.27	0.59	1.22
O_2	3.21	0.06	16.84	0.04
N_2	90.09	96.13	45.96	96.6
H_2	0.05	0.006	35.46	0.026
He	2.05	1.9	0.9	0.13
CO	0.1	<0.01	<0.01	<0.01
NO_x	0.9	0.54	0.16	0.15

[a] Value at beginning of the experiment.
[b] Typical SNF pool temperature.
[c] Value just prior to withdrawal of gas sample.
[d] Average temperature of container inside element (based on previous experiments).

Table 4.4. Estimated change in gas composition for selected experiments as a result of radiolysis

Experiment	Material[a]	Δ O_2 (mol)	Δ CO_2 (mol)	Δ H_2 (mol)
^{60}Co Np Tube 1	NpO_2 (650°C)	-4.1×10^{-5}	5.3×10^{-6}	6.2×10^{-8}
^{60}Co Np Tube 2	NpO_2 (650°C) + 8 wt % H_2O	3.9×10^{-5}	8.7×10^{-6}	9.8×10^{-5}
^{60}Co Np Tube 3	NpO_2 (650°C) + 1 wt % H_2O	-1.7×10^{-5}	1.3×10^{-5}	6.2×10^{-6}
^{60}Co Np Tube 4	NpO_2 (800°C) + 1 wt % H_2O	-4.5×10^{-5}	3.7×10^{-5}	1.5×10^{-6}
HFIR Np Tube 1	NpO_2 (650°C)	-2.4×10^{-4}	2.4×10^{-5}	5.3×10^{-7}
HFIR Np Tube 2	NpO_2 (650°C) + 1 wt % H_2O	-4.0×10^{-4}	2.4×10^{-8}	9.3×10^{-8}
HFIR Np Tube 3	NpO_2 (650°C) + 8 wt % H_2O	1.8×10^{-4}	-4.2×10^{-7}	1.2×10^{-3}
HFIR Np Tube 4	NpO_2 (800°) + 1 wt % H_2O	-2.9×10^{-4}	1.9×10^{-5}	3.0×10^{-7}
Alpha Np Tube 1	NpO_2 (650°C)	-5.4×10^{-5}	6.5×10^{-6}	8.7×10^{-7}
Alpha Np Tube 2	NpO_2 (650°C) + 1 wt % H_2O	5.2×10^{-5}	-9.6×10^{-8}	1.1×10^{-4}
Alpha Np Tube 3 (first gas sample)	NpO_2 (650°C) + 8 wt % H_2O	8.7×10^{-4}	1.2×10^{-6}	1.7×10^{-3}
Alpha Np Tube 4	NpO_2 (800°C) + 1 wt % H_2O	7.5×10^{-6}	4.1×10^{-7}	8.1×10^{-5}
Alpha Np Tube 5	NpO_2 (650°C) + 0.5 wt % H_2O	*b*	*b*	6.9×10^{-6}

[a] Value in parenthesis denotes preparation temperature.

[b] Excess O_2 was initially present in transducer region of sample; therefore, change in O_2 and CO_2 cannot be estimated.

Table 4.5. Estimated H_2 production as a percentage of initial amount of water available for radiolysis

Experiment	Material[a]	Ratio of H_2 production to water available for radiolysis (mol %)	Ratio of $O_2 + CO_2$ production to water available for radiolysis (mol %)
^{60}Co Np Tube 2	NpO_2 (650°C) + 8 wt % H_2O	0.55	0.27
^{60}Co Np Tube 3	NpO_2 (650°C) + 1 wt % H_2O	0.28	*b*
^{60}Co Np Tube 4	NpO_2 (800°C) + 1 wt % H_2O	0.068	*b*
HFIR Np Tube 2	NpO_2 (650°C) + 1 wt % H_2O	0.0042	*b*
HFIR Np Tube 3	NpO_2 (650°C) + 8 wt % H_2O	6.7	0.99
HFIR Np Tube 4	NpO_2 (800°C) + 1 wt % H_2O	0.014	*b*
Alpha Np Tube 2	NpO_2 (650°C) + 1 wt % H_2O	6.8	3.2
Alpha Np Tube 3 (after first gas sample)	NpO_2 (650°C) + 8 wt % H_2O	13	6.6
Alpha Np Tube 4	NpO_2 (800°C) + 1 wt % H_2O	4.7	0.46
Alpha Np Tube 5	NpO_2 (650°C) + 0.5 wt % H_2O	0.8	*c*

[a] Value in parenthesis denotes preparation temperature.
[b] For this sample, there was a net consumption of O_2.
[c] Not available, because the initial O_2 composition over the sample was not well known.

The NpO_2 samples containing ≤ 1 wt % H_2O that were irradiated in HFIR SNF elements (Figs. 4.6, 4.7, and 4.9) exhibited an overall pressure decrease. The gas analyses for these samples showed that the O_2 was almost completely consumed while only a trace of H_2 was produced. The CO_2 production was ≤10% of the O_2 consumption for HFIR Np Tube 1 and HFIR Np Tube 4. Only a trace of CO_2 was produced for HFIR Np Tube 2. By contrast, the sample containing 8% water (Fig. 4.8) had a net pressure increase. In this experiment, the pressure appeared to peak and then slowly decrease. The gas analysis for the 8% sample showed that a rather large amount of H_2 (~35 vol %, Table 4.3) was produced. It also appears from this table alone that a stoichiometric amount of O_2 was produced; however, closer examination of the net change in each component (Table 4.4) shows that the net O_2 production was 15% of the hydrogen production. Only in the case of HFIR Np Tube 3 was the H_2 production a significant fraction of the available H_2O (Table 4.5).

4.3 ALPHA RADIOLYSIS EXPERIMENTS

Table 4.6 provides a summary of the alpha irradiation experiments that were performed. Irradiation times ranged from 110 to 295 days. Considering the higher dose rate of the ^{244}Cm as compared with the ^{238}Pu (see Fig. 3.8), this would correspond to equivalent irradiation times ranging from 21 to 57 years for the SRS neptunium.

Table 4.6. Summary of alpha irradiation experiments performed

Experiment	Material[a]	Mass (g)	^{244}Cm added (mg)	Total dose (MGy)[b]
Alpha Np Tube 1	NpO_2 (650°C)	2.95	18.72	280
Alpha Np Tube 2	NpO_2 (650°C) + 1 wt % H_2O	2.96996	18.66	439
Alpha Np Tube 3	NpO_2 (650°C) + 8 wt % H_2O	3.175	18.66	410
Alpha Np Tube 4	NpO_2 (800°C) + 1 wt % H_2O	3.130	19.68	439
Alpha Np Tube 5	NpO_2 (650°C) + 0.5 wt % H_2O	2.96475	18.72	166

[a]Value in parenthesis denotes preparation temperature.
[b]Dose calculated by depositing all of the alpha decay energy in the sample (i.e., NpO_2 + H_2O).

4.3.1 Pressure Measurements

Pressure within the sample containers was monitored throughout the irradiations, and the pressure data from each of the experiments are shown in Figs. 4.10–4.14. G-values, which were calculated from the slope of the curves, are also presented in these figures.

The dry NpO_2 sample (Fig. 4.10) exhibited a steady pressure decrease. As seen in Fig. 4.10, a gas sample was withdrawn from Alpha Np Tube 1 after a dose of about 140 MGy. The tube was then backfilled with O_2 to a total pressure of about 1350 torr. The pressure again decreased, although at what appears to be at a higher rate than previously seen. Additionally, with increasing dose, the pressure appears to approach a steady state. After about 280-MGy total dose, this tube (which contained dry NpO_2) was opened and 0.5 wt % moisture was added. This sample then became experiment Alpha Np Tube 5 (Fig. 4.14).

Both of the samples that contained 1 wt % moisture (Figs. 4.11 and 4.13) exhibited similar behavior. The pressure steadily increased and approached what appeared to be a plateau. A gas sample was withdrawn from Alpha Np Tube 2 (Fig. 4.11) after a dose of about 140 MGy. The tube was then vented to the glove box and isolated. The experiment continued, whereupon the pressure increased slightly, followed by an overall decrease. Hence, the plateau that was seen just before gas sampling was probably a peak—one that would have been followed by a pressure decrease had a gas sample not been withdrawn.

Similar to Alpha Np Tube 2, a gas sample was withdrawn from Alpha Np Tube 4 after a dose of about 140 MGy (Fig. 4.13). This tube was then vented to the glove box and resealed, and the experiment continued. Again, the pressure increased slightly, followed by a decrease.

For Alpha Np Tube 3 (Fig. 4.12), gas samples were withdrawn after about 80- and 130-MGy total dose. The tube was vented to the glove box (no gas sample taken) after a dose of almost 250 MGy. It was then resealed, and the experiment was continued. However, a final gas sample was not withdrawn. Throughout the irradiation of Alpha Np Tube 3, a steady pressure increase was noted. After each sample withdrawal or pressure reduction, the rate of pressure increase slowed, as shown by comparing the G-values for each segment. These decreasing G-values again indicate the approach to a steady state.

The sample that contained the 0.5 wt % moisture (Fig. 4.14) showed a steady pressure increase to a plateau. This sample had originally been the dry NpO_2 (Alpha Np Tube 1), which had been exposed to excess oxygen. As seen in Fig. 4.14, a gas sample was withdrawn from Alpha Np Tube 5 after a total dose of about 130 MGy.

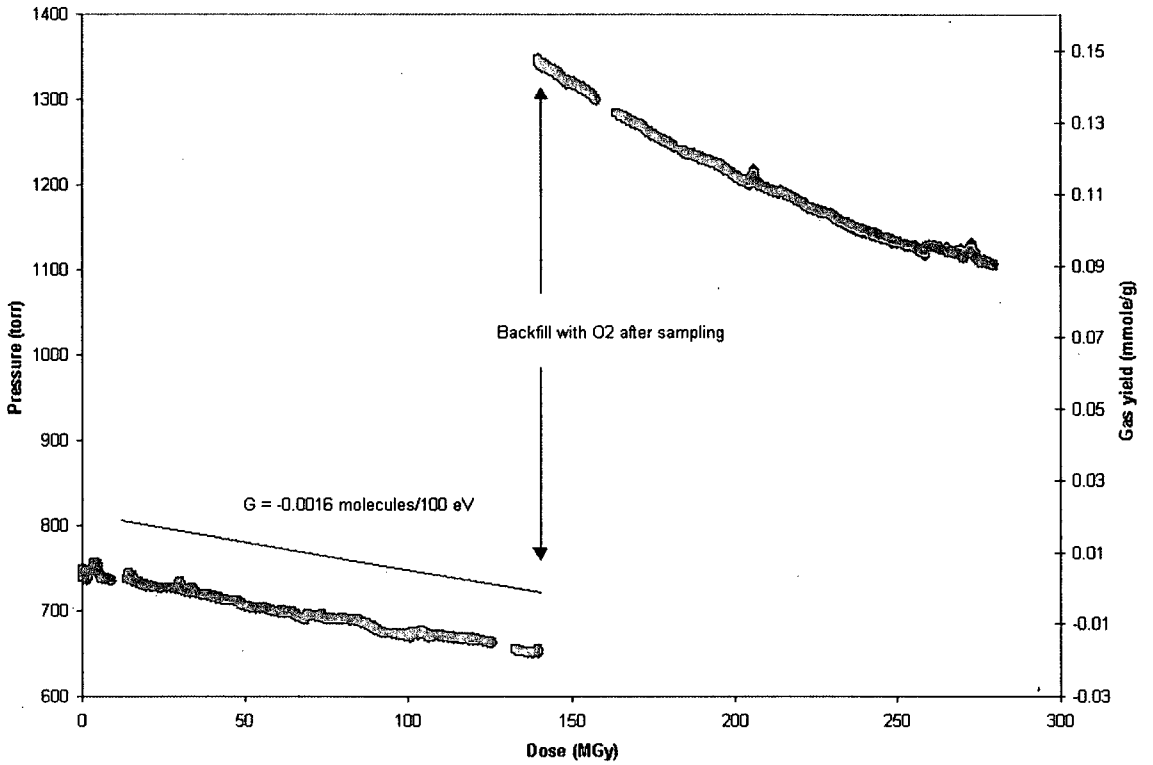

Fig. 4.10. Pressure and gas yield as a function of dose for sample Alpha Np Tube 1 [^{244}Cm alpha-irradiated NpO_2 (650°C)].

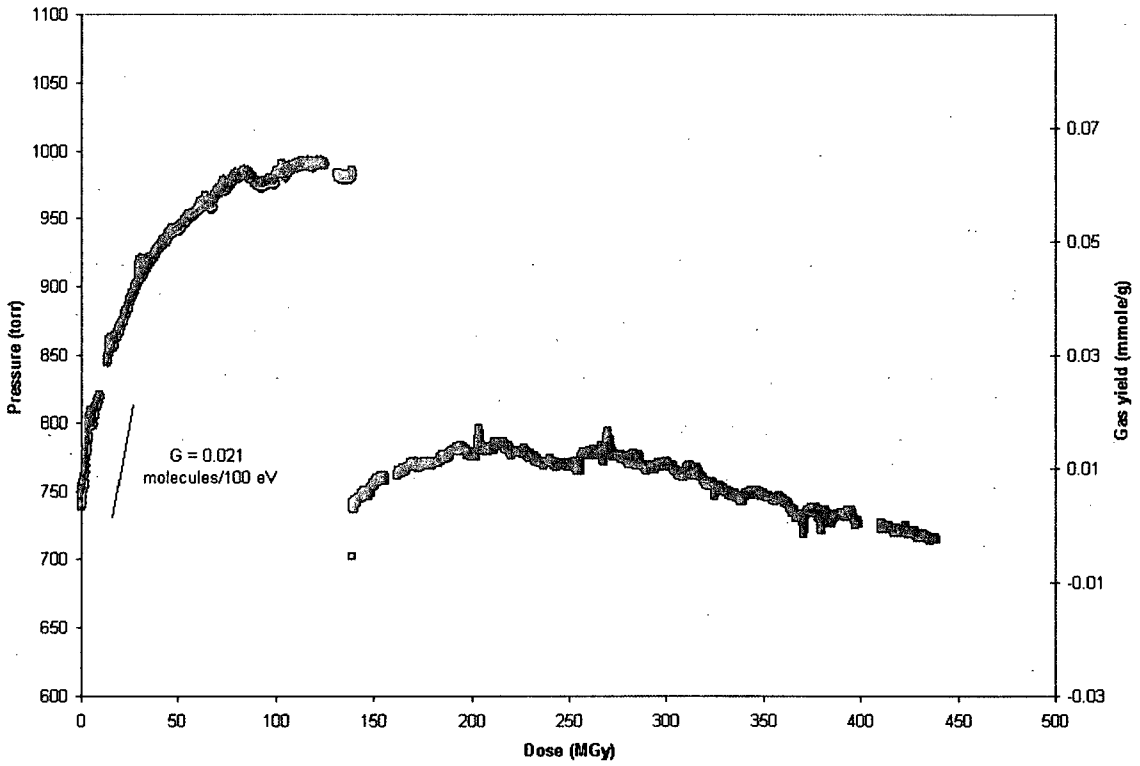

Fig. 4.11. Pressure and gas yield as a function of dose for sample Alpha Np Tube 2 [^{244}Cm alpha-irradiated NpO_2 (650°) + 1 wt % H_2O].

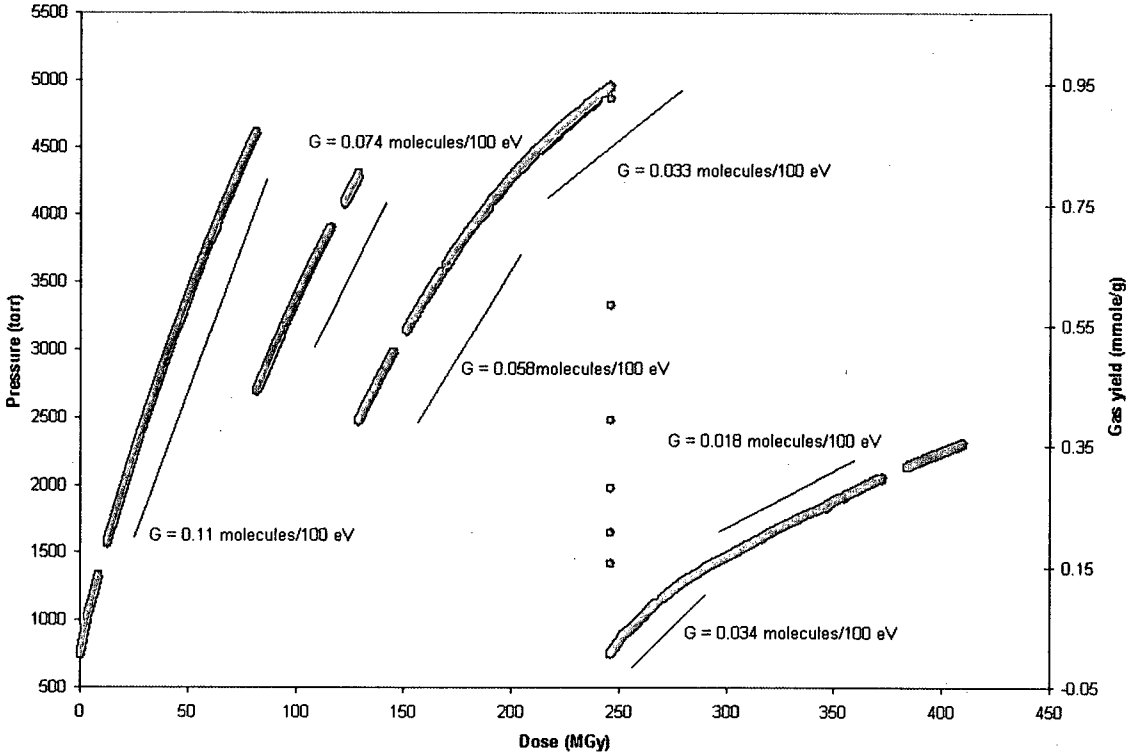

Fig. 4.12. Pressure and gas yield as a function of dose for sample Alpha Np Tube 3 [^{244}Cm alpha-irradiated NpO_2 (650°C) + 8 wt % H_2O].

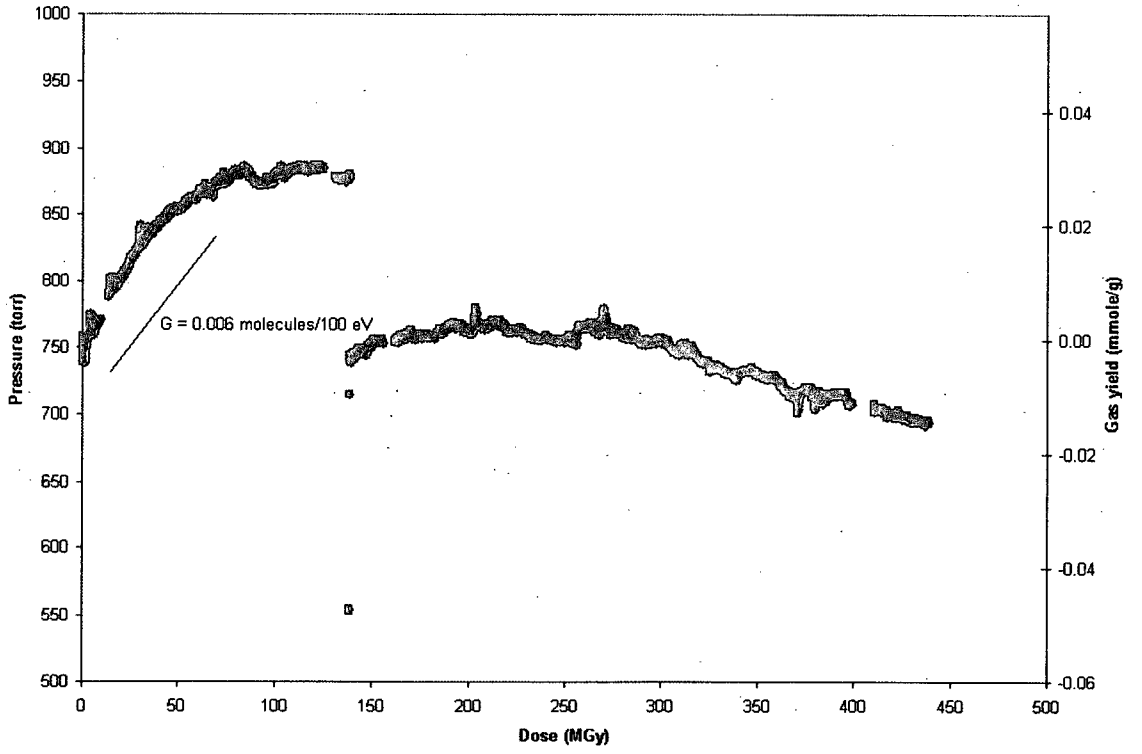

Fig. 4.13. Pressure and gas yield as a function of dose for sample Alpha Np Tube 4 [^{244}Cm alpha-irradiated NpO_2 (800°C) + 1 wt % H_2O].

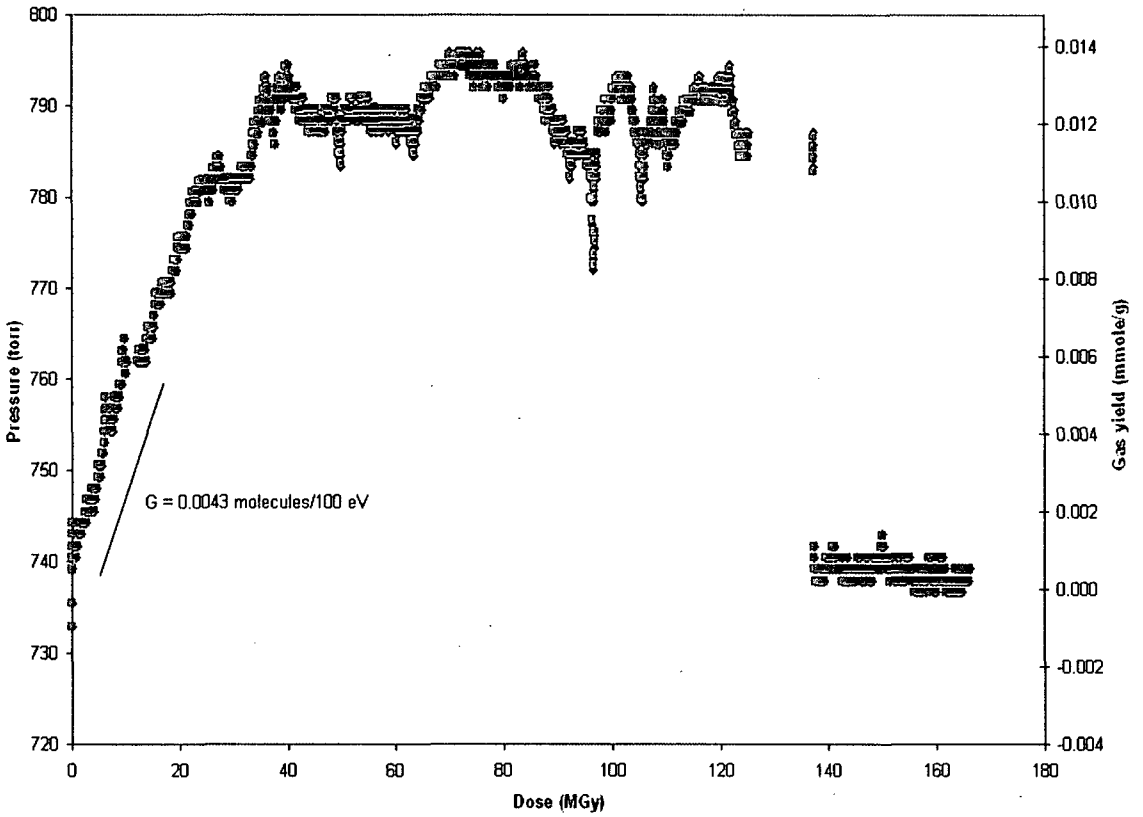

Fig. 4.14. Pressure and gas yield as a function of dose for sample Alpha Np Tube 5 [^{244}Cm alpha-irradiated NpO_2 (650°C) + 0.5 wt % H_2O].

4.3.2 Gas Analyses

Gas samples were periodically withdrawn from the containers during the experiments. Analytical results for these samples are presented in Table 4.7, which also includes pressure and temperature data. As in the gamma irradiation experiments, the values labeled as "initial" are those at the beginning of the experiment or, in the case of multiple gas samples, the value just after sampling. The "final" values are taken just prior to withdrawal of the gas sample.

The calculated changes in the moles of O_2, CO_2, and H_2 (assuming that the starting sample atmosphere was the standard air composition,[12] less any residual helium in the sample tubes) are shown in Table 4.4. (No such calculation was made for Alpha Np Tube 5. While air was present immediately over this sample, the sample initially had additional O_2 and helium that were present in the pressure-transducer region.) Table 4.5 provides (1) H_2 yields and (2) O_2-plus-CO_2 yields (for the samples that had a net oxygen production) as a mole percentage of the initial amount of water available for radiolysis.

Table 4.7. Results of mass spectrometric analysis of gas composition from alpha-irradiated NpO_2 samples

	Alpha Np Tube 1 NpO_2 (650°C)	Alpha Np Tube 2 NpO_2 (650°C) + 1 wt % H_2O	Alpha Np Tube 3 NpO_2 (650°C) + 8 wt % H_2O		Alpha Np Tube 4 NpO_2 (800°C) + 1 wt % H_2O	Alpha Np Tube 5 NpO_2 (650°C) + 0.5 wt % H_2O
			First gas sample	Second gas sample		
Initial atmosphere	Air	Air	Air	First gas sample composition (no helium)	Air	Air/excess O_2[a]
Initial pressure[b] (torr)	739	738	740	2683	740	735
Initial temperature[b] (°C)	19.5	17.2	18.3	18.9	19.5	19.8
Final pressure[c] (torr)	656	986	4601	4292	881	786
Final temperature[c] (°C)	19.6	19.6	18.9	18.5	19.1	23.0
	Gas composition (vol %)					
CO_2	0.9	0.1	0.04	0.025	0.07	0.02
Ar	0.65	0.54	0.2	0.1	0.61	0.47
O_2	7.4	17.27	28.9	30.16	14.26	42.63
N_2	52.0	44.4	17.52	7.95	50.79	54.11
H_2	0.12	11.72	50.26	58.57	9.54	1.27
He[d]	38.03	25.55	2.85	2.97	23.92	1.09
H_2O	0.2	0.1		0.2	0.2	
NO_x	0.6	0.39	0.05	0.02	0.6	0.4
CH_4	0.004	0.003	<0.01	<0.01	0.005	<0.01
CO	<0.01	<0.01	<0.01	<0.01	<0.01	0.006

[a] Tube 5 was made by taking the Tube 1 experiment and adding 0.5 wt % water. Prior to this addition, Tube 1 had been backfilled with O_2. Because the pressure transducer and sampling line were not flushed with air prior to the water addition, the initial atmosphere in the pressure-transducer region likely had an excess of O_2. The atmosphere directly over the sample was air.

[b] Value at beginning of experiment or just after previous gas-sampling operation.

[c] Value just prior to withdrawal of gas sample.

[d] Helium was an artifact of the sampling method.

The dry NpO_2 sample that was irradiated with the alpha from ^{244}Cm (Fig. 4.10) showed a pressure decrease to vacuum (i.e., a pressure less than atmospheric). The gas sample from this experiment confirmed that O_2 was consumed. After the gas sample was withdrawn, this container was backfilled with O_2 and the sample pressure continued to decrease, likely from further O_2 consumption. (A final gas sample was not withdrawn.)

Both of the alpha-irradiated NpO_2 samples that had 1 wt % sorbed moisture exhibited a pressure increase to an apparent steady-state plateau at ~100–130 MGy (Figs. 4.11 and 4.13). The sample prepared at 650°C increased about 250 torr, while that prepared at 800°C increased about 140 torr. The steady-state plateau represents a situation in which back reactions (i.e., H_2 and O_2 recombination) balance forward reactions (i.e., H_2 and O_2 production). The gas analysis results for these two experiments revealed that both H_2 and O_2 were produced. For Alpha Np Tube 2, a stoichiometric mixture of H_2 and O_2 was present at the plateau. However, for Alpha Np Tube 4, the O_2 production was only about 10% of the H_2 production (Table 4.4). A small amount of NO_x was also detected. After sampling, both tubes were vented with the glove-box atmosphere and then closed. Both experiments showed a small pressure increase followed by a decrease, probably indicating the consumption of some excess O_2 in the system, as was seen before in other experiments. However, a final gas sample was not taken.

The alpha-irradiated NpO_2 sample that contained 8 wt % H_2O exhibited a steady increase in pressure (Fig. 4.12). The initial gas analysis of a sample taken after 80-MGy total dose showed that both H_2 and O_2 were produced in stoichiometric proportions. A second gas sample after about 130 MGy showed further H_2 and O_2 production. As indicated in Fig. 4.12, the pressure increased at a decreasing rate; however, for this experiment, a pressure plateau had not been reached by the time the experiment was terminated.

The alpha-irradiated NpO_2 sample containing 0.5 wt % H_2O (equivalent to the limit established for the SRS material) showed a small pressure increase to a steady-state plateau (Fig. 4.14). The gas analysis showed that H_2 was produced. A conclusion about the production or depletion of O_2 cannot be made for this sample because of excess O_2 in the pressure-transducer region.* However, any O_2 production should be bounded by the results from the 1 wt % experiments.

*Alpha Np Tube 5 was prepared by opening Alpha Np Tube 1 and adding 0.5 wt % H_2O. However, the atmosphere in the experimental rig was not purged. Although glove-box air was directly over the NpO_2 sample, it is likely that a slug of O_2-rich air (from the previous operations on Alpha Np Tube 1) resided in the transducer region of the experimental rig.

4.4 OVERVIEW OF RADIOLYTIC MECHANISM

All of these experiments demonstrate some common trends. First, water radiolysis alone is a rapid process relative to other chemical processes that are occurring simultaneously. Second, when the water content is ≤1%, the overall pressure in the system *generally* decreases (or peaks after small pressure increases and then decreases). Third, oxygen is both produced and consumed as a result of radiolytic reactions and, in the long-term, consumption will be the dominant effect.* This consumption is especially evident when oxygen is added during the course of the experiment (see Fig. 4.10). Fourth, limiting pressures (steady-state plateaus) are either reached or approached. Fifth, minor products such as CO_2 and NO_x are produced. All of these phenomena are consistent with previously reported fundamental reactions and are discussed separately below.

Water radiolysis was extensively studied more than a half century ago,[16,17] when it was shown not only that the water is dissociated into *primary radical products* (ultimately forming H_2, O_2 and H_2O_2), but also that these primary radical products cause back reactions limiting the overall amount of *ultimate products*. Thus, a steady-state condition is quickly reached in which no further accumulation of ultimate products occurs—one in which the rate of dissociation of water is balanced by its rate of formation. Consequently, extreme gas product pressures from the radiolysis of water are not ordinarily possible.

Accompanying these water radiolysis reactions is another reaction in which the oxygen over solid actinide oxides in such a radiolytically activated system can oxidize the actinide solid (at least partially) to a higher oxidation state. Evidence for this is clearly seen in the oxidation of uranium oxides to higher oxidation states.[4,18,19] While a direct measurement of the oxidation state of the NpO_2 was not made (e.g., via X-ray diffraction), the disappearance of oxygen in the presence of NpO_2 is interpreted as being the result of the formation of higher neptunium oxidation states (e.g., Np_2O_5)—a reaction mechanism analogous to that observed for the uranium oxides.[4] This reaction largely accounts for the net pressure decrease in the system through the consumption of oxygen.

By using the NpO_2 sample from Alpha Np Tube 1 for the Alpha Np Tube 5 experiment, the competing reactions of (1) O_2 generation and consumption by H_2O radiolytic chemistry were separated from (2) the NpO_2 oxidation reaction. In this case, the NpO_2 was "presaturated" with oxygen prior to the addition of water in the Tube 5 test; and when the water was added, only the water radiolysis chemistry was evident (i.e., water radiolysis and back reactions to reach a steady state). The experiment in Tube 5 then showed a gradual rise to a steady-state pressure. Had this NpO_2 sample not been presaturated with

*Note that both of the alpha-irradiated samples that contained 1% H_2O appeared to reach a plateau. However, after withdrawal of a gas sample, the net effect was a pressure decrease. This result indicates that in the long term, a slower-acting mechanism (i.e., one that is slower than the forward-reaction production of O_2) will result in net O_2 consumption.

oxygen, we would predict a profile more like that of Fig. 4.11—one in which after the water radiolysis and back reactions would initially dominate, but then the slower oxygen consumption reaction by the NpO_2 would commence and begin to reduce the total pressure of the system.

Additionally, it appears that the radiochemical kinetics of such reactions (radiolysis of water and oxidation of the NpO_2) may be influenced by the type of radiation. In the case of the highly penetrating gamma radiation, the radiolysis reaction response occurs rapidly, followed by a decrease resulting from the radiolytically influenced oxidation of the NpO_2. The overall character of the gamma radiolysis experiments is then one that is dominated by oxidation of NpO_2. For the alpha radiolysis experiments, it appears that radiolysis of water dominates for a longer period of time as compared with that observed in the gamma experiments.

Also associated with the above reactions are a number of *impurity* reactions in which the primary products of water radiolysis combine with the N_2 accompanying the O_2 in the air atmosphere over the sample or with the carbon that is ubiquitous in many oxide preparations. Thus, trace amounts of NO_x and CO_2 are common impurity by-products of such oxide/water radiolysis reactions.

We can therefore explain the overall chemistry taking place during these radiolysis reactions as being a combination of the above phenomena and not just one of these isolated fundamental processes. Initially, a pressure increase often occurs in the encapsulated system, representing both a slight temperature effect and, more importantly, radiolysis of sorbed water to form some hydrogen and oxygen. This water radiolysis would reach a steady-state pressure were it not for the reaction of oxygen with the actinide oxide to form a higher oxidation state of the actinide and thus decrease the oxygen content of the atmosphere over the system. Evidence for this is seen in the "dry" oxide radiolysis experiments, in which there is no pressure increase (because there is no water to be radiolyzed)—only oxygen consumption. When there is an excessive amount of moisture (e.g., 8%, a case in which water would have to actually condense and puddle on the oxide), the water radiolysis reaction is dominant. Nevertheless, even here, *all* of the water on the sample is not radiolyzed, because of the accompanying back reactions of the primary water radiolytic products (i.e., the radicals) with the water products (H_2, O_2, etc.).

5. CONCLUSIONS

Two key results were demonstrated in these experiments. First, the water uptake experiments clearly indicated that the 0.5 wt % moisture limit that has been typically established for similar materials (e.g., uranium and plutonium oxides)[9,10] cannot be obtained in a practical environment. In fact, the uptake in a typical environment can be expected to be at least an order of magnitude less than this limit.

The second key result is the establishment of steady-state plateaus. These plateaus illustrate the presence of back reactions that limit the overall pressure increase and H_2 production. For example, in the case of the NpO_2 alpha radiolysis experiments containing 1 wt % H_2O, total decomposition of all the H_2O into H_2 and O_2 would result in a pressure increase of about 3450 torr. However, for these experiments, the actual pressure increase was only 140–250 torr. Similarly, for the alpha-irradiated 0.5 wt % H_2O sample, total decomposition would result in a pressure increase of about 1750 torr, while a rise of only 50 torr was observed. These results clearly demonstrate that 0.5 wt % H_2O on NpO_2 is safe for long-term storage—if such a moisture content could ever be practically reached. Additionally, there is evidence that another mechanism plays a role in O_2 consumption; namely, radiolytically-influenced oxidation of the NpO_2. This mechanism further limits pressurization in the long term.

In setting the storage standards for the actinide oxides, it has customarily been assumed[9,10] that radiolysis of sorbed moisture would produce stoichiometric amounts of H_2 and O_2 and would continue until all of the water had been radiolyzed to these products. However, these results support the observations of other laboratories that *many other radiolytic reactions* are concurrently active in such radiolytic processes and thus limit the overall accumulation of these products.

REFERENCES

1. A. S. Icenhour, L. M. Toth, G. D. Del Cul, and L. F. Miller, "Gamma Radiolysis Studies of Uranyl Fluoride," *Radiochim. Acta* **90**, 109–122 (2002).

2. A. S. Icenhour and L. M. Toth, *Gamma Radiolysis Study of $UO_2F_2 \cdot 0.4\ H_2O$ Using Spent Nuclear Fuel Elements from the High Flux Isotope Reactor*, ORNL/TM-2001/138, UT-Battelle, LLC, Oak Ridge National Laboratory, Oak Ridge, Tennessee, January 2002.

3. A. S. Icenhour, L. M. Toth, and H. Luo, *Water Sorption and Gamma Radiolysis Studies for Uranium Oxides*, ORNL/TM-2001/59, UT-Battelle, LLC, Oak Ridge National Laboratory, Oak Ridge, Tennessee, February 2002.

4. A. S. Icenhour and L. M. Toth, *Alpha Radiolysis of Sorbed Water on Uranium Oxides and Uranium Oxyfluorides*, ORNL/TM-2003/172, UT-Battelle, LLC, Oak Ridge National Laboratory, Oak Ridge, Tennessee, September 2003.

5. "Np Oxide Material Specification Agreement between the Savannah River Site and the Oak Ridge National Laboratory for the transfer of Neptunium Oxide," NMM-PRG-2002-011.7, Rev. 0, December 2002.

6. "Np Oxide Packaging Agreement between the Savannah River Site and the Oak Ridge National Laboratory for the Transfer of Neptunium Oxide," CBU-HCP-2003-00033, Rev. 0, March 2003.

7. J. A. Porter, "Production Technology of Neptunium-237 and Plutonium-238," pp. 289–293 in *Proceedings of the Symposium on Production Technology of Neptunium-237 and Plutonium-238, 146th Meeting of the American Chemical Society, January 1964*, Vol. 3, Issue 4, American Chemical Society, Washington, D.C., 1964.

8. A. S. Icenhour, *Radiolytic Effects on Fluoride Impurities in a U_3O_8 Matrix*, ORNL/TM-2000/157, UT-Battelle, LLC, Oak Ridge National Laboratory, Oak Ridge, Tennessee, May 2000.

9. *Criteria for Packaging and Storing Uranium-233-Bearing Materials*, DOE-STD-3028-2000, U.S. Department of Energy, Washington, D.C.

10. *Criteria for Preparing and Packaging Plutonium Metals and Oxides for Long-term Storage*, DOE-STD-3013, U.S. Department of Energy, Washington, D.C.

11. J. M. Duffey and R. R. Livingston, *Characterization of Neptunium Oxide Generated Using the HB-Line Phase II Flowsheet*, WSRC-TR-2003-00388, Rev. 0, Westinghouse Savannah River Company, Savannah River Site, Aiken, S.C., August 2003.

12. *CRC Handbook of Chemistry and Physics*, 73rd ed., D. R. Lide, ed., CRC Press, Boca Raton, Florida, 1992.

13. W. Primak and L. H. Fuchs, "Nitrogen Fixation in a Nuclear Reactor," *Nucleonics* **13**(2), 38–41 (1955).

14. P. Harteck and S. Dondes, "Producing Chemicals with Reactor Radiations," *Nucleonics* **14**(7), 22–25 (1956).

15. A. R. Jones, "Radiation-Induced Reactions in the N_2-O_2-H_2O System," *Radiat. Res.* **10**, 655–663 (1959).

16. C. J. Hochanadel, "Effects of Cobalt Gamma-Radiation on Water and Aqueous Solutions," *J. Phys. Chem.* **56**(5), 587–94 (1952).

17. A. O. Allen, C. J. Hochanadel, J. A. Ghormley, and T. W. Davis, "Decomposition of Water and Aqueous Solutions Under Mixed Fast Neutron and Gamma Radiation," *J. Phys. Chem.* **56**(5), 575–86 (1952).

18. G. Sattonnay et al., "Alpha-Radiolysis Effects on UO_2 Alteration in Water," *J. Nucl. Mater.* **288**, 11–19 (2001).

19. P. C. Burns and K. Hughes, "Studtite $[(UO_2)(O_2)(H_2O)_2](H_2O)_2$: The First Structure of a Peroxide Mineral," *Am. Mineral.*, **88**, 1165–68 (2003).

INTERNAL DISTRIBUTION

1. C. W. Alexander
2. J. M. Begovich
3. W. D. Bond
4–5. R. R. Brunson
6. R. M. Canon
7. T. B. Conley
8. G. D. Del Cul
9. R. H. Elwood, Jr.
10. L. K. Felker
11. L. L. Gilpin
12. S. Goluoglu
13. M. A. Green
14. J. N. Herndon
15. D. J. Hill
16. C. M. Hopper
17–21. A. S. Icenhour
22. A. M. Krichinsky
23. B. E. Lewis
24. S. C. Marschman
25. D. E. Mueller
26. P. E. Osborne
27. C. V. Parks
28. D. A. Reed
29. J. E. Rushton
30. C. M. Simmons
31. D. W. Simmons
32. R. G. Taylor
33–34. L. M. Toth
35. L. D. Trowbridge
36. R. M. Westfall
37–41. R. M. Wham
42. D. F. Williams
43. NSTD DMC
44. OTIC–RC, OSTI, CRL

EXTERNAL DISTRIBUTION

45. N. M. Askew, U.S. Department of Energy, Savannah River Site Operations Office, WSRC, Bldg. 773-A, Road 1A, Aiken, SC 29801
46. L. W. Boyd, DOE-ORO, U.S. Department of Energy, P.O. Box 2008 MS-6269, Oak Ridge, TN 37831
47. W. R. Brock, BWXT–Y-12, LLC, P.O. Box 2009, Oak Ridge, TN 37831
48. W. P. Carroll, DOE-HQ, NE-40/Germantown Building, U.S. Department of Energy, 1000 Independence Ave. S.W., Washington, DC 20585-1290
49. S. O. Cox, BWXT–Y-12, LLC, P.O. Box 2009, Oak Ridge, TN 37831
50. C. H. Delegard, Pacific Northwest National Laboratory, 902 Battelle Blvd., P.O. Box 999, Richland, WA 99352
51. J. M. Duffey, U.S. Department of Energy, Savannah River Site Operations Office, WSRC, Bldg. 773-A, Road 1A, Aiken, SC 29801
52. P. G. Eller, U.S. Department of Energy, Los Alamos National Laboratory, P.O. Box 1663, Los Alamos, NM 87545
53. H. C. Johnson, U.S. Department of Energy, Headquarters, EM-21, Forrestal Bldg., 1000 Independence Ave. S.W., Washington, D.C. 20585
54. R. A. Just, BWXT–Y-12, LLC, P.O. Box 2009, Oak Ridge, TN 37831
55. H. J. Keener, BWXT–Y-12, LLC, P.O. Box 2009, Oak Ridge, TN 37831
56. E. Kendall, NNSA, U.S. Department of Energy, P.O. Box 2001 MS-8193, Oak Ridge, TN 37831
57. R. R. Livingston, U.S. Department of Energy, Savannah River Site Operations Office, WSRC, Bldg. 773-A, Road 1A, Aiken, SC 29801
58. R. E. Mason, U.S. Department of Energy, Los Alamos National Laboratory, P.O. Box 1663, Los Alamos, NM, 87545

59. R. C. McBroom, DOE-ORO, U.S. Department of Energy, P.O. Box 2008 MS-6269, Oak Ridge, TN 37831
60. S. R. Martin, Jr., DOE-ORO, U.S. Department of Energy, P.O. Box 2008 MS-6269, Oak Ridge, TN 37831
61. T. R. Miller, BWXT–Y-12, LLC, P.O. Box 2009, Oak Ridge, TN 37831
62. L. Morales, U.S. Department of Energy, Los Alamos National Laboratory, P.O. Box 1663, Los Alamos, NM, 87545
63. M. T. Paffett, U.S. Department of Energy, Los Alamos National Laboratory, P.O. Box 1663, Los Alamos, NM, 87545
64. M. J. Plaster, BWXT–Y-12, LLC, P.O. Box 2009, Oak Ridge, TN 37831
65. K. H. Reynolds, DOE-ORO, U.S. Department of Energy, P.O. Box 2008 MS-6269, Oak Ridge, TN 37831
66. G. D. Roberson, U.S. Department of Energy, Albuquerque Operations Office, Bldg. 382-2, AL, Pennsylvania and H Street, Kirkland Air Force Base, Albuquerque, NM 87116
67. L. A. Worl, U.S. Department of Energy, Los Alamos National Laboratory, P.O. Box 1663, Los Alamos, NM 87545

SECTION 3 REFERENCES

10 CFR 71, *Packaging and Transportation of Radioactive Material,* Jan. 1, 2007.

ABAQUS/Standard, Version 6.4-1, 2003-09-29-11.18.28 46457, Abaqus, Inc., 2003.

ASME Boiler and Pressure Vessel Code, An American National Standard, Materials, Sect. II, *Materials,* Part D, American Society of Mechanical Engineers, New York, 2001 ed. with 2002 and 2003 addenda.

ASME Boiler and Pressure Vessel Code, An American National Standard, Rules for Construction of Nuclear Power Facility Components, Sect. III, Div. 1, Subsection NB, American Society of Mechanical Engineers, New York, 2001 ed. with 2002 and 2003 addenda.

ASME Boiler and Pressure Vessel Code, An American National Standard, Welding and Brazing Qualifications, Sect. IX, American Society of Mechanical Engineers, New York, 2001 ed. with 2002 and 2003 addenda.

ASTM D-2000, *Standard Classification System for Rubber Products in Automotive Applications*, American Society for Testing and Materials, Philadelphia, current revision.

ASTM E-2230-02, *Standard Practice for Thermal Qualification of Type B Packages for Radioactive Materials,* ASTM International, West Conshohocken, Pa., 2002.

Bailey, R. A., *Strain—A Material Database*, Lawrence Livermore Natl. Lab., Nov. 18, 1987.

Bailey, R. A., *THERM 1.2, A Thermal Properties DataBase for the IBM PC*, Lawrence Livermore Natl. Lab., Nov. 18, 1987.

Byington, G. A., *Vibration Test Report of the ES-2M Shipping Package*, GAB1296-2, Lockheed Martin Energy Systems, Inc., Oak Ridge Y-12 Plant, Sept. 3, 1997.

CRC Handbook of Chemistry and Physics, D. R. Lide, ed., 79th ed., CRC Press, Boca Raton, Fla. 1998.

Incropera, F. P., and D. P. DeWitt, *Fundamentals of Heat and Mass Transfer*, 2nd ed., John Wiley & Sons, New York, 1985.

MIL-HDBK-5H, *Metallic Materials and Elements for Aerospace Vehicle Structures*, Dec. 1 1998.

MSC.Patran, Version 12.0.044, MacNeal Schwendler Corp., 2004.

Nalgene Labware, http://www.nalgenelabware.com/products/productList.asp?search=1&catalog_no=2101.

NUREG/CR-6673, *Hydrogen Generation in TRU Waste Transportation Packages*, Lawrence Livermore Natl. Lab., May 2000.

OO-PP-986, rev. D, *Procurement Specification for 70A Durometer Preformed Packing (O-rings)*, Lockheed Martin Energy Systems, Inc., Oak Ridge Y-12 Plant, Jan. 26, 1999.

Parker O-ring Handbook, Catalog ORD 5700A/US, Parker Hannifin Corp., O-ring Div., Lexington, Ky., 2001.

SG 140.1, *Combination Test Analysis/Method Used to Demonstrate Compliance to DOE Type B Packaging Thermal Test Requirements (30 Minute Fire Test)*, U.S. DOE, Albuquerque Field Office, Nuclear Explosive Safety Division, Feb. 10, 1992.

Sudarsanam, S. B., et al., UT-Battelle, Presentation to Hydrogen Pipeline R&D, Project Review Meeting, *Hydrogen permeability and Integrity of hydrogen transfer pipelines*, January 2005, http://www1.eere.energy.gov/hydrogenandfuelcells/pdfs/03_babu_transfer.pdf.

Van Wylen, G. J., and R. E. Sonntag, *Fundamentals of Classical Thermodynamics*, 2d ed., John Wiley & Sons, Inc., New York, 1973.

4. CONTAINMENT

Design analysis, full-scale testing, and similarity of the ES-3100 prototypes have been used to demonstrate that the ES-3100 package with highly enriched uranium (HEU) is in compliance with the applicable containment requirements of Title 10 Code of Federal Regulations, Part 71 (10 CFR 71). The containment requirements of 10 CFR 71.51 are shown in Table 4.1. A bounding load case has been established for the ES-3100 package, and it assumes that the maximum HEU content is 35.2 kg (Sect. 1.2.3.6) with a decay heat load of 0.4 W (Sect. 1.2.3.7). This decay heat load and the volumes established for the convenience cans, spacers, silicone rubber pads, and the containment vessel void volume are discussed in Sect. 3.1.2 and Appendix 3.6.4. Sections 2 and 3 of this safety analysis report (SAR) also examine the effects of the lightest weight HEU content [2.77 kg (6.11 lb)]. The evaluations in Sects. 2, 3, and 4 have demonstrated that the ES-3100 shipping package with HEU content weight ranging from 2.77 kg (6.11 lb) to 35.2 kg (77.60 lb) meets the containment requirements specified in 10 CFR 71 for all conditions of transport. A summary of the containment boundary design and fabrication acceptance basis is given in Table 4.2. No credit is taken for the various convenience cans' ability to protect the HEU contents from being released.

Table 4.1. Containment requirements of transport for Type B packages [a]

Condition	Allowable release rate
Normal Conditions of Transport (NCT)	$R_N = 10^{-6}$ A_2 per hour = 2.78×10^{-10} A_2 per second
Hypothetical Accident Conditions (HAC)	$R_A = A_2$ in 1 week = 1.65×10^{-6} A_2 per second
	For ^{85}Kr, a value of 10 A_2 in 1 week is used

[a] From ANSI N14.5-1997, Sects. 5.4.1 and 5.4.2, and 10 CFR 71.51(a)(1) and (a)(2)

Table 4.2. Summary of the containment vessel design and fabrication acceptance basis

Nominal empty weight	15.10 kg (33.29 lb)
Air fill medium temperature at loading	25°C (77°F)
Air fill medium pressure at loading	101.35 kPa (14.70 psia)
Hydrostatic pressure test	1034 ± 34 kPa (150 ± 5) gauge
Helium acceptance leakage rate [a]	$L_T \leq 2.0 \times 10^{-7}$ cm³/s
Air acceptance leakage rate [a]	$L_T \leq 1 \times 10^{-7}$ ref-cm³/s
Air preshipment leakage rate	$L_T \leq 1 \times 10^{-4}$ atm-cm³/s

[a] Acceptance leakage testing includes fabrication, periodic (within 12 months of use), and maintenance testing. According to Sect. 2.1 of ANSI N14.5-1997, *leaktight* is defined as an air leakage rate of 1×10^{-7} ref-cm³/s; under the same conditions, this air leakage rate is ~ equal to a helium leakage rate of 2×10^{-7} cm³/s.

The analysis documented in Appendix 4.6.1 was conducted to establish the upper limit for the total activity and the maximum number of A_2s proposed for transport in the ES-3100 package. The maximum activity [3.2427×10^{-1} TBq (8.764 Ci)] of the contents occurs 10 years after initial fabrication. When the maximum activity-to-A_2 value (293.99) is reached at ~70 years from material fabrication, the corresponding activity is 3.2328×10^{-1} TBq (8.737 Ci). These values have been determined using a maximum of 35.2 kg of HEU with isotopic weight percents as shown in Table 4.3. By applying the maximum weight percents of isotopes ^{233}U, ^{234}U, ^{236}U and by incorporating the traces of ^{232}U and the transuranic isotopes, the maximum activity, minimum A_2 value, and the minimum leakage requirements were determined for the proposed contents and are summarized in Tables 4.4, 4.5, and 4.6. The mass and

isotopic concentrations used for the proposed content do not take into consideration limits based on shielding and subcriticality.

The initial composition of the content contains several isotopes of uranium (Sect. 1.2.3). As a result of radioactive decay, the ingrowth of uranium daughter products occurs, and these concentrations of daughter products will vary with time. The uranium isotopes and daughter products are considered a mixture of radionuclides, and the method for determining the mixture's A_2 value in Section IV, Appendix A, 10 CFR 71 is applied. The A_2 value for the most conservative set of contents defined in Sect. 1.2.3 has been calculated in Appendix 4.6.1. Since the HEU can be in the form of oxides (U_3O_8-Al, UO_2-Mg, UO_2, UO_3, and U_3O_8), uranyl nitrate crystals (UNX), or metal and alloy, the calculation of the mixture's A_2 used the various uranium isotopic A_2 values for fast, medium, and slow lung absorption criteria shown in Table A-1 of Appendix A of 10 CFR 71.

The mass and material compositions analyzed in this section of the SAR are not limited by the combustible gas requirements stated in NUREG-1609, Sect. 4.5.2.3. NUREG-1609, Sect. 4.5.2.3, requires the applicant to demonstrate that any combustible gases generated in the package during a period of one year do not exceed 5% (by volume) of the free gas volume in any confined region of the package. No credit should be taken for getters, catalysts, or other recombination devices. ~~The analysis described in Appendix 3.6.4 predicts the maximum normal operating pressure inside the containment vessel for the various packaging arrangements shown in Sect. 3.1.4.1.~~ The analysis conducted in Appendix 3.6.7 ~~further~~ evaluates the different packaging arrangements for the generation of hydrogen gas due to the radiolysis of water vapor, free water, interstitial water, polyurethane bags, and polyurethane or Teflon bottles. By limiting the mass and the material distribution ~~are described~~ as shown in Appendix 3.6.7, the combustible gas concentration limit stated in NUREG-1609 is not exceeded. These limits are further shown in Tables 1.3 and 1.3a. Getters, catalysts, or other recombination devices are not employed in any of the containment vessel packaging arrangements. The analysis conducted in Appendix 3.6.4 predicts the maximum normal operating pressure inside the containment vessel for the various packaging arrangements and masses discussed previously. This appendix also includes the hydrogen gas generation predicted by Appendix 3.6.7.

4.1 DESCRIPTION OF THE CONTAINMENT BOUNDARY

As shown in Table 4.4, the number of A_2s proposed for shipping exceeds 30 but is less than 3000. In accordance with NUREG 1609, the containment vessel is a Category II vessel. Since this vessel may be used for future contents that exceed 3000 A_2, the containment vessel category has been elevated to a Category I vessel. Therefore, the containment vessel is designed (using nominal dimensions for each component), fabricated, and inspected in accordance with the American Society of Mechanical Engineers (ASME) *Boiler and Pressure Vessel Code*, Sect. III, Division I, Subsection NB and Section IX.

4.1.1 Containment Boundary

The containment boundary consists of the vessel's body, lid assembly, and inner O-ring (Sect. 1, Fig. 1.3). Only the inner O-ring is considered part of the boundary. The outer O-ring is provided to allow a post-assembly verification leak check. Two methods of fabrication may be used to fabricate the containment vessel body as shown on Drawing M2E801580A012 (Appendix 1.4.8). The first method uses a standard 5-in., schedule 40 stainless-steel pipe per ASME SA-312 Type TP304L, a machined flat-head bottom forging per ASME SA-182 Type F304L, and a machined top flange forging per ASME SA-182 Type F304L. The nominal outside diameter of the 5-in. schedule 40 pipe is machined to match the nominal wall thickness of 0.254 cm (0.100 in.). Each of these pieces is joined with full-penetration circumferential weld as shown on sheet 2 of Drawing M2E801580A012 (Appendix 1.4.8). The weld filler material conforms to Sect. II, Part C, of the *ASME Boiler and Pressure Vessel Code*. All full-penetration welds are dye penetrant and radiographically inspected in accordance with Sect. III, Div. I, Sect. NB-5000, of the *ASME Boiler and Pressure Vessel Code*. The top flange is machined to match the schedule 40 stainless-steel 5-in. pipe, to provide two concentric half-dove-tailed O-ring grooves in the flat face, to provide locations for two 18-8 stainless-steel dowel pins, and to provide the threaded portion for closure using the lid assembly. The second method of fabrication uses forging, flow forming, or metal spinning to create the complete body (flat bottom, cylindrical body, and

Table 4.5. Regulatory leakage criteria for NCT [a]

Verification Activity	Fast Absorption		Medium Absorption		Slow Absorption	
	$L_{RN\text{-}air}$ (ref-cm³/s)	$L_{RN\text{-}He}$ (cm³/s)	$L_{RN\text{-}air}$ (ref-cm³/s)	$L_{RN\text{-}He}$ (cm³/s)	$L_{RN\text{-}air}$ (ref-cm³/s)	$L_{RN\text{-}He}$ (cm³/s)
Design	3.8473E-03	4.1336E-03	3.6868E-03	3.9662E-03	3.2845E-03	3.5462E-03

[a] The procedure used to calculate the above criteria is shown in Appendix 4.6.2. This data has been extracted from Table 1 in Appendix 4.6.2.

Table 4.6. Containment vessel verification tests criteria for NCT

Test Type	Test Values	Leakage test procedure
Design and compliance leakage testing		
Design verification of O-ring seal (air)	$L_T \leq 1.0 \times 10^{-4}$ ref-cm³/s	See Appendix 2.10.7
Design verification of containment vessel boundary (helium)	$L_T \leq 2.0 \times 10^{-7}$ cm³/s	See Appendix 2.10.7
Verification leakage testing		
Fabrication, periodic, and maintenance (helium)	$L_T \leq 2.0 \times 10^{-7}$ cm³/s	Y51-01-B2-R-140, Rev. A.1 (Appendix 8.3.1)
	$L_T \leq 1.0 \times 10^{-4}$ ref-cm³/s	Y51-01-B2-R-074, Rev. A.1 (Appendix 7.5.1)

The complete design verification testing of the ES-3100 package for NCT was conducted on test unit TU-4. Since the containment vessel was assembled at ambient conditions, the pressure was nominally 101.35 kPa (14.70 psia) at 25°C (77°F). In accordance with 10 CFR 71.71(b), the initial pressure inside each containment vessel should be the maximum normal operating pressure (MNOP). As calculated in Appendix 3.6.4, the bounding case MNOP is 138.43 kPa (20.077 psia). The stresses at the maximum normal operating pressure [37.07 kPa (5.377 psig)] are insignificant compared to the allowable stresses (Table 2.21). O-ring grooves are designed and fabricated in accordance with guidance from the *Parker O-ring Handbook*. In accordance with Fig. 3-2 of the *Parker O-ring Handbook*, the durometer of the O-ring, and the tolerance gap from the production drawings, the O-ring should be able to withstand ~800 psig before anti-extrusion devices are required. Therefore, conducting a compliance test with the MNOP in the containment vessel will have little, if any, effect on the results.

Following the design verification testing of paragraphs 10 CFR 71.71(c)(5) through 71.71(c)(10) excluding 71.71(c)(8), Test Unit-4 was subjected to the sequential testing of paragraphs 10 CFR 71.73(c)(1) through (c)(4). Upon removal of the containment vessel from the drum assembly, the cavity between the O-rings was leak checked. This unit recorded a leak rate between the O-rings of 2.4773×10^{-5} ref-cm³/s.

Following the O-ring leak test, the entire containment boundary of TU-4 was helium leak tested to a value $\leq 2 \times 10^{-7}$ cm³/s, thereby verifying a leak-tight boundary. The leak-test procedure followed to verify this criteria is documented in the ES-3100 test plan (Appendix 2.10.7). The maximum recorded helium leakage rate for this containment vessel was 2.0×10^{-7} cm³/s after 20 min of testing. Visual

inspection following the testing indicated that neither the vessel body, the O-rings, the seal areas, nor the vessel lid assembly were damaged during the tests. Pictures taken of the containment vessel top following testing showed that the closure nut had rotated a maximum of 0.15 cm (0.060 in.) from its original radial position obtained during assembly. Based on the pitch of the closure nut, this rotation translates into only 0.0013 cm (0.0005 in.) decompression of the O-rings. This compares to the original nominal compression of 0.064 cm (0.025 in.). Therefore, O-ring compression was maintained during compliance testing. Based on these results, the ES-3100 package meets and exceeds the containment criteria specified in 10 CFR 71.51 for NCT when used to ship the contents described in the introductory section of this chapter.

Following fabrication, the containment vessel undergoes hydrostatic pressure testing to 1034 kPa (150 psi) gauge. The hydrostatic test is conducted before the final leakage test. Following the hydrostatic pressure test, and prior to conducting the leakage test, the containment vessel and O-ring cavity must be thoroughly dried. Each vessel is then leak tested with either air or helium to $\leq 1 \times 10^{-7}$ ref-cm^3/s or 2×10^{-7} cm^3/s, respectively. This test ensures the containment vessel's integrity (walls, welds, inner O-ring seal) as delivered for use in accordance with paragraph 6.3.2 of ANSI N14.5-1997.

Following placement of the HEU content inside the containment vessel and joining the body and lid assembly, the volume between the containment vessel's O-ring seals is evacuated and checked to leak $\leq 1 \times 10^{-4}$ ref-cm^3/s. This leak-test procedure is a pressure rise air leak test prescribed in Section 7.1.2. This ensures that each containment vessel has been properly assembled in accordance with paragraph 7.6.4 of ANSI N14.5-1997.

The design verification tests were conducted following compliance tests in accordance with 10 CFR 71.71 and 71.73. The effectiveness of this closure system has been demonstrated by the NCT and HAC tests, which show that the complete containment system, including welds and O-ring seals, meet the leaktight criterion as defined in ANSI N14.5-1997 after the conclusion of the test series documented in *Test Report of the ES-3100 Package* (Appendix 2.10.7).

4.4 CONTAINMENT UNDER HYPOTHETICAL ACCIDENT CONDITIONS (TYPE B PACKAGES)

Requirements. A Type B package, in addition to satisfying the requirements of paragraphs 10 CFR 71.41 through 71.47, must be designed, constructed, and prepared for shipment so that under the tests specified in Sect. 71.73 ("Hypothetical Accident Conditions"), there would be no escape of ^{85}Kr exceeding 10 A_2 in one week, no escape of other radioactive material exceeding a total amount A_2 in one week, and no external radiation dose rate exceeding 10 mSv/h (1 rem/h) at 1 m (40 in.) from the external surface of the package.

Analysis. Calculations have been conducted in Appendix 4.6.2 to determine the regulatory leakage criteria to satisfy the above requirements. The results are shown in Table 4.7. These analyses assume that the total mass of uranium for each component is available for release as an aerosol (worst case). From experimental tests, the maximum aerosol density containing uranium particulate was reported by Curren and Bond to be 9.0×10^{-6} g/cm^3. This aerosol density is used to calculate the total activity concentration in ANSI N14.5-1997, Section B.15 examples 13, 27, and 29. Design leakage rate verification testing of the containment boundary (Table 4.8) was conducted on Test Units-1 through -6 and documented in test report (Appendix 2.10.7). Since each containment vessel was assembled at

ambient conditions, the pressure was nominally 101.35 kPa (14.70 psi) at 25°C (77°F). In accordance with 10 CFR 71.73(b), for these tests, the initial pressure inside each containment vessel should be the maximum normal operating pressure. As shown in Table 2.21, the stresses at the maximum normal operating pressure are insignificant compared to the allowable stresses. Therefore, conducting compliance testing with nominal pressure in the containment vessel would have little, if any, effect on the results. During the structural and thermal tests conducted on the ES-3100 for HAC, the drum experienced plastic deformation, and the insulation and impact limiter material experienced some deterioration, as anticipated (Sect. 2.7). The containment vessels did not exhibit any signs of damage and passed post-test leak tests and the subsequent 10 CFR 71.73(c)(5)–specified 0.9-m (3-ft) water immersion tests except for Test Unit-6. Test Unit-6 was subjected to the test specified by paragraph 10 CFR 71.73(c)(6). After completion of this test, the containment vessel was removed and the lid was drilled and tapped for a helium leak-check port. The entire containment boundary was then helium leak checked and passed the leaktight criteria. Also, no visible water was seen inside the inner O-ring groove of Test Unit-6 and no water was observed inside any of the other test units.

Table 4.7. Regulatory leakage criteria for HAC [a]

Verification activity	Fast absorption		Medium absorption		Slow absorption	
	$L_{RA\text{-}air}$ (ref-cm³/s)	$L_{RA\text{-}He}$ (cm³/s)	$L_{RA\text{-}air}$ (ref-cm³/s)	$L_{RA\text{-}He}$ (cm³/s)	$L_{RA\text{-}air}$ (ref-cm³/s)	$L_{RA\text{-}He}$ (cm³/s)
Design	1.3352E+01	1.2732E+01	1.2793E+01	1.2202E+01	1.1394E+01	1.0825E+01

[a] The procedure used to calculate the above criteria is shown in Appendix 4.6.2.

Table 4.8. Containment vessel design verification tests for HAC

Test Type	Test Values	Leakage test procedure
Design and compliance leakage testing		
Design verification of O-ring seal (air)	$L_T \leq 1.0 \times 10^{-4}$ ref-cm³/s	See Appendix 2.10.7
Design verification of containment vessel boundary (helium)	$L_T \leq 2.0 \times 10^{-7}$ cm³/s	See Appendix 2.10.7

To verify the entire containment boundary to the leaktight criteria, the containment vessels of Test Units-1 through -5 were helium leak tested using the procedure shown in the test report (Appendix 2.10.7). These test units had previously been subjected to the drop test stipulated in 10 CFR 71.71 (c)(6) and the sequential tests stipulated in 10 CFR 71.73 except for Test Unit-4, which had been first subjected to the testing in accordance with 10 CFR 71.71. The maximum recorded helium leak rate for any of these containment vessels was 2.0×10^{-7} cm³/s after 20 min of testing on Test Unit-4 as documented in Section 5.2 of the test report (Appendix 2.10.7). Test Units-2 and -5 displayed some unusual pulsing action during leak testing. The peak amplitude changed after adding helium in a manner expected for diffusion through the O-rings rather than a rise immediately following the addition of helium that would indicate a leak to the outside of the containment vessel. This is further discussed and graphically presented in Sect. 5.2.2 of the ES-3100 test report (Appendix 2.10.7). These measured leakage rates verify that the containment vessels are leaktight in accordance with ANSI N14.5-1997. Therefore, the containment boundary of the ES-3100 package was maintained during the HAC testing.

The 35.2 kg of HEU content is unirradiated; therefore, only very small quantities of fission gas products will be produced from spontaneous fission and subcritical neutron induced fission. Fission gas products are produced in such small quantities that they have no measurable effect on the releasable content source term or containment vessel pressurization. Fission gas products will not be considered further in this SAR.

4.5 LEAKAGE RATE TESTS FOR TYPE B PACKAGES

The maximum allowable release of radioactive material allowed by 10 CFR 71.51(a)(2) under HAC is A_2 in one week. Title 10 CFR 71.51(a)(2) also specifies that there be no escape of ^{85}Kr exceeding 10 A_2 in one week. ANSI N14.5-1997 specifies the leakage test methods and leakage rates that are accepted in Nuclear Regulatory Commission (NRC) Regulatory Guide 7.4 as demonstrating that a package meets the 10 CFR 71.51(a)(2) requirements for containment. The containment criteria for the ES-3100 package will be leaktight, defined in ANSI N14.5 paragraph 2.1 as having a leakage rate $\leq 1 \times 10^{-7}$ ref-cm^3/s, during the prototype tests. This leaktight criterion satisfies the design verification requirement stipulated in paragraph 7.2.4 of ANSI N14.5-1997. The requirements of ANSI N14.5-1997 are used for all stages of containment verification for the ES-3100 (i.e., design, fabrication, maintenance, periodic and preshipment). The design, fabrication, maintenance and periodic leakage rate limit is 1×10^{-7} ref-cm^3/s air (or 2.0×10^{-7} cm^3/s helium). The pass criterion for the preshipment leakage rate test, which demonstrates correct assembly of the containment vessels, is 1×10^{-4} ref-cm^3/s, which exceeds the requirements given in ANSI N14.5-1997, paragraph 7.6.4. In accordance with the definition of sensitivity of a leakage test procedure provided in Sections 2 and 7.6.4 of ANSI N14.5-1997, the minimum acceptable leakage rate that the procedure needs to be capable of detecting is 1×10^{-3} ref-cm^3/s. The requirements for the ES-3100 exceed the regulatory criterion by specifying a leakage rate of $\leq 1 \times 10^{-4}$ ref-cm^3/s, and equipment used in accordance with Section 7.6.4 of ANSI N14.5-1997 would not detect this leakage. The preshipment, fabrication, maintenance, and periodic leakage rate tests are required to be conducted on each containment vessel in accordance with ANSI N14.5-1997 and are specified in Chapters 7 and 8. These leakage rates are not dependent on filters or mechanical cooling.

The requirements of ANSI N14.5-1997 are used for all stages of containment verification for the ES-3100; the design (HAC test) leakage rate limit is 1×10^{-7} ref-cm^3/s (which is defined as leaktight in ANSI N14.5-1997). The packaging has been shown to maintain containment before and after prototype testing by leakage tests performed for containment verification to the requirements of ANSI N14.5-1997. Test Unit-4's containment vessel was subjected to both the NCT and HAC tests. Test Units-1 through -5 were subjected to the free drop stipulated in 10 CFR 71.71(c)(7) and to the sequential HAC test stipulated in 10 CFR 71.73. Following these tests, each containment vessel was helium leak tested in accordance with the test plan. Again, the test results verified that the containment vessels were leaktight. Thus, there could be no release of radioactive materials from the containment vessels. These leakage rates are not dependent on filters or mechanical cooling. These measured leakage rates verify that the containment vessels are leaktight in accordance with ANSI N14.5-1997.

Therefore, the ES-3100 package meets the containment criteria as specified in 10 CFR 71.73 for HAC when shipping the proposed 35.2 kg of HEU in the containment vessel.

arrangements in the ES-3100 package. The convenience cans are sealed inside the containment vessel in an environmentally controlled area. The ES-3100 package has been analyzed thermally in Sect. 3; it was evaluated at a maximum NCT gas temperature of 87.81°C (190.06°F) [100°F with solar insolation] and a maximum adjusted HAC gas temperature of 123.85°C (254.93°F).

The following analysis determines the maximum allowable O-ring seal air reference leakage rate for both NCT and HAC. The ANSI N14.5-1997 recommended method using a straight circular tube to model the leakage path is applied. Using this "standard" leakage hole model permits the calculation of equivalent reference leakage rates from which leak-test requirements can be established. Viscosity data for air and helium used in the following analyses were obtained from curve fitting routines at specific temperatures based on viscosity data for air (Handbook of Chemistry and Physics, 55th ed.) and helium (NBS Technical Note 631).

L_N and L_A correspond to the upstream volumetric leakage rate (L_u) at the upstream pressure (P_u).

$$L_N = 3.6984 \times 10^{-3} \text{ cm}^3/\text{s},$$
$$L_A = 2.1951 \times 10^{1} \text{ cm}^3/\text{s}.$$

Find the maximum pressure and temperature in the containment vessel:

Converting the temperature to degrees Kelvin:

$$T = 273.15 + T(°C),$$
$$T = 273.15 + 5 / 9\ (°F - 32)\ (K).$$

$$T_N = 273.15 + 5 / 9\ (190.06°F - 32)\ (K), \quad \text{(Sect. 3.4.1, for T = 190.06°F)}$$
$$T_N = 360.961 \text{ K.} \quad \text{NCT}$$

$$T_A = 273.15 + 5 / 9\ (254.93°F - 32)\ (K), \quad \text{(Sect. 3.5.3, for T = 254.93°F)}$$
$$T_A = 397.000 \text{ K.} \quad \text{HAC}$$

Converting the pressures from psia to atmospheres:

$$P_N = P \text{ (psia)} / 14.696 \text{ (psia/atm)}, \quad \text{where P is the pressure in Sect. 3.4.2}$$
$$P_N = 20.077 \text{ (psia)} / 14.696 \text{ (psia/atm)}, \quad \text{NCT}$$
$$P_N = 1.3662 \text{ atm.}$$

$$P_A = P \text{ (psia)} / 14.696 \text{ (psia/atm)}, \quad \text{where P is the pressure in Sect. 3.5.3}$$
$$P_A = 40.701 \text{ (psia)} / 14.696 \text{ (psia/atm)}, \quad \text{HAC}$$
$$P_A = 2.7695 \text{ atm.}$$

NCT Leakage Hole Diameter for the HEU Content

The following calculations determine the leakage hole diameter that generates the maximum allowable leakage rate during NCT. To keep these calculations conservative, the maximum values for temperature and pressure were used as steady-state conditions for NCT.

Input data for NCT with air fill gas:

L_N	=	3.6984×10^{-3} cm³/s,	Maximum upstream leakage
P_u	=	1.3662 atm,	Upstream pressure = 20.077 psia
P_d	=	0.2382 atm,	Downstream pressure = 3.5 psia, per 10 CFR 71.71(3)
a	=	0.3531 cm,	Leak path length, 0.139-in. O-ring section diameter
T	=	360.96 K,	Fill gas temperature = 190.06°F
μ	=	0.02141 cP,	Viscosity at temperature
M	=	29 g/g-mole.	Molecular weight of fill gas

The average pressure is:

P_a	=	$(P_u + P_d)/2$,	
	=	(1.3662 + 0.2382) / 2 ,	
P_a	=	0.8022 atm.	Average pressure during NCT

According to ANSI N14.5-1997, the flow leakage hole diameter is unknown. Therefore, the mass-like leakage flow rate must be calculated to calculate the average leakage flow rate.

Q is the mass-like leakage for flow using the upstream leakage, L_u, and pressure, P_u:

Q	=	$P_u L_u$,	(Eq. B1)
L_u	=	L_N.	NCT leakage
Q	=	(1.3662)(atm) (3.6984×10^{-3})(cm³/s),	
Q	=	5.0526×10^{-3} atm-cm³/s.	NCT mass-like leakage rate
Q	=	$P_a L_a$,	(Eq. B1)
L_a	=	Q / P_a = 5.0526×10^{-3} (atm-cm³/s) / (0.8022)(atm),	
L_a	=	6.2988×10^{-3} cm³/s.	NCT average leakage rate

Solve equations B2–B4 from ANSI N14.5-1997:

L_a	=	$(F_c + F_m)(P_u - P_d)$ cm³/s,	(Eq. B2)
L_a	=	$(F_c + F_m)$ (1.3662 - 0.2382),	
L_a	=	(1.1280) $(F_c + F_m)$ cm³/s.	
F_c	=	$(2.49 \times 10^6)\ D^4 / (a\ \mu)$ (cm³/atm-s),	(Eq. B3)
F_c	=	$(2.49 \times 10^6)\ D^4$ / ((0.3531) (0.02141)),	
F_c	=	$(3.2943 \times 10^8)\ D^4$ cm³/atm-s.	
F_m	=	$(3.81 \times 10^3)\ D^3\ (T / M)^{.5} / (a\ P_a)$ (cm³/atm-s),	(Eq. B4)
F_m	=	$(3.81 \times 10^3)\ D^3$ (360.96 / 29)$^{.5}$ / ((0.3531) (0.8022)),	
F_m	=	$(4.7454 \times 10^4)\ D^3$ cm³/atm-s.	

From the mass-like leakage calculation:

L_a	=	6.2988×10^{-3} cm³/s.	NCT average leakage rate

Find the leakage hole diameter that sets:

$$L_2 = L_a.$$

Using the equations:

$$L_2 = (1.1280)\,(F_c + F_m)\ cm^3/s,$$
$$F_c = (3.2943 \times 10^8)\,D^4\ cm^3/atm\text{-}s,$$
$$F_m = (4.7462 \times 10^4)\,D^3\ cm^3/atm\text{-}s.$$

To get a better guess on a new D use:

$$D = D_2\,(L_a / L_2)^{0.252}.$$

Now a guess must be made for D_2 to solve Eq. B2 for NCT:

D_2 = 0.001 cm, and solve for $L_a = 6.2988 \times 10^{-3}$ cm³/s. NCT average leakage rate

Diameter	F_c	F_m	L_2	L_a / L_2
1.0000E-03	3.2943E-04	4.7462E-05	4.2514E-04	1.4816E+01
1.9725E-03	4.9873E-03	3.6427E-04	6.0365E-03	1.0435E+00
1.9938E-03	5.2057E-03	3.7617E-04	6.2964E-03	1.0004E+00
1.9940E-03	5.2078E-03	3.7628E-04	6.2988E-03	1.0000E+00
1.9940E-03	5.2078E-03	3.7628E-04	6.2988E-03	1.0000E+00

The NCT leakage hole diameter for the HEU oxide content:

$D = 1.9940 \times 10^{-3}$ cm. NCT diameter

NCT Reference Air Leakage Rate for HEU Content

The leakage hole diameter found for the maximum allowable leakage rate for NCT will be used to determine the reference air leakage rate. O-ring seal leakage testing must ensure that no leakage is greater than the leakage generated by the hole diameter $D = 1.9958 \times 10^{-3}$ cm. Therefore, the NCT reference leakage flow rate ($L_{R,N}$) must be calculated to determine the allowable test leakage rate.

Input data for NCT reference air leakage rate:

D	=	1.9940×10^{-3} cm,	From NCT
a	=	0.3531 cm,	Leak path length, 0.139-in. O-ring section diameter
P_u	=	1.0 atm,	Upstream pressure
P_d	=	0.01 atm,	Downstream pressure
T	=	298 K,	Fill gas temperature, 77°F
M	=	29 g/g-mole,	Molecular weight of air
μ	=	0.0185 cP,	Viscosity of air at reference temperature

Calculate P_a:

$P_a = (P_u + P_d) / 2,$
$= (1.0 + 0.01) /2,$
$P_a = 0.505$ atm. NCT average pressure

$F_c = (2.49 \times 10^6) D^4 / (a \mu)$ (cm³/atm-s), (Eq. B3)
$F_c = (2.49 \times 10^6) (1.9940 \times 10^{-3})^4 / ((0.3531) (0.0185)),$
$F_c = (3.8122 \times 10^8) (1.9940 \times 10^{-3})^4,$
$F_c = 6.0265 \times 10^{-3}$ cm³/atm-s.

$F_m = (3.81 \times 10^3) D^3 (T / M)^{.5} / (a P_a)$ (cm³/atm-s), (Eq. B4)
$F_m = (3.81 \times 10^3) (1.9940 \times 10^{-3})^3 (298 / 29)^{.5} / ((0.3531) (0.505)),$
$F_m = (6.8501 \times 10^4) (1.9940 \times 10^{-3})^3 ,$
$F_m = 5.4307 \times 10^{-4}$ cm³/atm-s.

$L_u = (F_c + F_m) (P_u - P_d) (P_a / P_u)$ (cm³/s), (Eq. B5)
$L_u = (6.0265 \times 10^{-3} + 5.4307 \times 10^{-4})$(cm³/atm-s) (1.0 - 0.01)(atm) (0.505 / 1.0),
$L_u = (6.5696 \times 10^{-3})$(cm³/atm-s) (0.49995)(atm),
$L_u = 3.2845 \times 10^{-3}$ cm³/s.

The reference air leakage rate as defined in ANSI N14.5-1997, Sect. B.3, is the upstream leakage in air.

$L_{RN,Air} = 3.2845 \times 10^{-3}$ ref-cm³/s. For HEU oxide content

The same equations can be used to calculate an allowable leakage rate using helium for leak testing.

$M = 4$ g/g-mole, Molecular weight of helium
$\mu = 0.0198$ cP. Viscosity of helium at temperature

$F_c = (2.49 \times 10^6) D^4 / (a \mu)$ (cm³/atm-s), (Eq. B3)
$F_c = (2.49 \times 10^6) (1.9940 \times 10^{-3})^4 / ((0.3531) (0.0198)),$
$F_c = (3.5619 \times 10^8) (1.9940 \times 10^{-3})^4,$
$F_c = 5.6308 \times 10^{-3}$ cm³/atm-s.

$F_m = (3.81 \times 10^3) D^3 (T / M)^{.5} / (a P_a)$ (cm³/atm-s), (Eq. B4)
$F_m = (3.81 \times 10^3) (1.9940 \times 10^{-3})^3 (298 / 4)^{.5} / ((0.3531) (0.505)),$
$F_m = (1.8444 \times 10^5) (1.9940 \times 10^{-3})^3 ,$
$F_m = 1.4623 \times 10^{-3}$ cm³/atm-s.

$L_u = (F_c + F_m) (P_u - P_d) (P_a / P_u)$ (cm³/s), (Eq. B5)
$L_u = (5.6308 \times 10^{-3} + 1.4623 \times 10^{-3})$(cm³/atm-s) (1.0 - 0.01)(atm) (0.505 / 1.0),
$L_u = (7.0931 \times 10^{-3})$(cm³/atm-s) (0.49995)(atm),
$L_u = 3.5462 \times 10^{-3}$ cm³/s.

The allowable leakage rate using helium for leak testing is:

$L_{RN, He} = 3.5462 \times 10^{-3}$ cm³/s. NCT helium test value

HAC Leakage Hole Diameter for HEU Content

The calculation of a maximum allowable leakage rate hole diameter is based on the temperature and pressure of the fill gas aerosol for HAC, assuming the content is in an oxide powder form. Keeping this calculation conservative, the maximum values for temperature and pressure were used as steady-state conditions for a week. The maximum values were generated during the 30-min burn test for HAC.

Input data for HAC:

$L_A = 21.951\ cm^3/s$, Maximum exit leakage
$P_u = 2.7695\ atm$, Upstream pressure = 40.701 psia
$P_d = 1.0\ atm$, Downstream pressure
$T = 397.000\ K$, Fill gas temperature = 254.93 °F
$\mu = 0.02297\ cP$, Viscosity of air at temperature
$M = 29\ g/g\text{-}mole$, Molecular weight of air
$a = 0.3531\ cm$. Leak path length, 0.139-in. O-ring section diameter

$P_a = (P_u + P_d) / 2$
$= (2.7695 + 1.0) / 2$, HAC average pressure
$P_a = 1.8848\ atm$.

Q is the mass-like leakage for flow using the upstream leakage, L_u, and pressure, P_u:

$Q = P_u L_u$, (Eq. B1)
$L_u = L_A$. HAC leakage

$Q = (2.7695)(atm)\ (21.951)(cm^3/s)$,
$Q = 60.795\ atm\text{-}cm^3/s$. HAC mass-like leakage rate

$Q = P_a L_a$, (Eq. B1)
$L_a = Q / P_a$
$= 60.795\ (atm\text{-}cm^3/s) / (1.8848)(atm)$,
$L_a = 32.256\ cm^3/s$. HAC average leakage rate

Solve equations B2–B4 from ANSI N14.5-1997:

$L_a = (F_c + F_m)\ (P_u - P_d)\ (cm^3/s)$, (Eq. B2)
$L_a = (F_c + F_m)\ (2.7695 - 1.0)$,
$L_a = 1.7695\ (F_c + F_m)\ cm^3/s$.

$F_c = (2.49 \times 10^6)\ D^4 / (a\ \mu)\ (cm^3/atm\text{-}s)$, (Eq. B3)
$F_c = (2.49 \times 10^6)\ D^4 / ((0.3531)\ (0.02297))$,
$F_c = (3.0706 \times 10^8)\ D^4\ cm^3/atm\text{-}s$.

$F_m = (3.81 \times 10^3)\ D^3\ (T / M)^{.5} / (a\ P_a)\ (cm^3/atm\text{-}s)$, (Eq. B4)
$F_m = (3.81 \times 10^3)\ D^3\ (397.00 / 29)^{.5} / ((0.3531)\ (1.8848))$,
$F_m = (2.1184 \times 10^4)\ D^3\ cm^3/atm\text{-}s$.

From the mass-like leakage calculation:

L_a = 32.256 cm^3/s. HAC average leakage rate

Find the leakage hole diameter that sets:

L_2 = L_a.

Using the equations:

L_2 = 1.7695 ($F_c + F_m$) cm^3/s,
F_c = (3.0706×10^8) D^4 $cm^3/atm\text{-}s$,
F_m = (2.1184×10^4) D^3 $cm^3/atm\text{-}s$.

To get a better guess on a new D use:

$D = D_2 (L_a / L_2)^{0.252}$.

Now a guess must be made for D_2 to solve Eq. B2 for HAC:

D_2 = 0.01 (cm), and solve for L_a = 32.256 (cm^3/s). HAC average leakage rate

Diameter	F_c	F_m	L_2	L_a / L_2
1.0000E-02	3.0706E+00	2.1184E-02	5.4709E+00	5.8959E+00
1.5638E-02	1.8363E+01	8.1012E-02	3.2637E+01	9.8833E-01
1.5592E-02	1.8148E+01	8.0300E-02	3.2255E+01	1.0000E+00
1.5592E-02	1.8148E+01	8.0300E-02	3.2255E+01	1.0000E+00

The HAC leakage hole diameter for the HEU oxide content is:

D = 1.5592×10^{-2} cm. HAC diameter

HAC Reference Air Leakage Rate for HEU Content

The leakage hole diameter found for the maximum allowable leakage rate for HAC will be used to determine the reference air leakage rate. O-ring seal leakage testing must assure that no leakage is greater than the leakage generated by the hole diameter D = 1.3119×10^{-2} cm. Therefore, the HAC reference air leakage rate ($L_{R,A}$) must be calculated to determine the acceptable test leakage rate for post-HAC leakage testing.

Input data for HAC reference air leakage rate:

D = 1.5592×10^{-2} cm, From the HAC of transport
a = 0.3531 cm, Leak path length, 0.139-in. O-ring section diameter
P_u = 1.0 atm, Upstream pressure

P_d = 0.01 atm, Downstream pressure
T = 298 K, Fill gas temperature, 77°F
M = 29 g/g-mole, Molecular weight of air
μ = 0.0185 cP. Viscosity at temperature

Calculate P_a:

$P_a = (P_u + P_d) / 2$
$= 0.505$ atm. HAC average pressure

$F_c = (2.49 \times 10^6) D^4 / (a \mu) (cm^3/atm\text{-}s)$, (Eq. B3)
$F_c = (2.49 \times 10^6) (1.5592 \times 10^{-2})^4 / ((0.3531) (0.0185))$,
$F_c = (3.8122 \times 10^8) (1.5592 \times 10^{-2})^4$,
$F_c = 2.2531 \times 10^1 \ cm^3/atm\text{-}s$.

$F_m = (3.81 \times 10^3) D^3 (T / M)^{.5} / (a P_a) (cm^3/atm\text{-}s)$, (Eq. B4)
$F_m = (3.81 \times 10^3) (1.5592 \times 10^{-2})^3 (298 / 29)^{.5} / ((0.3531) (0.505))$,
$F_m = (6.8501 \times 10^4) (1.5592 \times 10^{-2})^3$,
$F_m = 2.5966 \times 10^{-1} \ cm^3/atm\text{-}s$.

$L_u = (F_c + F_m) (P_u - P_d) (P_a / P_u) (cm^3/s)$, (Eq. B5)
$L_u = (2.2531 \times 10^1 + 2.5966 \times 10^{-1})(cm^3/atm\text{-}s) (1.0 - 0.01)(atm) (0.505 / 1.0)$,
$L_u = (22.791 \times 10^1)(cm^3/atm\text{-}s) (0.49995)(atm)$,
$L_u = 11.394 \ cm^3/s$.

The HAC reference air leakage rate as defined in ANSI N14.5-1997, Sect. B.3, is the upstream leakage in air.

$L_{RA,Air}$ = 11.394 ref-cm^3/s. for HEU oxide content

The same equations can be used to calculate an allowable leakage rate using helium for leak testing.

M = 4 g/g-mole, Molecular weight of helium
μ = 0.0198 cP. Viscosity of helium at temperature

$F_c = (2.49 \times 10^6) D^4 / (a \mu) (cm^3/atm\text{-}s)$, (Eq. B3)
$F_c = (2.49 \times 10^6) (1.5592 \times 10^{-2})^4 / ((0.3531) (0.0198))$,
$F_c = (3.5619 \times 10^8) (1.5592 \times 10^{-2})^4$,
$F_c = 2.1052 \times 10^1 \ cm^3/atm\text{-}s$.

$F_m = (3.81 \times 10^3) D^3 (T / M)^{0.5} / (a P_a) (cm^3/atm\text{-}s)$, (Eq. B4)
$F_m = (3.81 \times 10^3) (1.5592 \times 10^{-2})^3 (298 / 4)^{.5} / ((0.3531) (0.505))$,
$F_m = (1.8444 \times 10^5) (1.5592 \times 10^{-2})^3$,
$F_m = 6.9915 \times 10^{-1} \ cm^3/atm\text{-}s$.

$L_u = (F_c + F_m) (P_u - P_d) (P_a / P_u) (cm^3/s)$, (Eq. B5)
$L_u = (2.1052 \times 10^1 + 6.9915 \times 10^{-1})(cm^3/atm\text{-}s) (1.0 - 0.01)(atm) (0.505 / 1.0)$,
$L_u = (2.1751 \times 10^1)(cm^3/atm\text{-}s) (0.49995)(atm)$,
$L_u = 10.875 \ cm^3/s$.

The allowable leakage rate using helium for leak testing for HAC is:

$L_{RA, He}$ = 10.875 cm^3/s. HAC helium test value

Table 1. Regulatory leakage criteria for 35.2 kg of HEU

Years from fabrication		NCT		HAC	
		$L_{RN\text{-}air}$ (ref-cm^3/s)	$L_{RN\text{-}He}$ (cm^3/s)	$L_{RA\text{-}air}$ (ref-cm^3/s)	$L_{RA\text{-}He}$ (cm^3/s)
Fast absorption	0	3.8774E-03	4.1649E-03	1.3456E+01	1.2831E+01
	5	3.8594E-03	4.1461E-03	1.3394E+01	1.2772E+01
	10	3.8568E-03	4.1434E-03	1.3384E+01	1.2763E+01
	20	3.8551E-03	4.1417E-03	1.3379E+01	1.2758E+01
	30	3.8538E-03	4.1403E-03	1.3374E+01	1.2754E+01
	40	3.8524E-03	4.1389E-03	1.3369E+01	1.2749E+01
	50	3.8508E-03	4.1372E-03	1.3364E+01	1.2744E+01
	60	3.8491E-03	4.1354E-03	1.3358E+01	1.2738E+01
	70	3.8473E-03	4.1336E-03	1.3352E+01	1.2732E+01
Medium absorption	0	3.7140E-03	3.9946E-03	1.2888E+01	1.2292E+01
	5	3.6975E-03	3.9774E-03	1.2831E+01	1.2238E+01
	10	3.6951E-03	3.9749E-03	1.2822E+01	1.2230E+01
	20	3.6937E-03	3.9734E-03	1.2817E+01	1.2225E+01
	30	3.6925E-03	3.9723E-03	1.2813E+01	1.2221E+01
	40	3.6913E-03	3.9710E-03	1.2809E+01	1.2217E+01
	50	3.6899E-03	3.9695E-03	1.2804E+01	1.2213E+01
	60	3.6884E-03	3.9679E-03	1.2799E+01	1.2208E+01
	70	3.6868E-03	3.9662E-03	1.2793E+01	1.2202E+01
Slow absorption	0	3.3003E-03	3.5628E-03	1.1450E+01	1.0927E+01
	5	3.2879E-03	3.5497E-03	1.1406E+01	1.0886E+01
	10	3.2865E-03	3.5483E-03	1.1401E+01	1.0881E+01
	20	3.2863E-03	3.5481E-03	1.1401E+01	1.0881E+01
	30	3.2863E-03	3.5481E-03	1.1401E+01	1.0881E+01
	40	3.2861E-03	3.5479E-03	1.1400E+01	1.0880E+01
	50	3.2857E-03	3.5475E-03	1.1399E+01	1.0879E+01
	60	3.2852E-03	3.5469E-03	1.1397E+01	1.0877E+01
	70	3.2845E-03	3.5462E-03	1.1394E+01	1.0875E+01